Charles University

Faculty of Medicine in Pilsen

Ph.D. Study program: Anatomy, Histology and Embryology

Branch of Study: D4AH5112

Ing. Anna Zavaďáková

ROLE OF FIBROBLASTS IN REGULATION OF WOUND HEALING

ROLE FIBROBLASTŮ V REGULACI PROCESU HOJENÍ

Ph.D. Thesis

Supervisor: Ing. Lucie Vištejnová, Ph.D.

Pilsen 2020

PREFACE

I declare that I prepared the Ph.D. thesis independently and that I stated all the information sources and literature. This work or a substantial portion thereof has not been submitted to obtain another academic degree or equivalent.

Pilsen,…….

…….

Anna Zavaďáková

ACKNOWLEDGEMENT

I would like to thank to my supervisor Ing. Lucie Vištejnová, Ph.D. for the best leadership I could wish for. I thank her for motivation, patience and especially for the hours of discussions about not only scientific topics which shaped me also as a person. Moreover, I would like to thank to all my colleagues for the unique friendly atmosphere they created.

Anna Zavaďáková

ABSTRAKT

Dermální fibroblasty hrají důležitou roli regulaci procesu hojení. Migrují do místa poranění, množí se a produkují řadu signalizačních molekul (např. prozánětlivé interleukiny IL6 a IL8) a složky mimobuněčné hmoty (např. kolagen typu I., hyaluronan, fibronektin). Narušení rovnováhy a načasování syntézy a odbourávání těchto molekul může vést k abnormálnímu hojení. Pro rány je typické současné působení několika stresových faktorů např. snížený přísun živin, zánět, bakteriální kontaminace, oxidační stres atd. Dosavadní *in vitro* výzkumy dermálních fibroblastů v procesu hojení simulovaly a popisovaly vliv vždy pouze jednoho z těchto faktorů. Tato dizertační práce se jako první zabývá chováním dermálních fibroblastů v prostředí dvou současně působících klíčových stresových faktorů rány v 2D *in vitro* kultuře a v 3D kolagenových hydrogelech, které byly připravovány v naší laboratoři.

V první části této práce je popsáno chování dermálních fibroblastů v podmínkách rány tvořené dvěma stresovými faktory – nízkým množstvím živin (2% FBS) a prozánětlivou složkou ve formě bakteriálního lipopolysacharidu (LPS). Studované parametry chování buněk zahrnují metabolickou aktivitu, proliferaci, morfologii, migraci, produkci IL6 a IL8, syntézu kolagenu typu I a produkci matrix metalloproteináz (MMPs) 2 a 9. Byla prokázána zvýšená metabolická aktivita v prostředí nízkých živin a LPS, zatímco proliferace v obou podmínkách byla v čase konstantní. Dále byla prokázána zvýšená migrace buněk v přítomnosti LPS. Produkce prozánětlivých IL6 a IL8 bylo potencováno LPS. Prostředí nízkých živin zmírňovalo změnu fibroblastů v myofibroblasty a tento efekt byl přítomností LPS umocněn. Remodelační schopnost buněk projevující se zvýšením produkce MMP2 byla ovlivněna v prostředí nízkých živin. Produkce kolagenu nebyla ovlivněna ani jedním stresovým faktorem.

V druhé části této práce je model rozšířen o přítomnost rozpustných faktorů produkovaných bakteriemi běžně se vyskytujících v ranách (*Staphylococcus aureus* a *Pseudomonas aeruginosa*). Změny chování dermálních fibroblastů jsou studovány 1) v jednodruhových podmínkách (v prostředí jednoho bakteriálního druhu) a 2) ve třech tzv. polybakteriálních podmínkách (působení obou bakteriálních druhů současně), které se liší způsobem přípravy. Studované parametry buněk zahrnují proliferaci, morfologii, migraci, produkci IL6 a IL8 a syntézu kolagenu typu I. Proliferace buněk byla snížená rozpustnými

faktory z *P. aeruginosa* a směsí rozpustných faktorů obou použitých bakteriálních druhů. Morfologie byla výrazně narušena rozpustnými faktory z *P. aeruginosa* a *S. aureus* kultivovanými společně. Pouze směs rozpustných faktorů potlačila migraci buněk. Dále byl prokázán prozánětlivý účinek *P. aeruginosa* na dermální fibroblasty projevující se zvýšenou produkcí IL6 a IL8. Syntéza kolagenu ovlivněna rozpustnými faktory nebyla. Rozpustné faktory z *S. aureus* neměly na fibroblasty žádný vliv.

Třetí část této dizertační práce porovnává chování dermálních fibroblastů v 2D a 3D kultuře. Obdobně jako v první části je i v 3D kultuře studován vliv nízkých živin a přítomnosti LPS na chování buněk. Studované parametry zahrnují schopnost kontrakce kolagenového hydrogelu, metabolickou aktivitu, proliferaci a změny v morfologii. Typ kultivace metabolickou aktivitu neovlivňoval. Metabolická aktivita v čase vzrůstala v 2D i 3D kultuře. Podmínky rány – nízké živiny a přítomnost LPS – na metabolickou aktivitu buněk v 2D a 3D kultuře vliv také neměly. Zatímco proliferace buněk v 2D kultuře mírně vzrůstala, v 3D kultuře buňky neproliferovaly. V podmínkách rány byla proliferace buněk v 2D i 3D kultuře konstantní. Dále byla prokázána narušená schopnost kontrakce v prostředí nízkých živin a LPS. Morfologie buněk se v 2D a 3D kultuře lišila. V 2D kultuře byly buňky zploštělé a vřeténkovité, v 3D kultuře měly buňky tvar hvězdicovitý.

V poslední části předkládané práce je popsána optimalizace metod pro stanovení absolutního počtu buněk v 2D a 3D kulturách. Metody pro stanovení absolutního počtu buněk se dosud nepoužívá a jejich popis tak tvoří významnou část této práce. Metoda pro stanovení absolutního počtu buněk v 2D kultuře je zde použita pro stanovení buněčné proliferace v čase a pro vztažení dat získaných jinými metodami na počet buněk v daném čase.

Tato dizertační práce objasňuje chování dermálních fibroblastů v podmínkách rány v 2D a 3D *in vitro* kulturách a optimalizuje metody pro stanovení absolutního počtu buněk. Největšími přínosy této práce shledáváme 1) ve vytvoření dvoufaktorového *in vitro* modelu rány a rozsáhlém studiu chování dermálních fibroblastů v tomto prostředí a 2) v možnosti využití unikátních metod pro stanovení absolutního počtu buněk v dalším výzkumu nejen dermálních fibroblastů.

ABSTRACT

Dermal fibroblasts participate actively in the regulation of wound healing process. They migrate and proliferate during the proliferative phase into the wound site and respond to signals from damaged tissue by secretion of a various pro-inflammatory molecules (e.g. interleukins IL6 and IL8) and extracellular matrix components (e.g. collagen type I, hyaluronan, fibronectin). The disruption of the balance and timing of synthesis and degradation of these molecules can lead to the transition of normal to abnormal non-healing process. Several stress factors act simultaneously in this type of wounds – impaired nutrition supply, inflammation, bacterial contamination, oxidative stress etc. However, the latest *in vitro* research of dermal fibroblasts in wound healing apply most often only one stress factor. This thesis deals with the response of dermal fibroblasts to the wound conditions. For the first time, a comprehensive study of the functional response of the cells to the two key wound stress factors is described in 2D culture and 3D self-made collagen hydrogel culture.

In the first part of the thesis response of dermal fibroblasts to the wound conditions applying two stress factors - low nutrition (2% FBS) and inflammation simulated by bacterial lipopolysaccharide (LPS) - is characterized. The functional response of the cells includes metabolic activity, proliferation, changes in morphology, migration, production of IL6 and IL8, synthesis of collagen type I and production of matrix metalloproteinases (MMPs) 2 and 9. It was shown that the low nutrition and the LPS promote metabolic activity of the cells; however, this promotion was not followed by increased proliferation. Further, the LPS potentiated the migration of the cells. The pro-inflammatory phenotype of the cells evidenced by increased production of IL6 and IL8 was potentiated by LPS. Moreover, the change of fibroblasts to myofibroblasts decreased by the low nutrition and even more by the LPS. The remodeling capability of the cells was influenced only by low nutrition when documented by increased MMP2 and unchanged MMP9 activities. Finally, the production of collagen type I was not affected by neither factors.

In the second part the model of wound contamination is improved by soluble factors secreted by bacterial species present in wounds. The responses of dermal fibroblasts to soluble factors from *Staphylococcus aureus* and *Pseudomonas aeruginosa* are characterized. Further, the effects of the three types of conditioned media originated in

different steps of *S. aureus* and *P. aeruginosa* media preparation (polybacterial conditions) on dermal fibroblasts are characterized. The functional response of the cells includes proliferation, changes in morphology, migration, production of IL6 and IL8 and synthesis of collagen type I. Proliferation of the cells was suppressed by conditioned medium from *P. aeruginosa* and polybacterial mixture of the both bacterial species. The cell morphology was affected by together cultivated polybacterial conditions. Further, only the polybacterial mixture of the both bacterial species suppressed the migration of the cells. The pro-inflammatory phenotype of the cells was potentiated only by *P. aeruginosa* conditioned medium. The production of collagen type I was not affected by neither factors. Finally, soluble factors from *S. aureus* did not affect the functions of dermal fibroblasts at all.

In the third part of the thesis the responses of dermal fibroblasts cultivated in 3D culture are characterized and compared with their responses in 2D culture. Moreover, the functional response of the cells in wound conditions applying the two stress factors in 3D culture was examined. The functional responses of the cells examined in these parts include contraction ability, metabolic activity, proliferation and changes in morphology. The metabolic activity was independent on the type of culture and was increasing in time. The proliferation of the cells was increasing in time in 2D culture and constant in 3D culture. The wound conditions did not affect the metabolic activity and the cell proliferation in both types of culture. The contraction ability of the cells was disrupted by both low nutrition alone and the low nutrition in combination with LPS. The spindle-shaped morphology of the cells was flattened in 2D culture, while in 3D culture the shape was more elongated and stellate.

In the last part the methods for the absolute cell number determination in both 2D and 3D cultures as the quantitative approach how to analyze cell proliferation is developed since suitable method for absolute cell number determination in 2D and 3D cultures has not been optimized. In this thesis, the method for absolute cell number determination in 2D was used for monitoring of cell proliferation in time and for IL6, IL8, MMPs and collagen type I relation to cell number at each time point.

Taken together, results of this thesis helped to describe behavior of dermal fibroblasts in 2D and 3D *in vitro* model under wound conditions. Our results can serve as a valuable tool in the early stages of therapeutics development.

TABLE OF CONTENTS

1. INTRODUCTION

1.1 The process of wound healing

1.1.1 Physiological wound healing

Damage of any tissue initiates a cascade of events leading to repair of the wound. The acute wound healing is a process of at least four phases overlapping in time – hemostasis, inflammation, proliferation and remodeling. Each phase is characterized by presence of certain active cell types (**Figure 1**). Immediately after tissue injury platelets aggregate at the wound site and form a blood clot which reestablishes hemostasis. In addition, platelets secrete a spectrum of growth factors, e.g. platelet-derived growth factor (PDGF), transforming growth factor β (TGFβ) or fibroblast growth factors (FGFs) that together with dead cells and debris attract other cells from local tissue and blood to the wound site (Stadelmann et al., 1998; Singer and Clark, 1999).

Neutrophils represent cell type, which initiate the inflammatory phase of the healing process. They infiltrate the trauma through damaged capillaries or by diapedesis, the passage of the cells through the vessel wall. The main functions of activated neutrophils are 1) to clear the wounded area of bacteria and tissue debris via phagocytosis, 2) to produce reactive oxygen species (ROS), 3) to secrete signaling molecules (e.g. vascular endothelial growth factor (VEGF) and matrix metalloproteinase 9 (MMP9)) activating angiogenesis, 4) to release neutrophil protein granules and chromatin make up extracellular fibers, so called neutrophil extracellular traps that kill bacteria and 5) to release tissue-repairing cytokines TGFβ and interleukin (IL)10 during neutrophil apoptosis (Singer and Clark, 1999; Brinkmann et al., 2004; Wang, 2018).

Together with neutrophils the mast cells inflow the wound site. Mast cells are involved in all phases of wound healing. They enhance inflammation through secretion of pro-inflammatory mediators that induce vascular permeability and recruit neutrophils. The proliferative phase is supported by secreted mediators enhancing keratinocyte and endothelial cell proliferation resulting in re-epithelization and angiogenesis. The released mediators affect the collagen production by fibroblasts and collagen maturation and remodeling (Wulff and Wilgus, 2013).

The short-lived neutrophils are together with microbes and tissue debris phagocytized by macrophages that differentiate from circulating monocytes. Pro-inflammatory M1 macrophages clean the wound from bacteria, foreign particles and dead cells. When acute wounds start to heal the M1 macrophages transform to M2 macrophages with anti-inflammatory effects. The M2 macrophages enhance the proliferation and migration of fibroblasts, endothelial cells and keratinocytes to promote repair of dermis, re-epithelization and angiogenesis (Krzyszczyk et al., 2018).

The subsequent proliferative phase consists of 1) the migration of fibroblasts from various sources resulting in the formation of granulation tissue, 2) the restoration of the skin surface by keratinocyte migration and proliferation and 3) blood supply re-establishment by angiogenesis.

The proliferative phase of wound healing starts with fibroblast migration into the wound initiated mainly by PDGF. PDGF promotes fibroblast chemotaxis, proliferation and production of extracellular matrix (ECM) components e.g. fibronectin, collagen and hyaluronic acid resulting in formation of granulation tissue (Li et al., 2004). Besides maintaining the structural integrity of the tissue fibroblasts respond to signals from damaged tissue, to e.g. cytokines, chemokines, growth factors, ECM components and lack of oxygen. Moreover, fibroblasts produce a number of these molecules as a response to the changing wound environment and participate on the regulation of the level of inflammation (Tandara and Mustoe, 2004; Behm et al., 2012; Vistejnova et al., 2014). Activated fibroblasts secrete IL6, IL8, cyclooxygenase-2 and hyaluronan which further regulate the immune cells (Smith et al., 1997).

The restoration of the epidermis starts at the early beginning of the wound healing. The keratinocytes cover the granulation tissue as they lose their adhesion to each other and to the basal lamina and migrate from the margins over the provisional matrix. The loss of adhesion and the migration is regulated by several mediators such as cytokines (e.g. IL1, IL6), growth factors (e.g. epidermal growth factor (EGF), heparin-binding EGF-like growth factor (HB-EGF), TGFα and FGFs), matrix metalloproteinases (e.g. MMP1, MMP2 and MMP3). When the dermis has been restored activated keratinocytes revert to their normal phenotype. TGFβ is the main regulator in the revert (Pastar et al., 2014).

Angiogenesis is mediated by pro-angiogenic factors, mostly VEGF-A, FGF2, PDGF and TGFβ. Endothelial cells invade the wound, form new blood vessels and re-establish the blood supply. A portion of the newly formed vessels are covered by pericytes. Pericytes are cells which stabilize and protect the capillaries (DiPietro, 2016).

In the later stages of proliferative phase, multiple skin cells such as keratinocytes, fibroblasts, endothelial cells and immune cells produce MMPs in response to a range of signals including cytokines (e.g. EGF, HGF, FGF, VEGF, PDGF, tumor necrosis factor α (TNFα), keratinocyte growth factor (KGF), TGFβ, interleukins and interferons), hormones, intercellular contact or contact with ECM (Caley et al., 2015). In skin, MMPs regulate cell-cell and cell-matrix interactions through modulating and releasing cytokines, growth factors and biologically active fragments of ECM. MMPs modify cell surface receptors and proteins of cell junctions and regulate multiple cellular processes e.g. cell death and inflammation (Krishnaswamy et al., 2017).

The remodeling phase occurs during months to years in the form of scar tissue. The main phenomenon of this phase is reorganization of ECM. The provisional matrix is replaced by permanent collagen-rich ECM produced by fibroblasts. Moreover, some of the fibroblasts change their phenotype into the contractile myofibroblasts which contain α smooth muscle actin (α-SMA). The phenotype change is dependent primarily on PDGF and TGFβ (Greaves et al., 2013). While collagen type III is synthesized in the early stages of wound healing, collagen type I is mainly synthesized in the remodeling phase and maturates through a number of cross-links between the fibers. Moreover, the collagen in scar is made from densely packed collagen compared to the reticular pattern in unwounded skin. Also capillaries are reduces after wound closure. Interestingly, the skin appendages are usually not regenerated after wounding which results in altered skin functions (Sorg et al., 2017).

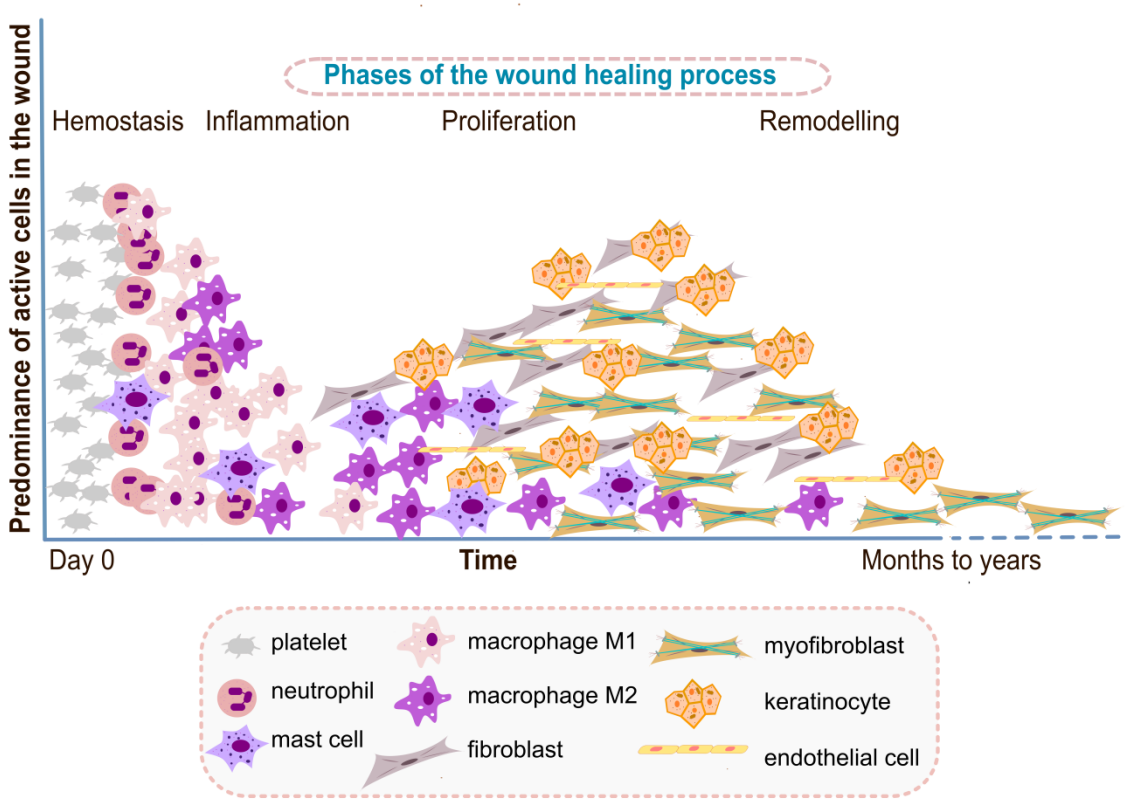

Figure 1 Predominance of active cell types in the wound**.** Immediately after injury, hemostasis is characterized by fast onset of platelets followed by neutrophils, macrophages and mast cells during inflammation. Predominant populations of fibroblasts, keratinocytes, endothelial cells and myofibroblasts are found during proliferation and remodeling lasting up to years.

1.1.2 Disorders in wound healing

The aim of the inflammatory phase is to clear wound from bacteria and debris. Neutrophils and macrophages play the major role in this process. Non-healing wounds show long-term inflammation and impaired cellular response. One of the characteristics of non-healing wounds is excessive neutrophil infiltration. Higher number of neutrophils leads to over-production of ROS resulting in direct ECM and membrane damage, delayed keratinocyte migration and re-epithelization and cell senescence. Moreover, neutrophils produce elastase and MMPs which degrade growth factors and components of the ECM. Thus, although the production of growth factors is increased in non-healing wounds, their bioavailability is decreased affecting their pro-healing benefits (Zhao et al., 2016; Makrantonaki et al., 2017).

Macrophages have a reduced ability to phagocytize dead neutrophils, which accumulate and create an augmented inflammatory environment. Since the transition from M1 macrophages to M2 macrophages is accelerated by neutrophil clearance, M1 macrophages accumulate in the non-healing wounds (Krzyszczyk et al., 2018). Activated macrophages produce nitric oxide which may generate toxic radicals resulting in tissue damage and augmented inflammation (Makrantonaki et al., 2017). Both neutrophils and macrophages produce elevated level of pro-inflammatory cytokines, e.g. IL1β and TNFα, which increase the level of MMPs and simultaneously decrease the level of tissue inhibitors of MMPs (TIMPs). The disturbed balance results in impaired cell functions, e.g. migration, proliferation, collagen production and ECM degradation which prevent tissue renewal in the proliferative phase of wound healing (Zhao et al., 2016).

Also the microbial flora of the non-healing wounds is abnormal. There is excessive numbers of pathogens and other commensal bacterial species. Besides direct damage pathogens attract leukocytes producing cytokines, proteases and ROS. The pathogens often form a biofilm on wounds to provide an optimal environment for bacteria to escape host immune response and antibiotic action resulting in chronic infection (Zhao et al., 2016; Makrantonaki et al., 2017). There is evidence that up to 90% of chronic wounds are covered by biofilm compared with 6% of acute wounds (Wolcott et al., 2016).

In proliferative phase all processes are affected during abnormal wounds healing. While keratinocytes resides only the basal layer of the skin in acute wounds, they reside even the suprabasal layer creating hyperproliferative epidermis in non-healing wounds with impaired migratory capacity (Pastar et al., 2014; Martin and Nunan, 2015). Necrotic debris often covers the non-healing wounds creating a pleasant environment for bacteria amplifying the influx of neutrophils and macrophages (Eming et al., 2007; Landén et al., 2016).

Most fibroblasts are prematurely senescent. They exhibit impaired proliferative and migratory capacity and abnormal morphology. Senescent fibroblasts are unresponsiveness to growth factors (Wall et al., 2008; Martin and Nunan, 2015). Moreover, they exhibit different secreted protein profile, e.g. increased level of pro-inflammatory cytokines and collagen type III in contrast to decreased level of collagen

type I and fibronectin (Vitellaro-Zuccarello et al., 1992; Kumar et al., 1993; Jin et al., 2001). There is higher myofibroblast differentiation rate in fibroblasts isolated from non-healing wounds (Schwarz et al., 2013).

Abnormal angiogenesis lead to impaired nutrient delivery and hypoxia (Li et al., 2017). It takes place depending on the co-occurring associated diseases. In diabetics, high glucose inhibits the normal angiogenesis. The formation of new blood vessels is poor with decreased enter of inflammatory cells and their growth factors. VEGF, essential growth factor for angiogenesis, is deficient in diabetic wounds. In contrast, VEGF is elevated in the circulation of venous stasis ulcer patients. The VEGF increase is caused by hypoxia which further results in the formation of pericapillary fibrin cuffs, compromised transcutaneous oxygen throughput and deteriorated vascular permeability. In addition, increased level of proteases and decreased level of their inhibitors are present (Kumar et al., 2015).

1.2 Stress factors responsible for disorders in wound healing

Despite the different causes of the transition of acute wounds to a non-healing state, abnormal wounds have a lot in common. However, the balance and timing are crucial, i.e. the imbalance in pro-inflammatory and anti-inflammatory molecules synthesis, collagen synthesis and degradation and correct timing of cell enter and activity. Moreover, the coexistence of bacterial colonization, local hypoxia and aging contribute to the abnormal wound healing.

Non-healing wounds are colonized by diverse populations of bacteria (Wolcott et al., 2016). The effect of bacterial species of non-healing wounds is often synergetic resulting in previously non-virulent bacterial species to become virulent (Dow et al., 1999). The most prevalent bacteria in wounds are *Staphylococcus aureus* (23.3%) and *Pseudomonas aeruginosa* (14.8%). *Staphylococcus aureus* was found often in patients with chronic wounds (48.8%) compared with patients with acute wounds (9.5%) (Wong et al., 2015). The lack of oxygen gives an opportunity for anaerobic bacteria (Wolcott et al., 2016). Bacteria on the wound bed proliferate, form micro-colonies and secrete substances for biofilm formation. Biofilms are organized microbes associated with exopolymers (proteins, polysaccharides and nucleic acids). Exact composition of biofilm may vary depending on bacterial species and other conditions of the chronic wound environment. Biofilms help attachment of bacteria and maintain their close contact. A key process in the formation of biofilms is quorum sensing (Omar et al., 2017). Biofilms are resistant to antimicrobial treatment. The exopolymer protects wound biofilm from the inflammatory process – it blocks complement activation, suppress the proliferation of lymphocytes and compromise detection of opsonins on bacterial cell walls by phagocytes (Wilson, 2001; Donlan and Costerton, 2002; Malic et al., 2011). Besides biofilms, bacteria attract leukocytes, which results in amplification of cytokine, protease and ROS production promoting the inflammatory environment (Schreml et al., 2010). Bacteria derived proteases and ROS degrade ECM and growth factors, which disrupt cell migration and wound closure (Demidova-Rice et al., 2012). Moreover, wound bacteria often produce toxins causing collagen degradation, stress and malnutrition (Rahim et al., 2017).

Tissue injuries become often hypoxic mainly due to the disruption of vasculature (arteriosclerosis, angiopathy, venous hypertension) and increased O_2 consumption by cells within the injured area and the adjacent tissue (Schreml et al., 2010; Lokmic et al., 2012). Although the limitation of oxygen in wounds has many reasons, the consequence is hypoxic wound environment characterized by insufficient nutrition and oxygen delivery to the wounded tissue (Li et al., 2017). Non-healing wounds require increased level of oxygen due to high energy demand of energy-consuming processes such as cell proliferation, migration, protein (e.g. collagen) synthesis, and bacterial defense, increased production of ROS by phagocytes (respiratory burst) and signaling based on redox reactions (Schreml et al., 2010; Castilla et al., 2012). On the molecular level, initial implication of hypoxia is the impairment of mitochondrial oxidative phosphorylation resulting in reduced ATP production which leads to a loss of transmembrane potential following cell swelling. Calcium ions accumulation in the cells activates pathways resulting in cell membrane disruption and promotion of inflammatory cascades (Schreml et al., 2010). The released pro-inflammatory cytokines e.g. IL1 and TNFα attract and activate neutrophils and macrophages. Moreover, endothelial cells express prominent amount of intracellular adhesive molecule 1 (ICAM1) and vascular cell adhesion molecule 1 (VCAM1) and their ligands leukocyte function-associated antigen 1 and very late antigen 1 on neutrophils and macrophages, which further facilitate their extravasation and invasion into the wound site synthetizing pro-inflammatory cytokines e.g. IL1α, IL1β, IL6 and TNFα in an autocrine manner (Peschen et al., 1999). The balance between ROS and antioxidant production is disrupted. The synthesis of nitric oxide, an effective antioxidant, is dependent on oxygen (Soneja et al., 2005). Therefore it decreases in a hypoxic environment. Nitric oxide directly detoxifies ROS to form peroxynitrite, which is further used for oxidative killing of bacteria (Kurahashi and Fujii, 2015). In addition, nitric oxide can make a switch between pro- and anti-inflammatory actions through the transcriptional factor NF-κB (Connelly et al., 2001). Excessive ROS production causes oxidative damage and stimulates transduction pathways leading to increased expression of serine proteases, MMPs and pro-inflammatory cytokines (Schreml et al., 2010). Many studies show that even slightly reduced oxygen level significantly increases risk of infection (Knighton et al., 1990; Hopf et al., 1997).

Delayed wound healing mostly occurs in elderly persons, possibly due to cellular senescence. Nevertheless, cells isolated from chronic wounds show senescent phenotype regardless the age of the patient (Mendez et al., 1998; Vande Berg et al., 1998). Factors that can cause a cellular senescence include oxidative stress and strong proteolytic milieu caused by bacterial infection and toxins. Aging is associated with cellular inability to proliferate, resistance to apoptosis, altered gene expression and decreased response to growth factors (Mendez et al., 1998; Telgenhoff and Shroot, 2005; Glass et al., 2013; Wang and Dreesen, 2018). The premature neutrophil influx occurs with decreased respiratory burst activity, reduced phagocytic ability and impaired chemotaxis (Ashcroft et al., 2002). Moreover, the neutrophils produce increased level of proteases, which are known to degrade ECM components, e.g. collagen and fibronectin. Further characteristics of aged skin are impaired macrophage function, decreased proliferation of keratinocytes and dermal atrophy. Wound closure, re-epithelization and granulation tissue fill is delayed or decreased (Kim et al., 2015). Senescent fibroblasts show reduced proliferation (Agren et al., 1999). They produce increased level of MMPs and decreased level of their inhibitors. Aged keratinocytes are more susceptible to hypoxia than adult young keratinocytes. While aged keratinocytes have depressed migratory activity when exposed to hypoxia, young keratinocytes showed increased migratory activity due to the different activation of MMPs in the young and the old (Xia et al., 2001). To establish capillary network endothelial cells must receive VEGF signal. Aged mice macrophages produce less VEGF compared with young mice macrophages (Swift et al., 1999). Therefore aged macrophages may contribute to poor angiogenesis. On the other hand, senescent fibroblasts and endothelial cells secrete PDGF-AA which cause differentiation of fibroblasts into myofibroblast phenotype and thus helps wound to heal more quickly (Demaria et al., 2014).

1.3 Dermal fibroblasts in wound healing

1.3.1 Origin and physiological functions of dermal fibroblasts

Dermal fibroblasts are mesenchymal cells of dermis that provide maintenance and support for skin. They build and maintain a scaffold, e. g. extracellular matrix (ECM), on which other cells migrate and perform their functions. They make up a diverse population of cells with distinct function in skin, other organs and in the wound healing process. Dermal fibroblasts are dynamic cells occurring in functionally and morphologically heterogeneous subpopulations, which are involved in all phases of wound healing (Nolte et al., 2008).

In healthy tissue, normal dermal fibroblasts can be found in at least two subpopulations – papillary fibroblasts, which reside in the upper dermis, and reticular fibroblasts, which reside in the deeper dermis (Sorrell and Caplan, 2004). These subpopulations differ in morphology, proliferation rate, response to growth factors, secretion of ECM molecules e.g. collagen, decorin, fibromodulin; organization of ECM and production of various molecules e.g. cytokines, growth factors, MMPs, TIMPs, podoplanin and transglutaminase 2 (Sorrell and Caplan, 2004; Wang et al., 2004; Honardoust et al., 2012; Janson et al., 2012). While the papillary fibroblasts may be primarily involved in immune responses and re-epithelization, the main functions of reticular fibroblasts include cytoskeletal organization and cell motility (Mine et al., 2008; Janson et al., 2012). In contrast, another study showed that reticular fibroblasts promote vascularization and re-epithelization when compared to papillary fibroblasts (Wang et al., 2004). Interestingly, it has been shown that reticular fibroblasts mainly contribute to wound healing of human skin wounds (Woodley, 2017).

There is a special type of fibroblasts typically occurring in later phases of wound healing. It has been shown that fibroblasts under mechanical tension and action of PDGF differentiate into protomyofibroblasts. When subjected to TGFβ1 they transform to myofibroblasts containing α-SMA. The contractile myofibroblasts are involved in the production of ECM and maturation of granulation tissue (Gabbiani, 2003; Hinz et al., 2007). The functions of dermal fibroblasts on molecular level in inflammatory and proliferative phase of wound healing are discussed in section 1.1.2

1.3.2 Disorders in functions of dermal fibroblasts

The heterogeneity of fibroblasts is important in wound healing. While the initial phases of wound healing are mediated by the lower lineage of fibroblasts expressing α-SMA, the later phases of wound healing are mediated by the upper dermis fibroblasts, which are recruited during re-epithelization and are involved in hair follicle formation (Driskell et al., 2013).

There is evidence that functions of fibroblasts in wound healing are disordered mainly by negative impact of associated diseases, primarily the chronic diseases e.g. diabetes mellitus or peripheral venous diseases.

Non-healing wounds are prone for bacterial infection as the wounds remain open for a prolonged period of time. The wound bed provides a surface and nutrients for bacterial growth, while poor blood supply and hypoxia discourage host defense (Kirker et al., 2012). Bacteria harm healing is both direct (production of toxins, metabolic wastes, alteration in pH and oxygen levels) and indirect (activation of host neutrophils) manner (Thomson, 2000). Bacteria colonizing chronic wounds induce apoptosis of keratinocytes and colonize dermal tissue. It often exists as a biofilm, surface attached polymicrobial communities forming complex structures. When compared to planktonic bacteria, biofilms are more resistant to antibiotics (Kirker et al., 2012). The composition of the chronic wound microbiome is not wound type-dependent and there is no significant difference in the abundance of these bacterial species across wound types. The most prevalent species include *Staphylococcus*, *Pseudomonas*, *Stenotrophomonas*, *Finegoldia, Enterococcus* and *Corynebacterium* (Wolcott et al., 2016). *S. aureus* and *P. aeruginosa* are the most studied bacterial species relating to dermal fibroblasts. Both planktonic- and biofilm-conditioned medium of methicillin resistant *S. aureus* (MRSA) significantly decreased the viability and migration ability of dermal fibroblasts after 24 hours. The proliferation was significantly decreased and simultaneously the apoptosis was significantly increased after 48 hours. The production of pro-inflammatory cytokines (IL6, IL8, TNFα), growth factors (TGFβ1, HB-EGF, VEGF) and MMP1 and MMP3 depended on the presence of either planktonic or biofilm MRSA suggesting that all phases of wound healing could be disturbed by the presence of the bacteria. Moreover, the soluble factors from planktonic MRSA generally induced a stronger response of dermal fibroblasts (Kirker et al., 2012). Lipoteichoic acid and protein-A

from *S. aureus* induced a release of hepatocyte growth factor (HGF) from dermal fibroblasts, a proliferation factor of keratinocytes, while LPS and porins from *P. aeruginosa* did not (Baroni et al., 1998). The co-infection by *S. aureus* and *P. aeruginosa* resulted in delayed wound healing compared to single species infection *in vivo* (Hotterbeekx et al., 2017); however, the impact of the simultaneously acting of the both bacterial species on cells has not been studied *in vitro*.

The high consumption of oxygen may lead to local hypoxia, even in well-oxygenated wounds. During the inflammatory phase, many cells including fibroblasts produce ROS (Hopf and Rollins, 2007). Extended exposure to ROS leads to inactivation of antioxidants produced by fibroblasts, such as superoxide dismutase, catalase and glutathione peroxidase (Richards et al., 2011). ROS promote fibroblast proliferation, TGFβ1 signaling resulting in increased migration, collagen and fibronectin production and bFGF expression by fibroblasts. Moreover, ROS promote angiogenesis via stimulation of VEGF synthesis by fibroblasts, macrophages and keratinocytes (Kunkemoeller and Kyriakides, 2017). Acute hypoxia may stimulate dermal fibroblast proliferation, collagen synthesis and expression of TGFβ1; whereas chronic hypoxia decreases these processes (Siddiqui et al., 1996). Hypoxic environment in combination with an insufficient nutriment supply leads to wound ischemia and decreased collagen synthesis by dermal fibroblasts. In turn, diminished collagen synthesis prevents the formation of net of ECM requiring vessels (Siddiqui et al., 1996; Sen, 2009). A decrease in the production of collagen leads to a reduction in the tensile strength of healing wounds (Jonsson et al., 1991). Moreover, in the remodeling phase, the replacement of collagen type III by collagen type I is strictly oxygen dependent (Schreml et al., 2010).

Most fibroblasts present in chronic wounds prove to be prematurely senescent (Wall et al., 2008). Senescent fibroblasts have an abnormal morphology and decelerated migratory and proliferative capacities and increased cell death (Loots et al., 1999; Tandara and Mustoe, 2004; Wall et al., 2008). They show an increased generation of MMPs, decreased level of TIMPs (Tandara and Mustoe, 2004), exhibit different profiles of secreted proteins, which results in increased level of pro-inflammatory cytokines, collagen type III and decreased level of collagen type I (Vitellaro-Zuccarello et al., 1992; Kumar et al., 1993; Jin et al., 2001). Fibroblasts, which originate in chronic

wounds, are unresponsive to growth factors. The amounts of growth factors, their receptors and downstream molecules in the signaling pathways are diminished (Cha et al., 2008). Although there is an increased level of growth factors in chronic wounds, they are fragmented by MMPs, which are increased in chronic wounds. Moreover, the decreased levels of TIMPs contribute to the chronicity (Bullen et al., 1995).

Long-term hyperglycemia, one of the manifestations of diabetic patients, may lead to the production of advanced glycation end products (AGEs). The accumulation of glycated collagen in the skin functions differently compared with normal collagen. AGEs can inhibit fibroblast proliferation, increase the collagen production, decrease the production of hyaluronic acid, disturb the balance between the accumulation and remodeling of ECM by MMPs and induce cell apoptosis. Moreover, AGEs contribute to abnormal expression of cytokines, growth factors and MMPs (Arya, 2014; Singh et al., 2014).

While in the dermis of unwounded tissue myofibroblasts represent only 1% of the fibroblast population, in fibroblasts derived from wounds 30-40% are myofibroblasts (Germain et al., 1994). Similarly, Schwarz et al. observed nearly 50% more myofibroblasts in the culture of fibroblast isolated from chronic wounds compared to the fibroblasts originated in acute wounds (Schwarz et al., 2013)

1.4 *In vitro* models of dermal fibroblasts in wound conditions

1.4.1 2 dimensional (2D) cultures of dermal fibroblasts

For *in vitro* studies cell lines or primary cultures are commonly used. The advantages of the cell lines are that the cells are identically the same features that have evaded normal cellular senescence enabling cultivation for a long time. On the other hand, the cell lines are transformed to become immortal. Genetically manipulated cell lines may alter their phenotype, native functions and their natural responsiveness to stimuli. Moreover, serial passage of cell lines can cause genotypic and phenotypic variation which can also cause heterogeneity in cultures at a single point in time. Therefore, cell lines may not adequately represent primary cells and may provide different results (Kaur and Dufour, 2012).

Primary cells are derived from tissue removed directly from a donor. Therefore, primary cells represent more relevant cell culture compared with cell lines. The primary human dermal fibroblasts are isolated from the skin specimens of healthy persons; however, there are some disadvantages to using primary cultures. Unlike cell lines, primary cells have a limited lifetime. The gender, age and tissue origin of the donor influence the robustness of the cell culture. Moreover, a population of primary cells will always be more heterogeneous than a culture of cell lines, making results of experiments more variable (Carter and Shieh, 2015).

Dermal fibroblasts are cultivated in widely used Dulbcco´s Modified Eagle Medium (DMEM) supplemented with 10% fetal bovine serum (FBS), penicillin (100 U/ml)/streptomycin (0.1 mg/ml), 0.5% L-glutamin and 1.0% non-essential amino acids in CO_2 incubator at 37°C, 5% CO_2 and 95% humidity up to 80% confluence and then passaged. The medium change is performed 3 times a week. 3^{th} – 6^{th} passage is used for experiments.

For wound environment modeling the particular stress factors simulating wound environment are added to culture media. One of such stress molecules with inflammatory stimuli is bacterial lipopolysaccharide (LPS). Fibroblasts treatment with LPS caused decrease in viability and increased production of chemokines monocyte chemoattractant protein 1 (MCP1), macrophage inflammatory protein 2 (MIP2),

cytokine-induced neutrophil chemoattractant (CINC) and chemokine (C-C motif) ligand 5 (CCL5, RANTES) (Xia et al., 1997; Basso et al., 2015).

Although there is an insufficient oxygen and nutrition income into a wound site (Schreml et al., 2010; Lokmic et al., 2012; Li et al., 2017), it is possible to cultivate dermal fibroblasts in hypoxic conditions (hypoxic box) or with the lack of nutrition (decreased level of serum in the culture medium) (Kanafi et al., 2013). Breit et al. has shown that dermal fibroblast culture in hypoxic conditions (0.5% O_2) have decreased proliferation rate and migration ability and extensively increased production of VEGF-A, indicating the important role of fibroblasts as endothelial cell attractant supporting neo-angiogenesis in the early phases of wound healing. Myofibroblast differentiation was also induced by hypoxia (Breit et al., 2011). Decreased proliferation and migration of dermal fibroblasts under hypoxic conditions (0.5% O_2) was also observed by Oberringer et al. (Oberringer et al., 2007). Dermal fibroblasts in lack of nutrition conditions have not been studied since now. Mesenchymal stem cells (MSCs) cultured under lack of nutrition (2% FBS) maintained their normal growth and morphology just for the first 2 passages, but they did not grow further. Upon comparison to normal MSC growth conditions, the number of migrated cells cultured in 5% FBS-supplemented media was decreased (Kanafi et al., 2013).

There is an evidence of bacteria in wound environment, primarily in chronic wounds (Bill et al., 2001; Bessa et al., 2015; Serra et al., 2015; Wong et al., 2015; Wolcott et al., 2016; Rahim et al., 2017). In *in vitro* wound bacteria experiments one bacterial species or combination of two bacterial species is usually used. The experiments with planktonic- or biofilm-conditioned culture medium of *S. aureus* on dermal fibroblasts were performed. While migratory ability, metabolic activity and cell death by apoptosis was the same in both planktonic- and biofilm-conditioned culture medium, production of cytokines, growth factors and proteases were affected differently. Planktonic-conditioned culture medium induced more IL6, IL8, VEGF, TGFβ1, HB-EGF, MMP1 and MMP3 secretion by dermal fibroblasts than biofilm-conditioned culture medium. On the contrary, biofilm-conditioned culture medium induced more TNFα and suppressed MMP3 (Kirker et al., 2012). In the *in vitro* study the co-presence of the bacterial species were more virulent than monoculture infection with either species. Moreover, the ability of *P. aeruginosa* and *S. aureus* to survive the

antibiotic treatment increased when the strains were grown together (DeLeon et al., 2014). Soluble factors originated in *S. aureus* induced secretion of different pro-inflammatory molecules by dermal fibroblasts than soluble factors originated in *P. aeruginosa* (Baroni et al., 1998).

Another possibility of wound environment modeling is the oxidative stress establishment. Oxidative stress is induced by chemical compounds e.g. hydrogen peroxide, or free radical generators e.g. 2,2-azobis(2-amidinopropane)dihydrochloride (AAPH) or 3-morholinosydnonimine hydrochloride (SIN-1) (Takabe, 2001; Tanigawa et al., 2014). Hydrogen peroxide (0.1 - 2 mM) induced apoptotic cell death in fibroblasts (Takahashi et al., 2002; Formichi et al., 2006; Tanigawa et al., 2014). AAPH lowered the metabolic activity and increased lipid peroxidation in dermal fibroblasts in dose dependent manner. Moreover, AAPH induced cell death by apoptosis (Giampieri et al., 2014). Both AAPH and SIN-1 induced peroxyl radicals and peroxylnitrite and decreased level of antioxidants (Takabe, 2001).

A special attention may be taken to hyperglycemia which is often present in diabetic wounds. High glucose culture medium is a way how hyperglycemia is commonly created (Kruse et al., 2016; Senthil et al., 2016). Dermal fibroblasts in normoglycemic (5.6 mM) and hyperglycemic (23, 26 and 50 mM) conditions were studied. The <26 mM glucose concentrations did not have any noticeable effect on metabolic activity of dermal fibroblasts after 5 days culture, while dermal fibroblasts did not survive in glucose concentrations >26 mM (Kruse et al., 2016). 15 mM glucose significantly decreased metabolic activity even after 3 days culture and 50 mM glucose even after 2 days culture. Moreover, the exposure of dermal fibroblasts to high glucose (30 mM) for 3 days accelerated G0/G1arrest and senescence (Senthil et al., 2016). Extensively increased proliferation of dermal fibroblasts in high glucose medium was concentration dependent. Moreover, the migratory ability of dermal fibroblasts was impaired even in the lowest tested glucose concentration (5.6 mM) (Kruse et al., 2016).

Except the models of wound environment which use the addition of stress factors to the culture medium, the commonly used model is based on the study of fibroblasts isolated directly from the wounds (Hehenberger et al., 1998; Wall et al., 2008; Schwarz et al., 2013). Dermal fibroblasts derived from chronic wounds displayed decreased adhesion, proliferation and ability to withstand oxidative stress resulting in

early onset of senescence compared with normal fibroblasts. Moreover, chronic wound fibroblasts expressed lower levels of chemokine genes and are not able to correctly express a stromal address code providing a requirement to guidance of infiltrating leukocytes to the site of injury (Hehenberger et al., 1998; Wall et al., 2008). The rate of myofibroblasts was higher in the fibroblasts isolated from chronic wounds compared to well healing wound fibroblasts (Schwarz et al., 2013). Late passage of dermal fibroblasts from chronic wounds displayed significantly greater senescence-associated β-galactosidase compared to patient-matched normal dermal fibroblasts (Wall et al., 2008).

The cultivation of dermal fibroblasts with wound exudate containing serum components and tissue-derived proteins from patients is another way of wound modeling *in vitro*. Although wound exudate is a very relevant source of real stress factors, the disadvantage of its use is low availability. Chronic wound exudate induced an increase in fibroblast proliferation and viability in the first 3 days followed by a strong decrease after 7 days of culture with dermal fibroblasts. Moreover, the exudate caused cytoskeletal changes and lack of myofibroblast differentiation (De Mattei et al., 2008). Exudate isolated from acute wounds stimulated fibroblast migration while exudate isolated from chronic wounds inhibited their activation and migration and induced the degradation of the collagen matrix (Manuela et al., 2017).

1.4.2 3 dimensional (3D) cultures of dermal fibroblasts

The 2D fibroblast culture overlooks many aspects, e.g. mechanical stimuli and cell-matrix interactions, important for normal skin physiology. When fibroblasts are cultivated on glass or plastic substrate the cellular responses such as cell adhesion, proliferation and migration are known to differ from that in native skin. The ECM establishes the environment providing mechanical support and a scaffold for fibroblasts and other cells in the skin. 3D culture models are a bridge between animal models and cellular monolayers. Therefore 3D cultures, where the cell environment takes into account the spatial organization of the cells, have been developed and provide a useful tool for functional and biomechanical analysis of cell-matrix interactions (Bott et al., 2010; Rolin et al., 2014; Smithmyer et al., 2014). Moreover, there is evidence that cells

cultured in 3D exhibit functional characteristics that are more similar to their *in vivo* behavior when compared to cell culture in 2D (Abbott, 2003).

Hydrogels are a valuable tool in study of wound healing *in vitro*. Hydrogels are crosslinked polymer networks often used for mimicking the native ECM. One of their main advantages is the possibility to study not only proteins of ECM but also mechanical properties, e.g. modulus of elasticity. Naturally-derived native ECM components, such as collagen, fibrin and hyaluoronic acid are often used for the culture of fibroblasts *in vitro* (Smithmyer et al., 2014). In these models differentiation, proliferation, migration, secretion of proteases, contraction and extracellular matrix remodeling have been examined (Helary et al., 2005; Bott et al., 2010; Rolin et al., 2014; Thievessen et al., 2015).

Despite that many advantages of 3D naturally-derived cultures, there are some disadvantages – prolonged cell culture formation, worse performance, batch-to-batch variability which may substantially reduce the reproducibility of experimental outcomes and lack of standardized methods for characterization of the cells (Bott et al., 2010; Kapałczyńska et al., 2018). While for estimation of cell proliferation and migration the commonly methods are available in 2D culture, it is hardly to estimate these parameters in 3D. Therefore it is necessary to develop analytical tools for 3D cell culture systems.

Collagen is a natural material which represents about 30% of all proteins in human body. Collagen type I is an important component of ECM in the skin, making it relevant material for construction of 3D environment for wound healing studies. Collagen is a critical determinant for cell shape and mechanical tension, which is known to regulate many cellular functions (Hynes, 2009). The synthesis of collagen is visualized in **Figure 2**. Collagen is a molecule consisting of three polypeptide α-chains. In endoplasmic reticulum α-chains are woven together to form a pro-collagen molecule. It contains repeating proline-hydroxyproline-glycine sequences allowing formation of fibrillary structure (O'Leary et al., 2011; Dong and Lv, 2016). The monomers of pro-collagen are transferred outside the cell by exocytosis in COP II vesicles. During or after the releasing process, terminal amino acid sequences are enzymatically removed from α-chains of the pro-collagen so that pro-collagen becomes tropo-collagen. The final collagen fibers are formed in the extracellular space by crosslinking (Kruger et al., 2013). Collagen type I hydrogels are commonly used for fibroblast culture making

natural viscoelastic environment for the cells. It is cytocompatible and present native sites for cell adhesion (Caliari and Burdick, 2016).

Collagen type I for hydrogel construction may originate in many organisms, e.g. bovine, porcine or equine (Garcia et al., 2007; Bedran et al., 2014; Böhm et al., 2017); however, the most frequently collagen used is isolated from rat tendons (Maione et al., 2015; Rossi et al., 2015; Babaei et al., 2016). There are two most common arrangements of the 3D models: 1) seeded cells on the top of collagenous layer (Helary et al., 2005; Rolin et al., 2014), or 2) cells encapsulated into the collagenous hydrogel (Grinnell et al., 2006; Garcia et al., 2007; Shamis et al., 2011; Babaei et al., 2016; Füller and Müller-Goymann, 2018). While there are benefits to collagenous layer studies, hydrogels with encapsulated cells more closely mimics the *in vivo* environment.

Fibroblasts alone or in co-culture with keratinocytes seeded on the top of the hydrogels, the so called human skin equivalents (HSE), are usually used for study of wound healing in 3D. The hydrogels are wounded after the HSE is prepared. Normal or abnormal fibroblasts (e.g. isolated from diabetic foot ulcers) are usually used for the wound healing studies (Maione et al., 2015; Reijnders et al., 2015; Rossi et al., 2015). These models are used for study of proliferation of the cells, re-epithelization and production of ECM and wound healing mediators (Maione et al., 2015; Reijnders et al., 2015). The most modern 3D wound healing models are constructed from several cell types. Kreimendahl et al. encapsulated endothelial cells and fibroblasts together into the hydrogel, which was further covered by keratinocytes and macrophages (Kreimendahl et al., 2019). Even though such a complex 3D cultures are established, any of the models mentioned use one or more wound environment stressors present in wound environment of the skin.

To highlight the potential of collagen based 3D cell cultures to investigate cell-matrix interactions important in wound healing; we present here the influence of collagen hydrogel on behavior of dermal fibroblasts in 3D. Additionally, we also compare the behavior of dermal fibroblasts under pathological conditions of non-healing wounds versus those cultured in normal conditions which since now has not been studied.

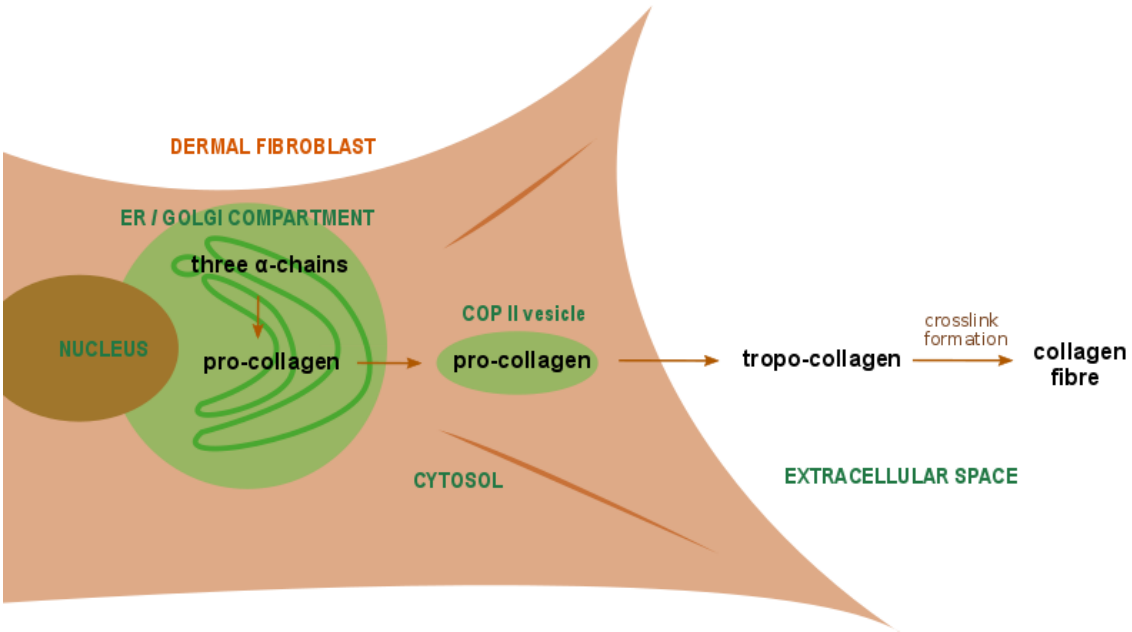

Figure 2 Collagen synthesis. In endoplasmic reticulum α-chains are woven together to form a pro-collagen molecule. The monomers of pro-collagen are transferred outside the cell by exocytosis in COP II vesicles. During or after the releasing process, terminal amino acid sequences are enzymatically removed from α-chains of the pro-collagen so that pro-collagen becomes tropo-collagen. The final collagen fibers are formed in the extracellular space by crosslinking.

2. HYPOTHESIS AND AIMS

Recent *in vitro* models of dermal fibroblasts simulating wound conditions are arranged in 2D or in 3D. To simulate wound conditions mostly only one stress factor is applied, e.g. lipopolysaccharide (LPS) from G^- bacteria as a pro-inflammatory stimuli, conditioned media from wound bacteria as a bacterial contamination or increased pro-inflammatory molecules (IL1, IL6). The relevant 2D and 3D cultures utilizing simultaneously acting more than one stress factor of wound conditions are missing.

Before we establish the hypotheses it is important to highlight that we are aware of the large spectrum of simultaneously acting stress factors in wounds. Therefore, with respect to the scope of this thesis, we focus only on the two stress factors, low nutrition and pro-inflammatory stimuli (LPS and bacteria), which we consider as the most important stress factors. Similarly, we focus only on the two bacterial species.

We establish these hypotheses:

1. The functions of dermal fibroblasts in 2D culture are more likely impaired due to the simultaneously acting low nutrition+LPS conditions than low nutrition conditions alone.
2. The different bacterial species and even different bacterial strains impair the functions of dermal fibroblasts in 2D culture diversely.
3. The three types of conditioned media from the two bacterial species (polybacterial conditions) impair the functions of dermal fibroblasts diversely.
4. The functions of dermal fibroblasts in 2D culture do not correspond to those in 3D culture.
5. The functions of dermal fibroblasts in 3D culture are impaired due to the simultaneously acting low nutrition+LPS conditions.

The aims of the thesis are as follows:

1. To simulate wound conditions *in vitro* applying low nutrition conditions or low nutrition+LPS conditions and to describe the responses of dermal fibroblasts on these conditions in 2D culture. The responses of dermal fibroblasts cover their

functions in real tissue and include metabolic activity, proliferation, changes in morphology, migration, production of pro-inflammatory factors such as IL6 and IL8, synthesis of collagen type I and production of MMP2 and MMP9, and contraction ability including differentiation in myofibroblast phenotype.

2. To expose the dermal fibroblasts to bacterial conditions (soluble factors from *S. aureus* and *P. aeruginosa*) and to describe the responses of dermal fibroblasts on these conditions in 2D culture. The responses of dermal include proliferation, changes in morphology, migration, production of pro-inflammatory factors such as IL6 and IL8 and synthesis of collagen type I.
3. To study the impact of the three types of the polybacterial conditions originated in different steps of *S. aureus* and *P. aeruginosa* media preparation on dermal fibroblasts in 2D culture. The responses of dermal fibroblasts include proliferation, changes in morphology, migration, production of pro-inflammatory factors such as IL6 and IL8 and synthesis of collagen type I.
4. To describe the responses of dermal fibroblasts cultured in 3D self-made collagen hydrogel culture and to compare it with their responses in 2D culture.
5. To simulate wound conditions *in vitro* applying low nutrition+LPS conditions and to describe the responses of dermal fibroblasts on these conditions in 3D culture. The responses of dermal fibroblasts cover their functions in real tissue and include metabolic activity, proliferation, changes in morphology and contraction ability.
6. To develop methods for the determination of total cell number in both 2D and 3D cultures as the quantitative approach how to analyze cell proliferation. This aim was defined during the solving of the aims mentioned above, since we realized that methods for determination of the total cell count in a whole sample are not available up to date.

3. MATERIALS AND METHODS

3.1 Isolation and culture of dermal fibroblasts

Normal human dermal fibroblasts (NHDF) were isolated from skin residues via the digestion-migration method following plastic surgery interventions. The isolation of NHDF from skin residues was carried out after approval by local ethics committee of the University Hospital in Pilsen, E. Benese 13, 305 99 Pilsen, Czech Republic, decision from 5th November 2015. The guidelines in the Declaration of Helsinki were followed. All donors gave written informed consent before intervention. Immediately following skin biopsy, the samples were immersed in physiological solution and transported to the cell culture lab for immediate isolation. The samples were washed in Hank's balanced salt solution (HBSS) (Sigma Aldrich) containing penicillin (100 U/ml)/streptomycin (0.1 mg/ml) (Biochrom, United Kingdom) and gentamicin (50 μg/ml) (Biochrom). The samples were cut into 3 mm^2 pieces and digested overnight at 37°C in Petri dishes (Techno Plastic Products, Trasadingen, Switzerland) in HBSS containing collagenase type I (100 U/ml, Thermo Fisher Scientific, USA). On the following day, the suspension containing the digested tissue was shaken intensively employing a vortex for 30 sec and filtered through a 100 μm nylon cell strainer (FalconTM, Thermo Fisher Scientific). The cell suspension was then transferred to a 75 cm^2 cultivation flask (Techno Plastic Products) containing 10 ml of medium composed of low glucose DMEM (Thermo Fisher Scientific), 10% heat-inactivated FBS (Thermo Fisher Scientific), penicillin (100 U/ml)/streptomycin (0.1 mg/ml) (Biochrom), 0.5% L-glutamin (Biosera, France) and 1.0% non-essential amino acids (Biosera). The NHDF were cultured at 37°C, 5% CO_2 up to 80% confluence and then passaged. The medium described here served as control conditions for all experiments. Only those NHDF from the 3^{rd} – 5^{th} passages were used in the experiments. The media were changed every 2^{nd} - 3^{rd} day of cell culture.

3.2 Origin and characterization of bacterial strains

Three bacterial strains were used in this thesis. One strain of *P. aeruginosa* (*PA*) and one strain of *S. aureus* (*SA*) were randomly chosen from Czech Collection of Microorganisms (CCM) (Brno, Czech Republic) and one strain of *P. aeruginosa* (*PA2*) was isolated from a patient at the University Hospital, Plzeň, Czech Republic.

Bacterial strains were maintained frozen in glycerol cryoprotective medium (Cryobank B, Itest, Czech Republic) in -80°C, resuscited on Columbia sheep blood agar (Oxoid, UK), once subcultured on the same medium and used for the tests. These bacterial strains were analyzed for associated virulence factors.

Gelatinase activity was tested by the modified method described by Su et al. (1991). Briefly, one colony of 12-hour bacterial cultures on Tryptone Soy Agar (TSA) (Sigma, Germany) were spot inoculated onto a 4 mm deep Luria Bertani (LB) agar (Merck, Darmstadt, Germany) with 5% (w/v) bovine gelatin (Sigma, Germany). After 24 hours incubation in 37°C the gelatin in medium was precipitated with Frasier Solution, the zone of complete gelatin lysis was read against the dark background and expressed semiquantitatively as follows: (+) – weak, (++) – moderate, (+++) – high gelatinase activity.

Hyaluronidase activity was tested by spot inoculation of one colony of 12-hour TSA bacterial cultures onto a 4 mm deep LB agar (Merck, Darmstadt, Germany) with 0.1% (w/v) of bovine serum albumin (Serva, Germany) and 0.5% (w/v) sodium hyaluronate (Contipro, Czech Republic). After 24 hours incubation in 37°C the hyaluronic acid was precipitated with 20% acetic acid (Sigma, Germany), the zone of complete hyaluronate lysis was read against the dark background and expressed as follows: (+) – weak hyaluronidase activity, (-) – negative hyaluronidase activity.

Before the strains were co-cultivated to test their leukocidal activity, the possible antagonism was tested by cross-inoculation of particular strains on Colmbia sheep blood agar (Oxoid, UK). Any inhibition of strain growth was interpreted as antagonism of particular strains. The presence of leucocidins produced by particular strains or strain combinations was tested on raw fraction of leukocytes isolated from fresh citrated porcine blood using a sucrose gradient (Centic et al., 1998). The isolated cells were exposed to the media from either overnight 16-18 hours culture or 70-74 hours culture of bacteria (or bacterial combination) in DMEM for 10 minutes, then stained with

trypan blue and counted (live/dead). The significant leukocidal activity was expressed as follows: (+) – significant leukocidal activity, (-) – not significant leukocidal activity.

The characterization of the bacterial strains was performed by experienced microbiologist Martin Sojka from the Regional Public Health Authority in Komarno, Slovakia.

3.3 *In vitro* simulation of wound conditions

3.3.1 Simulation of low nutrition and inflammation

Low nutrition conditions were simulated by means of a medium (3.1) containing only 2% of FBS and *low nutrition+LPS* conditions were simulated by means of a same medium containing 2% of FBS and 0.1 μg/ml of lipopolysaccharide (LPS) originated in pathogenic type of *E. coli* strain O111:B4 (Sigma Aldrich). The concentration of LPS was chosen in accordance to the preliminary experiments (data not shown) and the concentrations used in previous studies. The applied treatment conditions are summarized in **Table 1**.

3.3.2 Simulation of contamination by bacterial strains

Wound contamination by common bacterial strains was simulated as follow. Medium (3.1) was conditioned with soluble factors originated in *S. aureus* (*SA*), a strain from CCM database, or in *P. aeruginosa* (*PA*) a strain from CCM, or in *P. aeruginosa* (*PA2*), a strain originated from a patient wound. The medium without soluble factors served as control (*ctrl*) conditions.

Before preparation of bacterial conditions the bacteria were cultivated in Mueller-Hinton Broth (Difco, Becton Dickinson, Prague, Czech Republic) at 35°C for 18 hours. This is further referred as cultivation. After cultivation, bacteria were centrifuged at 4 500 × g and the pellet was resuspended in low glucose DMEM (Thermo Fisher Scientific) and incubated at 35°C for 12 hours. This is further referred as incubation. Afterwards the number of colony forming units per ml (CFU/ml) was estimated. After centrifugation at 24 000 × g and pH adjustment to 7.3 – 7.4 the bacteria conditioned DMEM was filtered through 0.22 μm filter and stored at -20°C for final bacterial conditioned media preparation.

Bacterial conditions were prepared as follow. The thawed bacteria conditioned DMEM was filtred through 0.22 μm filter and diluted with low glucose DMEM to the final concentration listed for each bacterial condition in **Table 1**. The diluted bacteria conditioned DMEM was finally complemented by 10% heat-inactivated FBS (Thermo Fisher Scientific), penicillin (100 U/ml)/streptomycin (0.1 mg/ml) (Biochrom), 0.5% L-glutamin (Biosera, France) and 1.0% non-essential amino acids (Biosera). The NHDF

were cultured in the bacterial conditions at 37°C, 5% CO_2 for 6 days without media exchange.

The final bacterial conditions, the media for NHDF containing bacterial soluble factors, were as follows: single strain conditions (*SA,* or *PA,* or *PA2*) or polybacterial conditions. The polybacterial conditions were of three types: 1) cultivated and incubated together (*SA+PAcu*), or cultivated separately but incubated together (*SA+PAin*), or cultivated separately, incubated separately, but mixed together just before application on the cells (*SA+PAmix*). For *SA+PAcu*, *SA+PAin* and *SA+PAmix* the *PA* bacterial strain (originated from CCM database) was used. The polybacterial conditions were of the three types according to various steps of media preparation, as the bacteria produce different soluble factors during the process. The applied treatment conditions are summarized in **Table 1**.

3.3.3 Summary of simulated wound conditions

The dermal fibroblasts were cultured in media composed of low glucose DMEM, heat-inactivated 2% or 10% FBS, penicillin (100 U/ml)/streptomycin (0.1 mg/ml), 0.5% L-glutamin and 1.0% non-essential amino acids. The treatment conditions used throughout the whole thesis are summarized in **Table 1**.

Table 1 Summary of applied treatment conditions throughout the thesis.

Abbreviation	Treatment conditions
control (ctrl)	10% FBS
low nutrition	2% FBS
low nutrition + LPS	2% FBS, LPS (0.1 µg/ml)
SA	*S. aureus* conditioned DMEM (1.5×10^7 CFU/ml)
PA 1.5	*P. aeruginosa* conditioned DMEM (1.5×10^7 CFU/ml) (origin: CCM database)
PA 0.25	*P. aeruginosa* conditioned DMEM (0.25×10^7 CFU/ml) (origin: CCM database)
PA2	*P. aeruginosa* conditioned DMEM (1.5×10^7 CFU/ml) (origin: patient)
SA+PAcu	conditioned DMEM from *S. aureus* (2.5×10^7 CFU/ml) and *P. aeruginosa* (origin: CCM database) (2.5×10^6 CFU/ml) cultivated and incubated together
SA+PAin	conditioned DMEM from *S. aureus* (2.5×10^7 CFU/ml) and *P. aeruginosa* (origin: CCM database) (2.5×10^6 CFU/ml) cultivated separately but incubated together
SA+PAmix	conditioned DMEM from *S. aureus* (2.5×10^7 CFU/ml) and *P. aeruginosa* (origin: CCM database) (2.5×10^6 CFU/ml) cultivated and incubated separately

3.4 Response of dermal fibroblasts to wound conditions in 2D culture

3.4.1 Metabolic activity

The metabolic activity was estimated using alamarBlue® assay that converted blue resazurin to pink resorufin. NHDF were seeded on 96-well plates (Techno Plastic Products) at a density of 6000 cells/cm^2 (for metabolic activity and cell proliferation) in 100 µl of medium and cultured overnight at 37°C and 5% CO_2. On the following day, the medium was changed - NHDF were treated with 150 µl media of particular conditions described in chapter 3.3. The media were collected and frozen at -80°C at time points 0, 1, 2, 3 and 5 or 6 days after the treatment for further analysis. NHDF attached on the plate were covered with medium with 10x diluted alamarBlue® solution (ThermoFisher Scientific) and incubated for 2 hours at 37°C, 5% CO_2. Subsequently, the fluorescence was measured at 530 nm (ex) and 590 nm (em) in a microplate reader (Synergy HT, Biotek, USA). The change in the metabolic activity over time was expressed as the ratio of the metabolic activity at days 1, 2, 3 and 5 or 6 to that at day 0 for each treatment. The results were expressed as the mean ± standard deviation. The number of independent NHDF donors was given in the graph captions.

3.4.2 Cell number determination

Cell proliferation was estimated by total nuclei count. After alamarBlue® assay, NHDF were stained by Hoechst #33342 (Thermo Fisher Scientific). Nine sequential images of each well covering whole well area were taken by Olympus UPlanFL N 4x/0.13 objective. The whole well area images composed of the nine sectional images were automatically compiled by VisiView® software (Visitron Systems, Germany) (**Figure 3**). Number of cells in each well was determined with use of Fiji software (National Institute of Health, Bethseda, USA). The image processing is described in chapter 3.4.3. The change of proliferation rate in time was expressed as ratio of cell count at day 1, 2, 3 and 5 or 6 to cell count at day 0 for each treatment. Results were expressed as mean of the cell number ± standard deviation. The number of independent NHDF donors was given in the graph captions.

In the case of comparison of cell proliferation in 2D and 3D the different protocol, according to previously published method with modification (Mio et al., 1996) was used. NHDF growing on well plates were stained by Calcein-AM (Sigma). Cells were collected by centrifugation and resuspended in phosphate buffer saline (PBS). Afterwards, NHDF were lysed in 1% Triton X-100 while shaking. The cell lysis suspension was frozen at -80°C. After thawing the fluorescence of the suspensions was measured at 485 nm (ex) and 528 nm (em) in microplate reader (Synergy HT, Biotek, USA). The change of proliferation data in time was expressed as ratio of relative fluorescence unit at day 1, 2, 3 and 6 to relative fluorescence unit at day 0. The results were expressed as mean ± standard deviation from 3 independent NHDF donors.

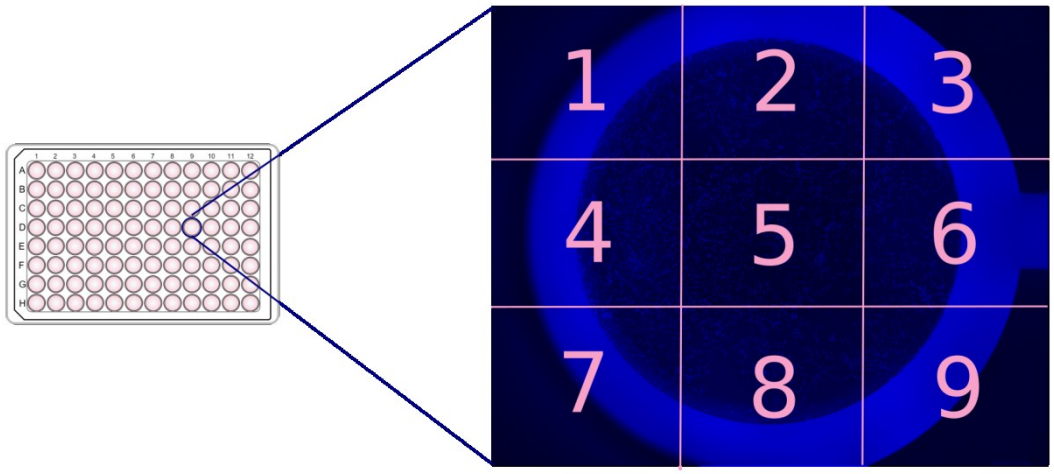

Figure 3 Nine sectional microscopic pictures compiled to cover the whole well area of 96-well plate. The total nuclei count in the well was determined from the compiled picture with Fiji software.

3.4.3 Optimization of cell number determination in 2D culture by image analysis

The preparation of NHDF and taking microscopy pictures foregoing image analysis is described in chapter 3.4.2. After this process, all nuclei were counted in each well by custom made protocol in Fiji software. The protocol included following steps (the details can be found in **Appendix 1** - 9.1):

1. Load the series of whole well area images (image sequence).
2. Adjust brightness and contrast of the image sequence to a*uto*.
3. Adjust and subtract the undesirable background of the image sequence.
4. Threshold nuclei in the image sequence to remove the background fluorescence.
5. *Convert to the mask* the image sequence and separate the touching nuclei by *watershed* tool.
6. Count the cells (nuclei) with the use of C*ell counter* tool after adjustment of the specific range of nuclei size and the circularity in the settings.

3.4.4 Cell morphology

The morphology of NHDF was observed by phase contrast microscopy. The pictures of NHDF were taken by Olympus UPlanFL N 10x/0.30 objective, Canon EOS1200D digital camera at days 0, 1, 2, 3 and 5.

3.4.5 IL6, IL8 and collagen type I quantification by ELISA

The media were collected at each time point 0, 1, 2, 3 and 5 or 6 days and stored at -80°C. Concentrations of IL6, IL8 and collagen type I were assessed by ELISA, using Human IL-6 ELISA Ready-SET-Go!™ Kit (eBioscience, USA), Human IL-8 ELISA Ready-SET-Go!™ Kit (eBioscience, USA) and Human Pro-Collagen I alpha 1 ELISA kit (Abcam, UK) respectively. The assays were performed according to the manufacturer´s protocol. The change in IL6, IL8 and collagen type I production was expressed as ratio of pg per 1000 cells at day 1, 2, 3 and 5 to pg per 1000 cells at day 1 in the case of simulation of low nutrition and inflammation, or as a ratio of pg per 1000 cells at day 1 and 6 in the case of simulation contamination by bacterial strains. The results were expressed as mean ± standard deviation. The number of independent NHDF donors was given in the graph captions.

3.4.6 MMP2 and MMP9 zymography

The media of treated cells were collected at time points 1 and 5 or 6 days and stored at -80°C. Pure media containing either 10% or 2% of FBS were analyzed to determine the basal MMP activities of media. The MMP2 and MMP9 were analyzed via gelatin zymography on an SDS-PAGE (7.5% separating gel, 4% stacking gel) containing 0.05% of gelatin and using PageRuler™ Plus Prestained Protein Ladder, 10 to 250 kDa (ThermoFisher Scientific, USA), as marker of molecular weight. Following electrophoresis, the gels were washed in 2.5% Triton X-100 for 30 min while being shaken so as to remove the SDS and to renature the MMPs in the gels. The gels were then incubated overnight in a gelatinase activation buffer (100 mM Tris-HCl, pH 7.4; 5 µM $CaCl_2$; 1 µM $ZnCl_2$), stained with Coomassie Brilliant Blue G-250 for 30 min and de-stained using de-staining solution. The gels were scanned using the ChemiDoc MP Imaging System (BioRad, USA). The MMP2 and MMP9 activities were determined via the software quantification of the degraded bands in Fiji software. The MMP activity was determined in two steps. First, the values of basal MMP activities of pure media were subtracted from those media of analyzed samples; second, the values of MMP activities were normalized to total cell number. The results were expressed as the mean ± standard deviation from 4 independent NHDF donors. The original scan of the gel (**Figure 9A**) is attached in **Appendix 2 -** 9.2).

3.4.7 Scratch wound assay

The NHDF were seeded on 6-well test plates (Techno Plastic Products) at a density of 30 000 cells/cm^2 in the culture medium and cultured overnight at 37°C and 5% CO_2. On the following day, the cell monolayers were scratched by a 10 µl pipette tip so as to create four crosses (wounded areas) per well thus mimicking the "wound bed". The detached cells were washed carefully in PBS and treated with particular wound conditions (3.3) but without FBS to eliminate the effect of cell proliferation and cultured for 5 or 6 days. Immediately following treatment, images of the four wounded positions in each well were captured using an Olympus UPlanFL N 4x/0.13 objective. The positions were saved by cellSens Dimension 1.12 microscope software (Olympus, Japan). Images of the migrating cells were taken at time points of 0, 1, 2, 3 and 5 or 6 days following treatment. Morphology of the cells in conditions of contamination by

bacterial strains was documented outside the scratch under the same microscope by phase contrast at day 6. The final images of scratch wound assay were analyzed using TScratch software (CSELab, Switzerland) via the quantification of the wounded areas (i.e. the areas without cells) as a percentage of the whole of the picture area. The change in the migration rate of the cells was expressed as the ratio of the wounded area at days 1, 2, 3 and 5 or 6 to the wounded area at day 0. The results were expressed as the mean ± standard deviation. The number of independent NHDF donors was given in the graph captions.

3.4.8 α-SMA and collagen type I visualization and α-SMA quantification

NHDF were seeded on a µ-Slide 4-well (Ibidi, Germany) at a density of 6000 cells/cm^2 (visualization) and on 96-well plate (quantification) in the medium and cultured overnight at 37°C and 5% CO_2. On the following day, the NHDF were treated with particular wound conditions (3.3.1). 5 days following treatment, the NHDF were fixed with fresh 4% paraformaldehyde. The cells were then permeabilized with cold 0.1% Triton X-100 solution for 15 minutes. After rinsing with PBS, the non-specific bonds were blocked with 5% bovine serum albumin in PBS for 30 minutes at room temperature. Subsequently, the samples were incubated overnight at 4°C with the following primary antibodies diluted in PBS: anti-alpha smooth muscle actin antibody (ab7817, Abcam) diluted to final concentration of 1 µg/ml or collagen I alpha I antibody (MAB 6220, R&D Systems) diluted to final concentration of 125 µg/ml. Following rinsing with PBS, secondary goat anti-mouse IgG H&L antibody conjugated with Alexa Fluor® 488 (ab150113) was applied to the samples (diluted in PBS to a final concentration of 1 µg/ml) for 1 hour at room temperature in the dark. The nuclei were stained with Hoechst #33342 in the final 10 minutes. An Olympus UPlanFL N 20x/0.50 objective was used for the visualization of the α-SMA. The visualization of the collagen type I was conducted using an Olympus LUCPlanFL N 40x/0.60 objective. With respect to the quantification of the α-SMA, the compilation of nine sequential images covering the whole well areas was used as described in chapter (3.4.2). The results were expressed as the mean of the α-SMA positive cell area at day 5 normalized to the cell count ± standard deviation from 3 independent NHDF donors.

3.5 Preparation of 3D culture

3.5.1 Isolation of rat tail collagen type I

The type I collagen used for preparing the 3D collagen hydrogel was isolated from rat tails. The tendons were removed from the rat tails and maintained 3 × 24 hours in PBS on a laboratory shaker at room temperature. PBS was exchanged every single day. Afterwards the procedure was repeated with citrate buffer (0.08 M, pH 3.7). Subsequently, the tendons were digested in 0.1 M acetic acid for 48 hours at 4°C. The collagen digested in acetic acid was homogenized with blender and the suspension was ultracentrifuged at the maximum speed (approx. 46 000 × g) for 1 hour in order to remove the tissue debris. The supernatant containing the collagen type I was lyophilized and stored in -20°C. The collagen solution for preparation of the 3D collagen hydrogel was prepared by dissolving the lyophilized collagen in 0.02 M acetic acid at 4°C at least 5 days to a concentration of 5 mg/ml and was stored at 4°C as a stock solution for maximal 1 month.

3.5.2 Preparation and culture of cell-seeded collagen hydrogels

3D collagen hydrogels containing NHDF were prepared in our lab as follows. 600 µl of collagen stock solution (5 mg/ml) was mixed properly with 290 µl of medium, 10 µl of sodium bicarbonate (Thermo Fisher Scientific) and 100 µl of NHDF suspension in medium on ice. The final collagen concentration was 3 mg/ml and final NHDF seeding density was 30 000 cells/ml (cell morphology, proliferation and contraction) and 40 000 cells/ml (metabolic activity). 10 000, 125 000, 250 000 and 375 000 cells were seeded in each collagen hydrogel for cell number determination in 3D. 0.5 ml of collagen suspension with NHDF was plated into the 24-well plate. The polymerization occurred at 37°C, 5% CO_2 and humidified atmosphere after 20 minutes. The change in pH from acidic to neutral and 37°C caused the collagen to polymerize into a gel. After collagen polymerization 0.5 ml of medium was carefully added on the top of the hydrogels. In the case of the cell contraction measurement 2-ml collagen hydrogels were plated into the 24-well plates. After the polymerization 1 ml of medium was carefully added on the top of the hydrogels.

3.6 Response of fibroblasts to 3D culture in normal and wound conditions

3.6.1 Cell morphology

At the day of the analysis the cell-seeded collagen hydrogels were stained by Calcein-AM solution in PBS (1:1000) and incubated for 45 min at 37°C, 5% CO_2. After washing with PBS the confocal imaging of the NHDF was conducted using an Olympus LUCPlanFL N 20x/0.50 objective.

3.6.2 Metabolic activity

The day after preparation of cell-seeded collagen hydrogels (3.5.2), NHDF were treated as describe in chapter (3.3.1). In time points 0, 1, 2, 3, and 6 days after treatment alamarBlue® assay was performed. The medium was replaced with medium containing 10× diluted alamarBlue® solution and the cell-seeded collagen hydrogels were incubated for 3 hours at 37°C, 5% CO_2. Afterwards, fluorescence was measured at 530 nm (ex) and 590 nm (em) in microplate reader (Synergy HT, Biotek, USA). The change of metabolic activity in time was expressed as ratio of metabolic activity at day 1, 2, 3 and 6 to metabolic activity at day 0 for each treatment. Results were expressed as mean ± standard deviation. The number of independent NHDF donors was given in the graph captions.

3.6.3 Cell proliferation

Cell proliferation was estimated according to previously published method with modification (Mio et al., 1996). The cell-seeded collagen hydrogels were digested in 0.5 ml of 0.25% Trypsin/EDTA for 15 minutes at 37°C, 5% CO_2. Afterwards 0.5 ml of collagenase I solution in HBSS (4 mg/ml) was added and incubated for at least 1 hour until the hydrogel was completely digested. Cells were collected by centrifugation at 500 × g for 10 minutes. The cell pellet was stained by Calcein-AM solution in PBS (1:1000) and incubated for 45 minutes at 37°C, 5% CO_2. Cells were collected by centrifugation at 500 × g for 10 minutes and washed with PBS. After washing, the cells were collected by centrifugation again and finally resuspended in 1 ml of 1% Triton X-100 for 30 minutes while shaking to finalize cell lysis. The lysed cells were frozen at -

80°C. After thawing, fluorescence was measured at 485 nm (ex) and 528 nm (em) in microplate reader (Synergy HT, Biotek, USA). The change of proliferation data in time was expressed as ratio of relative fluorescence unit at day 1, 2, 3 and 6 to relative fluorescence unit at day 0. Results were expressed as mean ± standard deviation from 3 independent NHDF donors.

3.6.4 Cell morphology

NHDF were observed by light microscopy the day after seeding into the collagen hydrogels. The pictures of NHDF in 3D cultures were taken by Olympus CKX41 microscope, CachN 10x/0.25 objective, Canon EOS1200D digital camera.

The sample preparation for fluorescence visualization of NHDF in 3D collagen hydrogel was performed as follows. The cell-seeded collagen hydrogels were stained by Calcein-AM solution in PBS (1:1000) and incubated for 45 minutes at 37°C, 5% CO_2.

3.6.5 Cell contraction

30 000 NHDF/ml were seeded into 2-ml collagen hydrogels as described in chapter (3.5.2). An equal volume of fresh culture medium was replaced three times a week. The force of contraction was determined from collagen hydrogel diameter measurement. The diameter of the hydrogels was measured with a caliper at time points of 7, 14, 21 and 28 days (seeded vs. non-seeded hydrogels) or 1, 6 and 13 days (NHDF in control vs. low nutrition and inflammation conditions). The results were expressed as the mean ± standard deviation. The number of independent NHDF donors was given in the graph captions.

3.7 Cell counting in cell-seeded 3D collagen hydrogels by stereology

Since any suitable method for total cell counting in 3D has not been optimized yet, this method based on stereology kindly discussed with prof. Peter Mouton (Stereology Resource Center, Inc. and Department of Computer Sciences and Engineering, University of South Florida, USA) was developed as the determination of cell number in 3D collagen hydrogels was essential for our purpose.

3.7.1 Cell staining and scaffold optical sectioning by fluorescence microscopy

The day after seeding (3.5.2), the collagen hydrogels were fixed with 4% paraformaldehyde for 30 minutes. After washing with PBS the cell-seeded collagen hydrogels were maintained in 0.2% Triton X-100 for 30 minutes followed by 30 minutes in 5% bovine serum albumin. NHDF in collagen hydrogels were stained by DAPI fluorescent staining solution.

The process of optical sectioning of collagen hydrogels was as follow. Nine Z-axis columns were located through the XYZ-axes of each collagen hydrogel (**Figure 4**). The columns included 30 separated Z stacks with 0.02 mm distance between each stack (height of column = 30 × 0.02 mm = 0.6 mm). Each column had an XY area of 2.34 mm^2, giving a total volume of each column of 1.4 mm^3 (0.6 mm × 2.34 mm^2) = 1.4 µl. Thus, the total volume of all 9 columns was at least 12.6 µl (1.4 µl × 9). 2D images of each section were taken by Olympus UPlanFL N 10x/0.30 objective and the pictures of columns were saved as image sequence (*.stk file) by VisiView® software. The number of cells was recalculated to the whole collagen hydrogel volume.

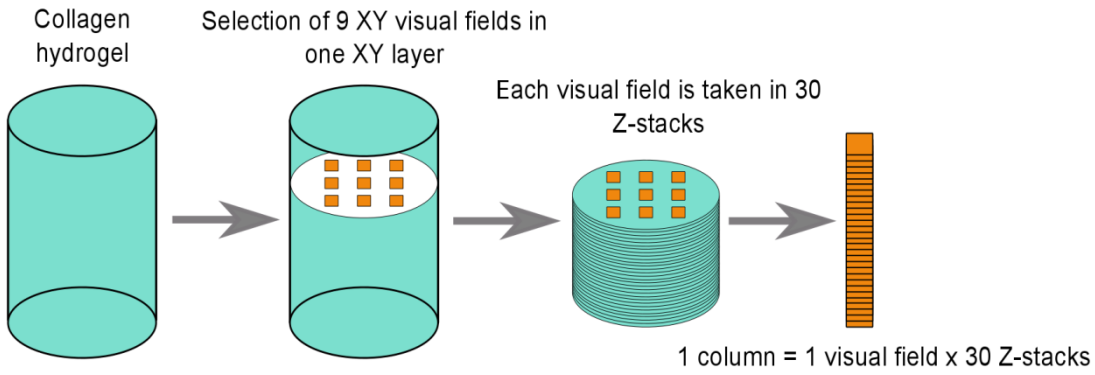

Figure 4 Sampling procedure. 3D collagen hydrogel sampled into 9 XY visual fields and 30 Z-stacks. Cell number was determined for each column. The number was recalculated to the whole collagen hydrogel volume.

3.7.2 Optimization of cell number determination by image analysis

Cell numbers were counted within columns using Fiji software and cell number in total volume of collagen hydrogel was estimated from each column using the optical dissector principle (Farel, 2003).

The protocol included following steps (the details can be found in **Appendix 3 -** 9.3):

1. Load the *.stk file of the image sequence (XYZ column).
2. Adjust brightness and contrast of each image sequence to *auto*.
3. Adjust and subtract the undesirable background of the image sequence.
4. Threshold nuclei in the image sequence to remove the background fluorescence.
5. Set the *3D object counter* to account for only the size range consistent with the size of dermal fibroblast nuclei; set the circularity to account for spherical and oval-shaped areas and start the counter.

3.7.3 Estimation of collagen hydrogel volume

The volume of collagen hydrogels was estimated according to Archimedes´ principle. 5-ml measuring cylinder with 0.1 ml marked lines was filled with precise 3 ml of PBS. Each collagen hydrogel was put into the cylinder with PBS and the volume increase was read on the cylinder scale. The increased volume responded to the volume of the collagen hydrogel.

3.7.4 Data analysis

The data for total cell number determination in the whole cell-seeded collagen hydrogel were recalculated from the cell number determined in the image sequences (XYZ column), i.e. for estimation of cell number in one collagen hydrogel, cell number from 9 image sequences (i.e. 9 columns) were recalculated to the total collagen hydrogel volume. The example of the recalculation of cell number in the whole collagen hydrogel from cell number in one column:

$$\frac{cell\ number\ in\ the\ column \times collagen\ hydrogel\ volume}{the\ column\ volume} = \frac{221\ cells \times 200\ \mu l}{1.4\ \mu l} = 31\ 571\ cells\ in\ hydrogel$$

This calculation was performed 9 times (from each of the 9 columns) and the mean of the values was considered as a result (total cell number) for one collagen hydrogel.

3.8 Statistical analysis

All the data was expressed as the mean ± standard deviation from 3-8 independent NHDF donors depending on the type of analysis conducted. The Shapiro-Wilk test was used to ascertain data normality and the Leven's test was employed for the assessment of the equality of the variances for a variable calculated for two or more groups.

The statistical significance of the differences between the *control*, *low nutrition* and *low nutrition+LPS* groups was determined via one-way ANOVA ($p<0.05$) followed by the Fisher's LSD test for the quantification of the α-SMA and MMP2; by the Kruskal-Wallis test ($p<0.05$) for the metabolic activity, proliferation and quantification of the IL6, IL8, collagen type I and MMP9 and by the Mann-Whitney U test ($p<0.05$) for the migration and the within groups statistics for the metabolic activity in the particular time points.

The statistical significance of the differences between the *PA, PA2, SA, PA+SAcu, PA+SAin, PA+SAmix* and *ctrl* groups was determined via one-way ANOVA ($p<0.05$) followed by the Fisher's LSD test for the migration; by the Kruskal-Wallis test ($p<0.05$) for the metabolic activity, proliferation and quantification of the IL6, IL8 and collagen type I and by the Mann-Whitney U test ($p<0.05$) for the within groups statistics for the quantification of collagen type I in the particular time points.

The statistical significance of the differences for metabolic activity and proliferation of dermal fibroblasts cultured in 2D and 3D was determined by the Mann-Whitney U test ($p<0.05$); and by the Wilcoxon test ($p<0.05$) for the contraction.

The statistical significance of the differences between the *control* and *low nutrition+LPS* groups in the 3D culture was determined by the Kruskal-Wallis test ($p<0.05$) for the contraction and by the Mann-Whitney U test ($p<0.05$) for the metabolic activity and proliferation.

The method for cell number determination in 3D was verified by the One-sample t-test ($p<0.05$).

All the statistical analyses were performed in Statistica v12 software (Tibco Software, Palo Alto, California, USA).

4. RESULTS

4.1 Response of fibroblasts to wound conditions in 2D culture

4.1.1 Low nutrition and inflammation

4.1.1.1 Metabolic activity

The effect of *low nutrition* and *low nutrition+LPS* conditions on NHDF metabolic activity was estimated by means of alamarBlue assay. NHDF were cultured 5 days under *control*, *low nutrition* and *low nutrition+LPS* conditions and the metabolic activity was estimated after 0, 1, 2, 3 and 5 days of treatment (**Figure 5a**). NHDF cultured under all three conditions exhibited increasing tendency in metabolic activity during whole cultivation period (Mann Whitney U test; $p<0.05$). The comparison of metabolic activity of NHDF cultured in particular conditions revealed no significant difference between the groups with the exception of the occurrence of significantly higher NHDF metabolic activity under *low nutrition* (4.08 ± 0.76) conditions compared to the *control* (2.60 ± 0.59) at day 3 (Kruskal-Wallis test; $p<0.05$).

4.1.1.2 Cell proliferation

The effect of *low nutrition* and *low nutrition+LPS* conditions on NHDF proliferation was evaluated by means of the total cell count (**Figure 5b**). The NHDF did not proliferate at 5 days under either *low nutrition* or *low nutrition+LPS* conditions. A comparison of the proliferation of NHDF under particular conditions and at particular time points revealed no significant difference between the *low nutrition* and *low nutrition+LPS* conditions at any time point. However, at days 3 and 5 the proliferation of NHDF was significantly lower under both *low nutrition* (1.86 ± 0.78 for day 3; 1.67 ± 0.41 for day 5) and *low nutrition+LPS* (1.89 ± 0.79 for day 3; 2.17 ± 1.11 for day 5) conditions than that of the *control* (3.30 ± 0.69 for day 3; 4.90 ± 0.90 for day 5) (Kruskal-Wallis test; $p<0.05$).

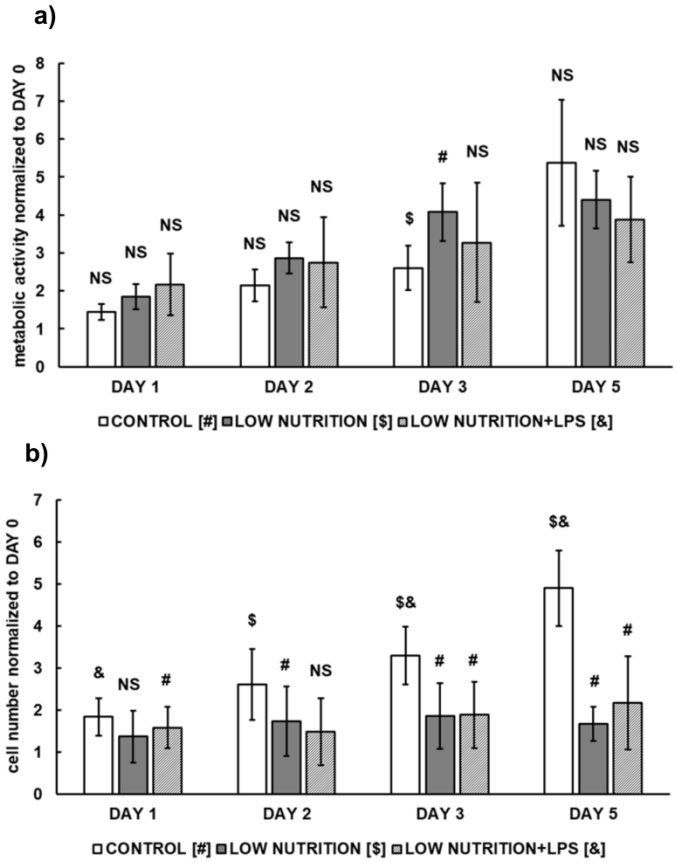

Figure 5 The metabolic activity of dermal fibroblasts is not influenced by the *low nutrition* and *low nutrition+LPS* wound stress factors while the cells did not proliferate. Metabolic activity of dermal fibroblasts (a) cultured for 5 days in *control*, *low nutrition* and *low nutrition+LPS* conditions was measured by alamarBlue assay every 24 hours and the change in the metabolic activity was expressed as a ratio of the signal at days 1-5 to the signal at day 0. Proliferation of NHDF (b) cultured for 5 days in *control*, *low nutrition* and *low nutrition+LPS* conditions was assessed by cell count every 24 hours and the change in the proliferation was expressed as a ratio of the cell number at days 1-5 to the cell number at day 0. The results are expressed as the mean ± standard deviation (n=8). *Control* = medium with 10% of FBS; *low nutrition* = medium with 2% of FBS; *low nutrition+LPS* = medium with 2% of FBS and 0.1 µg/ml of LPS. # = a significant difference from the *control* group, $ = a significant difference from the *low nutrition* group, & = a significant difference from the *low nutrition+LPS* group, NS = no significant difference between particular groups (Kruskal-Wallis test; $p<0.05$).

4.1.1.3 Cell morphology

The effect of *low nutrition* and *low nutrition+LPS* conditions on NHDF morphology was observed by phase contrast microscopy. NHDF were cultured 5 days under *control*, *low nutrition* and *low nutrition+LPS* conditions and the pictures of the cell morphology was taken after 0, 1, 2, 3 and 5 days of treatment **Figure 6**. The morphology of NHDF was typical spindle-shaped and remained stable for 5 days in all tested conditions.

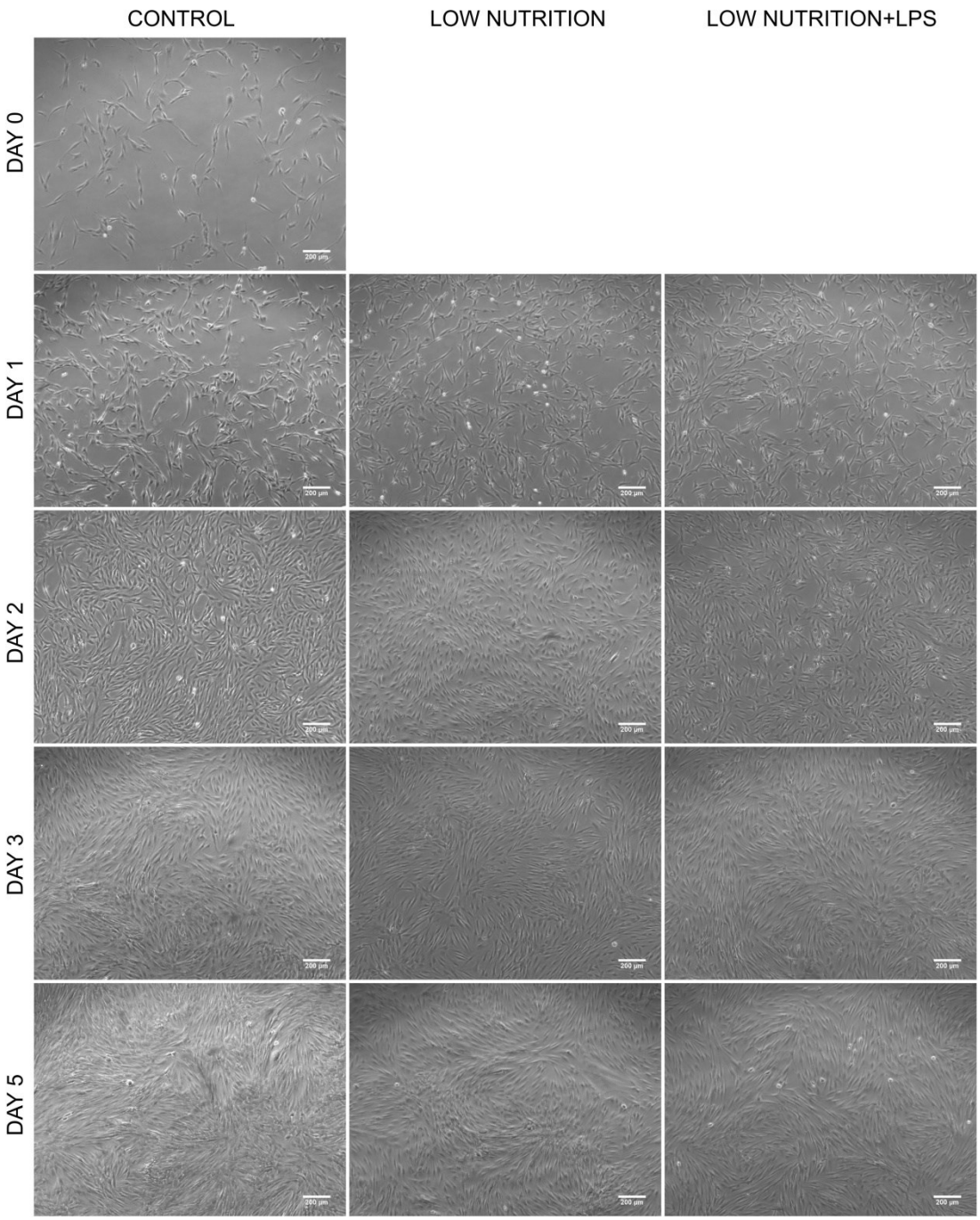

Figure 6 The morphology of dermal fibroblasts is not influenced by the *low nutrition* and *low nutrition+LPS* wound stress factors. The pictures of dermal fibroblasts in *control*, *low nutrition* and *low nutrition+LPS* conditions were taken by light microscope every 24 hours for 5 days. The scale bar represents 200 μm.

4.1.1.4 Migration

The effect of *low nutrition* and *low nutrition+LPS* conditions on NHDF migration was evaluated by means of scratch wound assay. The NHDF migrated for 5 days and the wounded area was measured 0, 1, 2, 3 and 5 days following wounding (**Figure 7**). Interestingly, the *low nutrition+LPS* conditions, particularly the addition of LPS promoted NHDF migration significantly since the day 2. After 2 day of migration, the wounded area under *low nutrition* conditions was determined at 71.5 ± 12.4% and under *low nutrition+LPS* conditions at 56.7 ± 7.0%. At the subsequent time points, the wounded area values were: 62.7 ± 11.0% (*low nutrition*) versus 42.2 ± 4.7% (*low nutrition+LPS*) after 3 days, 56.8 ± 13.3% (*low nutrition*) versus 36.5 ± 9.7% (*low nutrition+LPS*) after 5 days (Mann-Whitney U test; $p<0.05$).

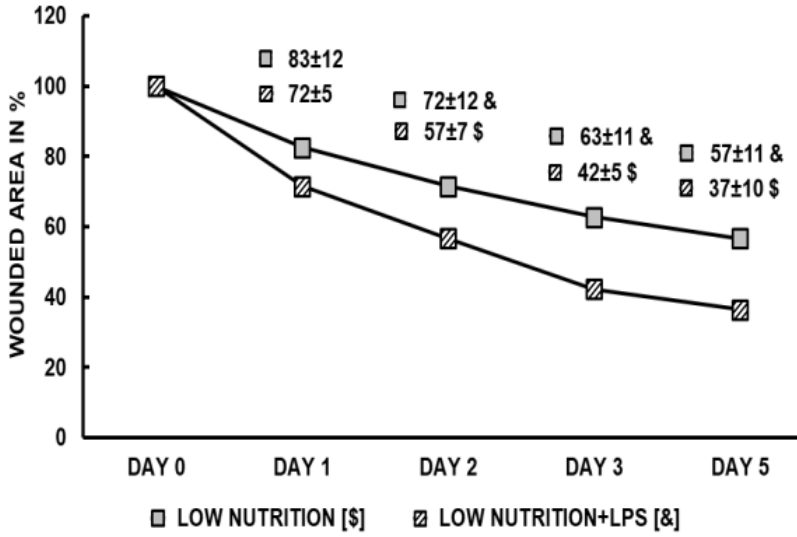

Figure 7 The migration of dermal fibroblasts is potentiated by *low nutrition+LPS* wound stress factor. Migration was measured by scratch wound assay. The wounded area (in %) was calculated as the ratio of the open area at days 1-5 to the open area at day 0. The results are expressed as the mean ± standard deviation (n=6). *Low nutrition* = medium with 2% of FBS; *low nutrition+LPS* = medium with 2% of FBS and 0.1 µg/ml of LPS. $ = a significant difference from the *low nutrition* group, & = a significant difference from the *low nutrition+LPS* group (Mann-Whitney U test; $p<0.05$).

4.1.1.5 Pro-inflammatory cytokine IL6 and IL8 production

The pro-inflammatory response of the NHDF under *low nutrition* and *low nutrition+LPS* conditions was estimated via the quantification of IL6 (**Figure 8a**) and IL8 (**Figure 8b**) in the cell culture media and normalized to the cell number at each day and then to value at day 1. The production of IL6 by the NHDF was significantly higher under the *low nutrition+LPS* conditions than it was under the *low nutrition* and *control* conditions over time from day 2 (Kruskal-Wallis test; $p<0.05$). The production values were determined at 1.35 ± 0.50 (*low nutrition+LPS*), 0.85 ± 0.18 (*low nutrition*) and 0.78 ± 0.20 (*control*) at day 2; 2.16 ± 1.04 (*low nutrition+LPS*), 0.83 ± 0.49 (*low nutrition*) and 0.78 ± 0.55 (*control*) at day 3 and 5.47 ± 2.07 (*low nutrition+LPS*), 1.07 ± 0.60 (*low nutrition*) and 1.16 ± 1.02 (*control*) at day 5. The production of IL8 by the NHDF exhibited a greater increasing tendency over time when cultured under *low nutrition+LPS* conditions than it did under the *low nutrition* and *control* conditions. However, the concentration of IL8 did not differ significantly between the groups at any of the time points (Kruskal-Wallis test; $p<0.05$).

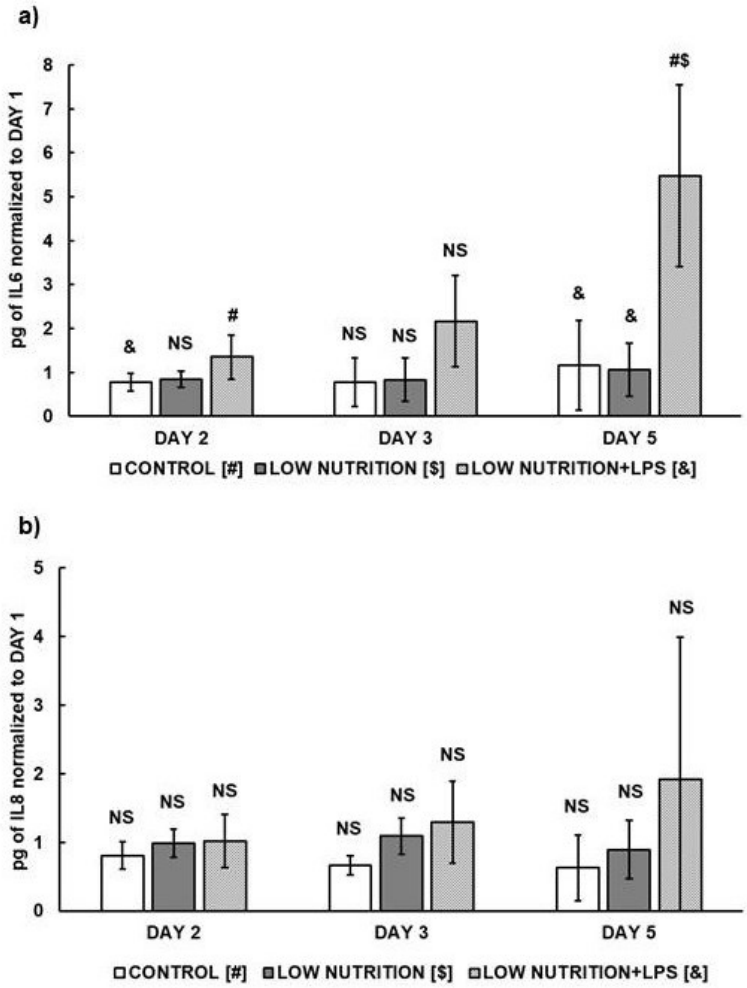

Figure 8 The production of IL6 and IL8 by dermal fibroblasts is potentiated by *low nutrition+LPS* wound stress factor. The production of IL6 and IL8 was estimated by means of ELISA. The change in the production of (a) IL6 and (b) IL8 is expressed as the ratio of pg produced by a single cell at days 1-5 to those produced by a single cell at day 1. The results are expressed as the mean ± standard deviation (n=6-8). *Control* = medium with 10% of FBS; *low nutrition* = medium with 2% of FBS; *low nutrition+LPS* = medium with 2% of FBS and 0.1 µg/ml of LPS. # = a significant difference from the *control* group, $ = a significant difference from the *low nutrition* group, & = a significant difference from the *low nutrition+LPS* group, NS = no significant difference between particular groups (Kruskal-Wallis test; $p<0.05$).

4.1.1.6 MMPs production

The effect of *low nutrition* and *low nutrition+LPS* conditions on the NHDF secretion of MMP2 and MMP9 was evaluated via gelatin zymography at the 1- and 5-day time points. The signal from MMP2 and MMP9 activity contained in pure cell culture media was subtracted from signal of tested samples and then normalized to the cell number (**Figure 9a-c**). Both *low nutrition and low nutrition+LPS* conditions were found to significantly promote the activity of MMP2 per cell at day 1 (**Figure 9b**) with an MMP2 per cell count of 1.25 ± 0.60 (*low nutrition+LPS*) and 0.58 ± 0.26 (*low nutrition)* versus -0.68 ± 0.37 (*control*). MMP9 increased significantly under *low nutrition* conditions at day 1 with an MMP9 per cell count of 0.38 ± 0.17 (*low nutrition*) versus -0.37 ± 0.33 (*control*). The negative values of *control* conditions were caused by higher activity in pure cell culture media (**Figure 9a**). At day 5 (**Figure 9c**), the activity of MMP2 per cell increased significantly under both *low nutrition* and *low nutrition+LPS* conditions with an MMP2 per cell count of 1.48 ± 0.50 (*low nutrition+LPS*) and 1.54 ± 0.82 (*low nutrition*) versus 0.35 ± 0.17 (*control*). The level of MMP9 per cell was not found to have changed at day 5 in *low nutrition* and *low nutrition+LPS* conditions; however, the level of MMP9 per cell in *control* conditions reached the values of *low nutrition* and *low nutrition+LPS* (One-way ANOVA; $p<0.05$ followed by Fisher's LSD for the MMP2; Kruskal-Wallis test; $p<0.05$ for the MMP9).

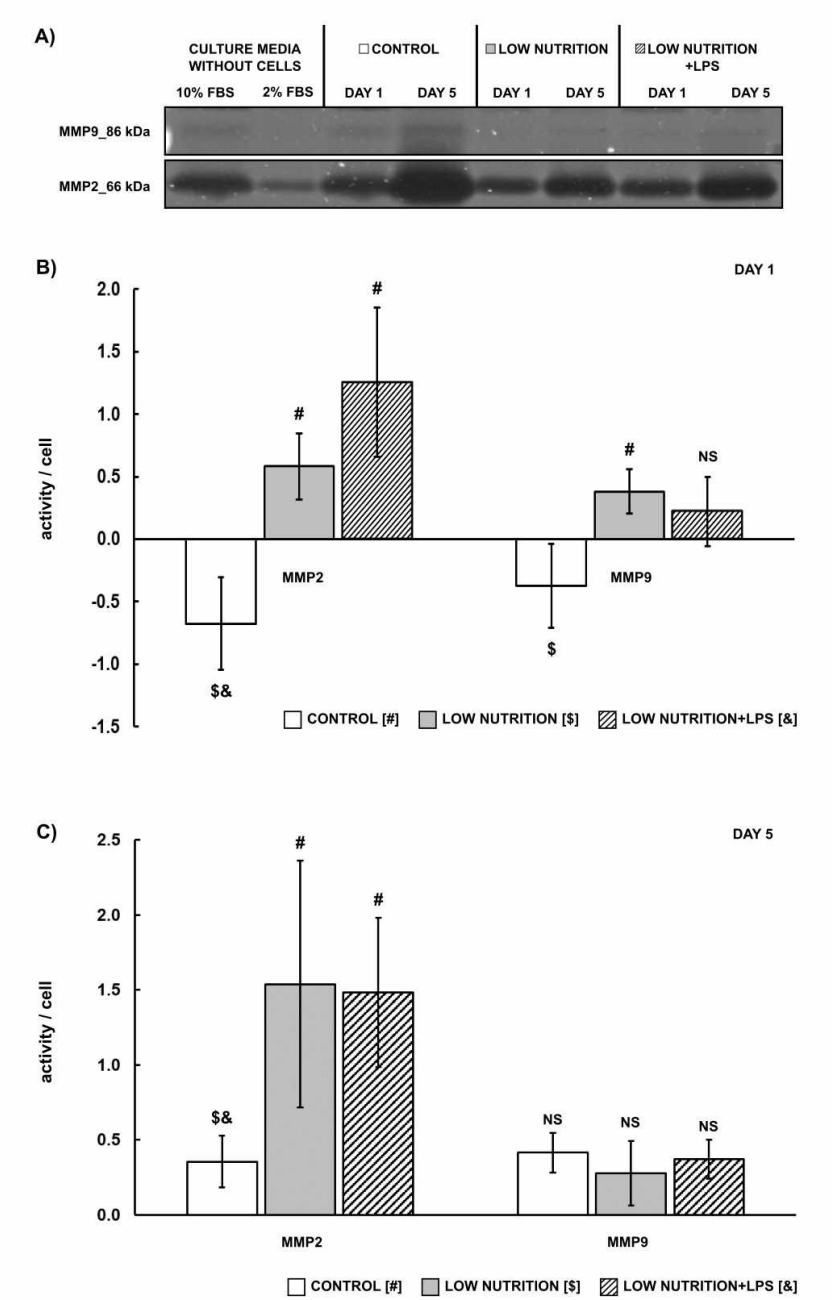

Figure 9 MMP activity of dermal fibroblasts is potentiated mainly by low nutrition conditions. MMP activity was assessed by means of zymography at days 1 and 5. Gel images (a) of particular culture conditions at day 1 and 5 including baseline MMP level in medium (medium without cells). Densitometric analysis of gel images (b, c). The graph depicts MMP activity as a fraction of the area of the sample (baseline MMP levels subtracted) normalized to the cell number. The results are expressed as the mean ± standard deviation (n=4). *Control* = medium with 10% of FBS; *low nutrition* = medium with 2% of FBS; *low nutrition+LPS* = medium with 2% of FBS and 0.1 μg/ml of LPS. # = a significant difference from the control group, $ = a significant difference from the low nutrition group, & = a significant difference from the low nutrition+LPS group, NS = no significant difference between particular groups (One-way ANOVA; $p<0.05$ followed by Fisher's LSD test (MMP2) and Kruskal-Wallis test; $p<0.05$ (MMP9)).

4.1.1.7 α-SMA synthesis

The expression of α-SMA by the NHDF was visualized and quantified after 5 days of culturing under the *control*, *low nutrition* and *low nutrition+LPS* conditions (**Figure 10a-d**). The expression of α-SMA decreased under *low nutrition* and *low nutrition+LPS* conditions after 5 days of culturing compared to the *control* conditions. Moreover, the *low nutrition+LPS* conditions decreased the expression of α-SMA compared to the *low nutrition* conditions with areas of α-SMA positive cells normalized to the total cell number of 169 ± 49 μm^2 (*control*), 145 ± 23 μm^2 (*low nutrition*) and 74 ± 40 μm^2 (*low nutrition+LPS*) (**Figure 10a**). The changes in the number of α-SMA positive cells were apparent both from the quantification analysis (**Figure 10a**) (One-way ANOVA; $p<0.05$ followed by Fisher's LSD test) and the microscopy images (**Figure 10b-d**).

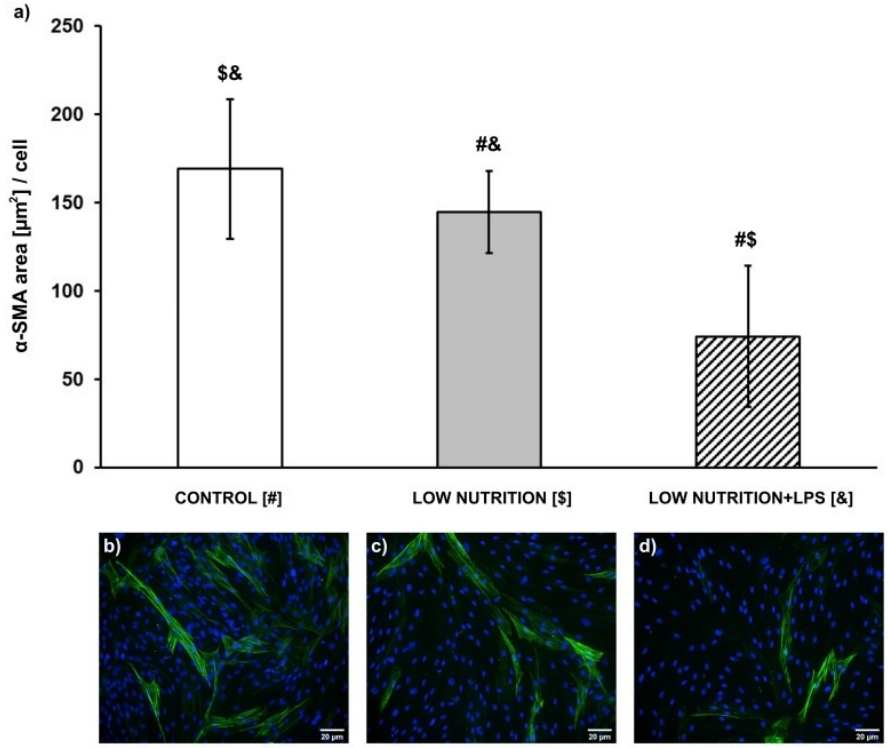

Figure 10 α-SMA expression by dermal fibroblasts is affected by the *low nutrition* and *low nutrition+LPS* wound stress factors. α-SMA was visualized by means of immunocytochemistry with fluorescence detection at day 5. The quantification of the α-SMA-positive cells (a) was normalized to the total cell number. The results are expressed as the mean of α-SMA-positive cells at day 5 normalized to the total cell number ± standard deviation (n=3). The α-SMA was stained by means of immunofluorescence (Alexa 488, green) and cell nuclei were stained with Hoechst #33342 (blue) in NHDF cultured in (b) *control*, (c) *low nutrition* and (d) *low nutrition+LPS* conditions. *Control* = medium with 10% of FBS; *low nutrition* = medium with 2% of FBS; *low nutrition+LPS* = medium with 2% of FBS and 0.1 µg/ml of LPS. # = a significant difference from the *control* group, $ = a significant difference from the *low nutrition* group, & = a significant difference from the *low nutrition+LPS* group, (One-way ANOVA; $p<0.05$ followed by Fisher's LSD test; $p<0.05$).

4.1.1.8 Collagen type I synthesis and visualization

The synthesis of intracellular collagen type I by NHDF was visualized using fluorescent microscopy after 5 days of cultivation under the *control*, *low nutrition* and *low nutrition+LPS* conditions. The production of collagen type I by NHDF was evaluated by means of ELISA from the culture media. The synthesis of intracellular collagen type I was found to be comparable under all the tested conditions (**Figure 11b-d**). The production of collagen type I increased during culturing in the *low nutrition+LPS*, *low*

nutrition and *control* media (**Figure 11a**); however, no difference was detected between the groups at any of the time points (Kruskal-Wallis test; $p<0.05$).

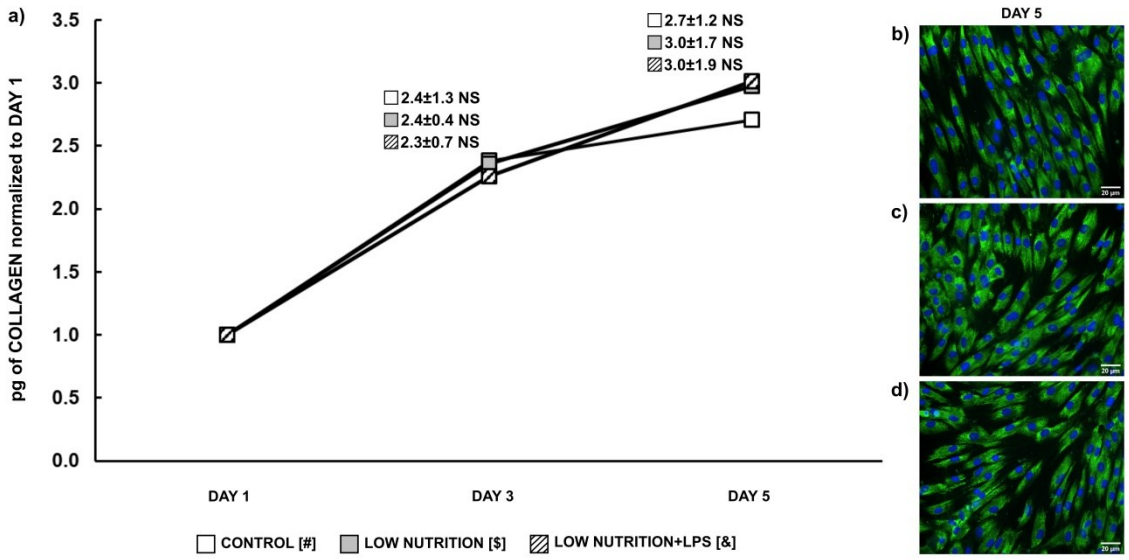

Figure 11 The synthesis and production of collagen type I by dermal fibroblasts is not affected by the neither of wound stress factors. The production of collagen type I was estimated by means of ELISA from the culture media (a). The change in the production of collagen type I is expressed as pg produced by 1 000 cells at days 1-5 divided by those produced by 1 000 cells at day 1. The results are expressed as the mean ± standard deviation (n=5-8). Visualization of intracellular collagen type I was performed at day 5 of NHDF cultivation under (b) *control*, (c) *low nutrition* and (d) *low nutrition+LPS* conditions. The collagen type I was visualized by means of immunofluorescence staining (Alexa 488, green). The cell nuclei were stained with Hoechst #33342 (blue). C*ontrol* = medium with 10% of FBS; *low nutrition* = medium with 2% of FBS; *low nutrition+LPS* = medium with 2% of FBS and 0.1 µg/ml of LPS. NS = no significant difference between particular groups (Kruskal-Wallis test; $p<0.05$).

4.1.2 Contamination by bacterial strains

4.1.2.1 Characterization of the bacterial strains

Characterized virulence factors of the bacterial strains associated with wound healing impairment are listed in **Table 2**. At least weak gelatinase production (+) was detected in all the tested strains. *PA2* showed high gelatinase activity (+++), the *SA* showed moderate gelatinase activity (++) and the *PA* showed weak gelatinase activity.

The only strain giving positive result in hyaluronidase production test was *SA* in low level. Hyaluronidase was not detected in *PA* and *PA2* strains.

Leukocidic activity was tested in all the strains in single strain cultures and in polybacterial cultures after overnight and 3 days (co-)cultivation. Only the *PA* and *SA* strains showed leukocidic activity when cultured overnight alone while the *PA2* did not. The polybacterial condition (*SA+PAcu)* showed leukocidic activity since the overnight culture. After 3 days of cultivation all the strains showed leukocidic activity when cultured alone.

Table 2 Gelatinase, hyaluronidase and leukocidic activity of the single strains *SA, PA,* and *PA2* and polybacterial conditions *SA+PAcu*; (+) – weak positive activity, (++) – moderate positive activity, (+++) – high positive activity, (-) – negative activity.

Bacterial strain	Gelatinase	Hyaluronidase	Leukocidic activity	
			Overnight	3 days
SA	++	+	+	+
PA	+	-	+	+
PA2	+++	-	-	+
SA+PAcu			+	+

4.1.2.2 Cell proliferation

The proliferation rate of NHDF was determined in the single strain bacterial conditions *SA*, *PA, PA2* of the same concentration (1.5 x 10^7 CFU/ml) (**Figure 12a**). The NHDF did not proliferate in *PA* conditions at days 2, 3 and 6 (1.08 ± 0.18 for day 2, 0.99 ± 0.34 for day 3 and 0.88 ± 0.27 for day 6) compared with *PA2* conditions (2.96 ± 0.39 for day 2, 4.11 ± 0.43 for day 3 and 4.70 ± 1.05 for day 6) and *ctrl* conditions (2.63 ± 0.31 for day 2, 3.56 ± 0.55 for day 3 and 4.04 ± 0.78 for day 6) (Kruskal-Wallis test; $p<0.05$; n=5-8).

The effect the three types of preparation of the polybacterial conditions on NHDF proliferation was evaluated by means of the total cell number determination (**Figure 12b**). The proliferation of NHDF was lower in all polybacterial conditions compared to *ctrl*. Significantly lower proliferation of NHDF was observed in *SA+PAmix* conditions at days 3 and 6 (2.38 ± 0.07 for day 3 and 2.25 ± 0.22 for day 5) compared with *ctrl* conditions (3.93 ± 0.45 for day 3 and 4.18 ± 0.35 for day 5) (Kruskal-Wallis test; $p<0.05$; n=3).

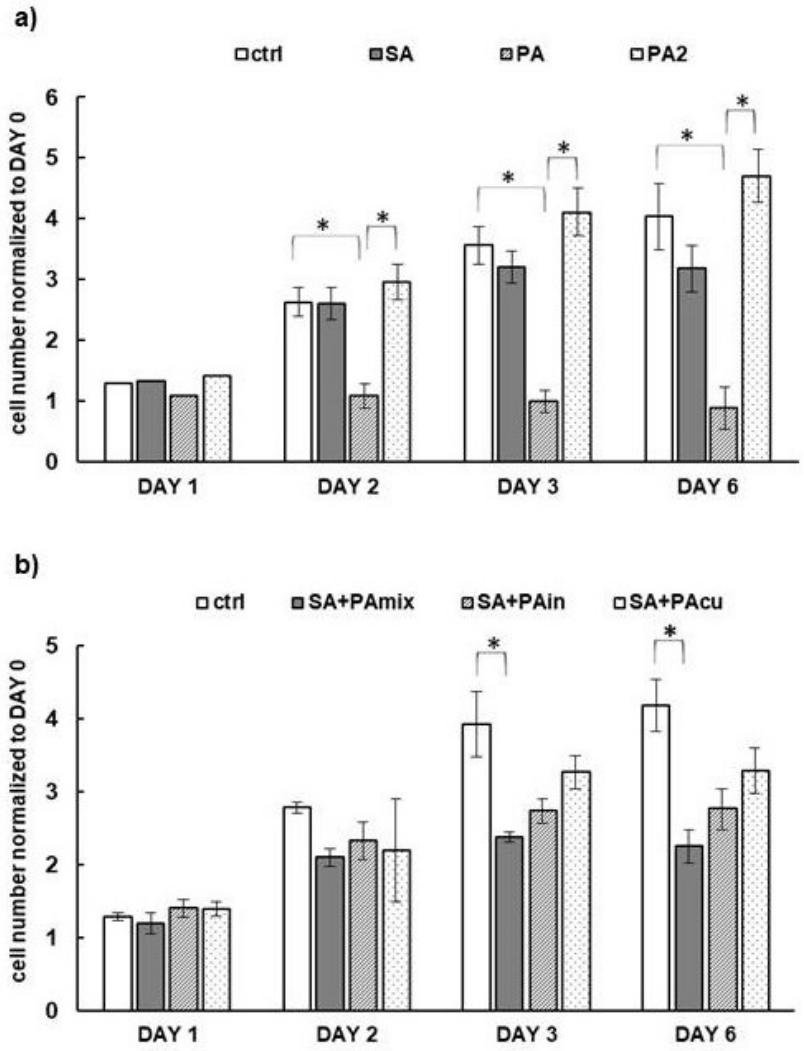

Figure 12 The proliferation of dermal fibroblasts is decreased in *PA* conditions at days 2, 3 and 6 compared to *SA* and *PA2* conditions of the same concentration of soluble factors. The proliferation of dermal fibroblasts is decreased in *SA+PAmix* conditions at day 3 and 6 compared to *SA+PAin*, *SA+PAcu* and *ctrl* conditions. Dermal fibroblasts were cultured (a) in the single strain bacterial conditions *SA, PA, PA2* of the 1.5×10^7 CFU/ml and (b) in polybacterial conditions *SA+PAin*, *SA+PAcu*, *SA+PAmix* of the 1.5×10^7 CFU/ml and *ctrl* conditions for 6 days. The proliferation rate was assessed by cell number determination every 24 hours and the change in the proliferation was expressed as a ratio of the cell number at days 1-6 to the cell number at day 0. The results are expressed as the mean ± standard deviation (n=3-8) (Kruskal-Wallis test; $p<0.05$). *Ctrl* = normal medium; *SA* = medium with soluble factors from *S. aureus*; *PA* = medium with soluble factors from *P. aeruginosa*, strain originated in the database; *PA2* = medium with soluble factors from *P. aeruginosa* originated in patient wound; *SA+PAmix* = medium with soluble factors from *SA* and *PA* cultivated separately, incubated separately, but mixed together just before application on the cells; *SA+PAin* = medium with soluble factors from *SA* and *PA* cultivated separately and incubated together*;* *SA+PAcu* = medium with soluble factors from *SA* and *PA* cultivated together and incubated together; * = a significant difference between particular groups.

4.1.2.3 Cell morphology

The effect of the bacterial conditions on NHDF morphology was evaluated by phase contrast microscopy. The cells were visualized at day 6 (**Figure 13**). NHDF exhibited normal morphology in *ctrl*, *PA*, *SA* and *SA+PAin* conditions, while the NHDF cultured in *SA+PAmix* and *SA+PAcu* conditions exhibited impaired morphology. In *SA+PAmix* conditions the NHDF were a little rounded after 6 days of the treatment, while in *SA+PAcu* conditions, the cells were shrunken and the culture comprised several dying cells. Interestingly, the decreased cell number in *SA+PAmix* conditions was apparent.

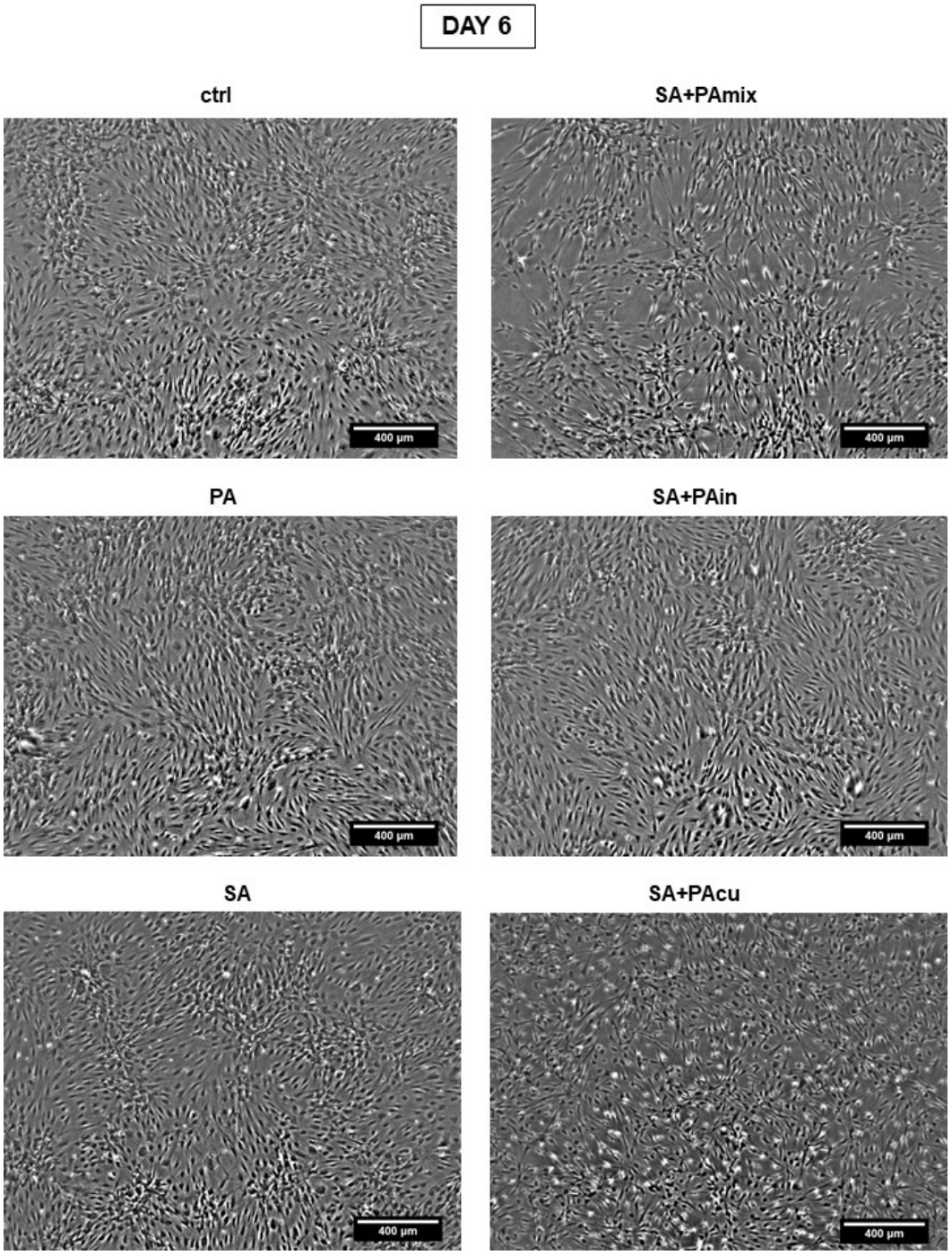

Figure 13 Cell morphology of the dermal fibroblasts is affected by *SA+PAcu* conditions 6 days after the treatment. Cell morphology was evaluated by phase contrast microscopy 6 days after the treatment. *Ctrl* = normal medium; *SA* = medium with soluble factors from *S. aureus; PA* = medium with soluble factors from *P. aeruginosa*, strain originated in the database*; SA+PAmix* = medium with soluble factors from *SA* and *PA* cultivated separately, incubated separately, but mixed together just before application on the cells; *SA+PAin* = medium with soluble factors from *SA* and *PA* cultivated separately and incubated together; *SA+PAcu* = medium with soluble factors from *SA* and *PA* cultivated together and incubated together. The scale bar represents 400 µm.

4.1.2.4 Migration

The effect of bacterial conditions on NHDF migration was evaluated by means of scratch wound assay. The NHDF migrated for 6 days and the wounded area was measured 1 day and 6 days following wounding using phase contrast microscopy (**Figure 14**). The single strain bacterial conditions exhibited no significant difference in NHDF migration neither the day after the treatment, nor 6 days after the treatment (**Figure 15a**). However, *PA* conditions slightly potentiated NHDF migration, although the effect was not significant. On the contrary, *SA+PAmix* conditions suppressed NHDF migration significantly after 6 days (79.02 ± 4.66%) compared to *ctrl* conditions (50.05 ± 9.64%) and to *SA+PAin* conditions (51.31 ± 0.30%). NHDF migration was not affected by *SA+PAin* and *SA+PAcu* conditions (**Figure 15b**) (One-way ANOVA; $p<0.05$ followed by Fisher´s LSD test; $p<0.05$; $n=3$).

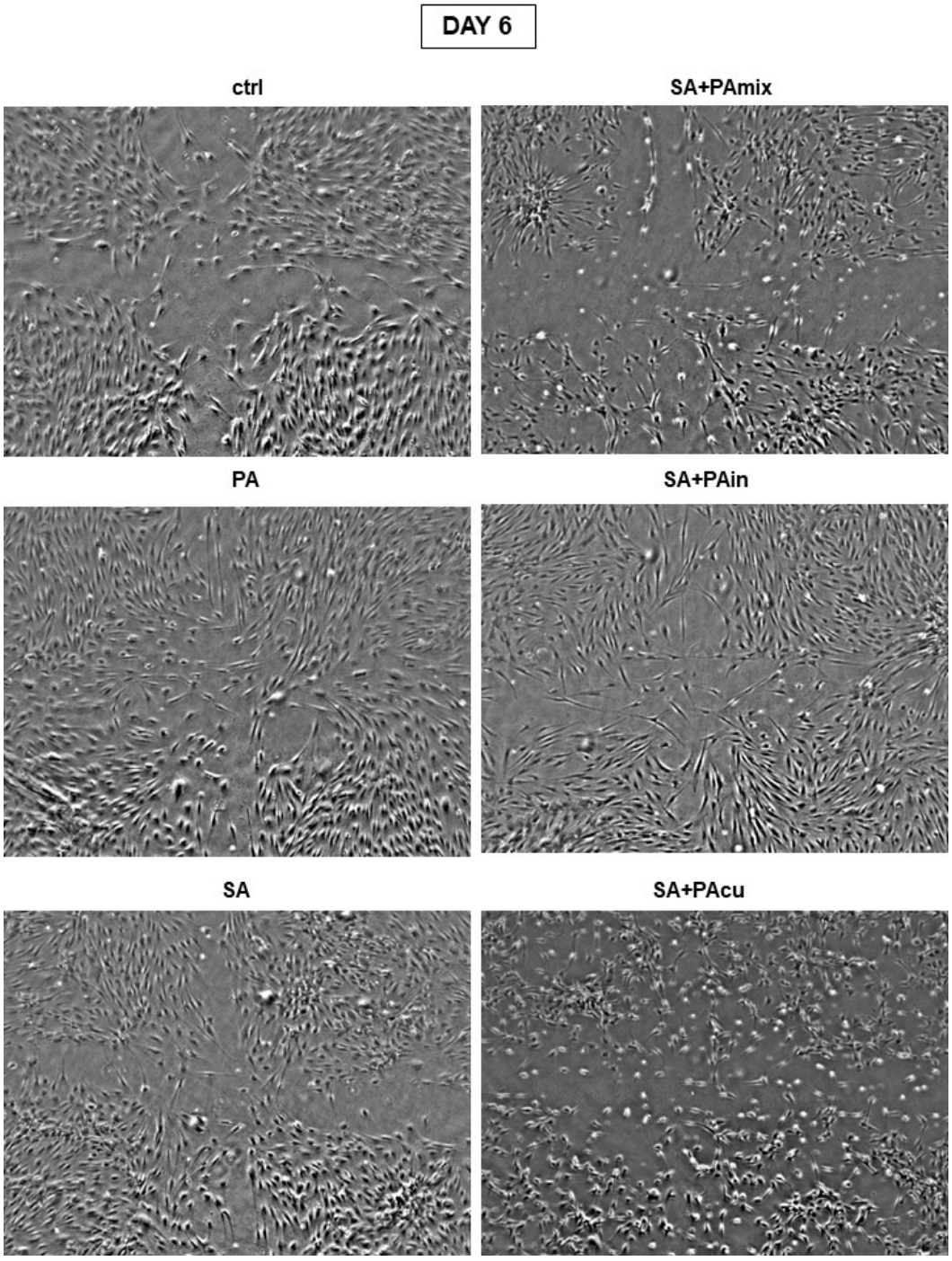

Figure 14 The migration of dermal fibroblasts is not affected by the single strain bacterial conditions (*PA, SA*), *SA+PAin* and *SA+PAcu* conditions, but is suppressed by *SA+PAmix* conditions when compared to *ctrl* conditions. Dermal fibroblasts were cultured in *PA*, *SA*, *SA+PAin*, *SA+PAcu*, *SA+PAmix* and *ctrl* conditions for 6 days. Migration was analyzed by scratch wound assay using phase contrast microscopy.

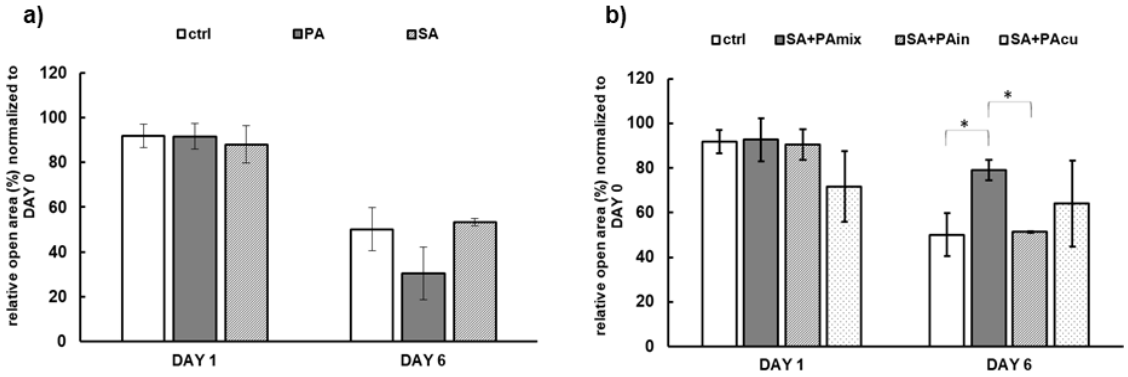

Figure 15 The migration of dermal fibroblasts is not affected by the single strain bacterial conditions (a), but is suppressed by *SA+PAmix* conditions when compared to *ctrl* and *SA+PAin* conditions (b). Dermal fibroblasts were cultured in *PA*, *SA*, *SA+PAin*, *SA+PAcu*, *SA+PAmix* and *ctrl* conditions for 6 days. Migration was analyzed by scratch wound assay. The wounded area (in %) was calculated as a ration of the open area at day 6 to the open area at day 0. The results are expressed as the mean ± standard deviation (n=3) (One-way ANOVA; $p<0.05$ followed by Fisher´s LSD test; $p<0.05$). *Ctrl* = normal medium; *SA* = medium with soluble factors from *S. aureus; PA* = medium with soluble factors from *P. aeruginosa*, strain originated in CCM*; SA+PAmix* = medium with soluble factors from SA and PA cultivated separately, incubated separately, but mixed together just before application on the cells; *SA+PAin* = medium with soluble factors from *SA* and *PA* cultivated separately and incubated together; *SA+PAcu* = medium with soluble factors from *SA* and *PA* cultivated together and incubated together; * = a significant difference.

4.1.2.5 Pro-inflammatory cytokine IL6 and IL8 production

The pro-inflammatory response of the NHDF to bacterial conditions was estimated via the quantification of IL6 and IL8 in the cell culture media and normalized to 1 000 cells at time points of 1 and 6 days. The production of IL6 and IL8 by NHDF was compared a) in different types of polybacterial conditions (*SA+PAmix*, *SA+PAin* and *SA+PAcu*), b) in bacterial conditions of the same concentration of soluble factors (1.5×10^7 CFU/ml) from two species (*SA* and *PA*) and c) in *PA* conditions of two concentrations – *PA 1.5* (1.5×10^7 CFU/ml) and *PA 0.25* (0.25×10^7 CFU/ml).

The different types of polybacterial conditions did not affect the production of IL6 by NHDF neither at day 1, nor at day 6 (**Figure 16a**). NHDF cultured in *PA* conditions for 6 days produced significantly higher amount of IL6 compared to *SA* and *ctrl*, when the production of IL6 was 11.8 ± 9.0 (*PA*, n=5), 2.9 ± 1.5 (*SA*, n=6) and 2.5 ± 1.3 (*ctrl*, n=6) (**Figure 16b**). NHDF cultured in 1.5×10^7 CFU/ml *PA* conditions produced significantly higher amount of IL6 compared with the production in 0.25×10^7 CFU/ml *PA* conditions at day 6, when the production was 11.8 ± 9.0 (*PA 1.5*, n=5)

and 3.0 ± 1.5 (*PA 0.25*, n=4) (**Figure 16c**) (Kruskal-Wallis test; $p<0.05$). The production of IL6 by the NHDF did not change in time.

The different types of polybacterial conditions did not affect the production of IL8 by NHDF neither at day 1, nor at day 6 (**Figure 17a**). NHDF cultured in *PA* conditions for 6 days produced significantly higher amount of IL8 compared to *SA*, when the production of IL8 was 8.4 ± 7.0 (*PA*, n=4) and 1.3 ± 0.3 (*SA*, n=6) (**Figure 17b**). NHDF cultured in *PA 1.5* conditions produced significantly higher amount of IL8 compared with *ctrl* at day and 6, when the production was 8.1 ± 3.5 (*PA 1.5*, n=4) and 2.6 ± 1.9 (*ctrl*, n=6) at day 1 and 8.4 ± 7.0 (*PA 1.5*, n=4) and 1.6 ± 0.7 (*ctrl*, n=6) at day 6, while NHDF cultured in *PA 0.25* conditions did not increase (**Figure 17c**) (Kruskal-Wallis test; $p<0.05$). The production of IL8 by the NHDF did not change in time.

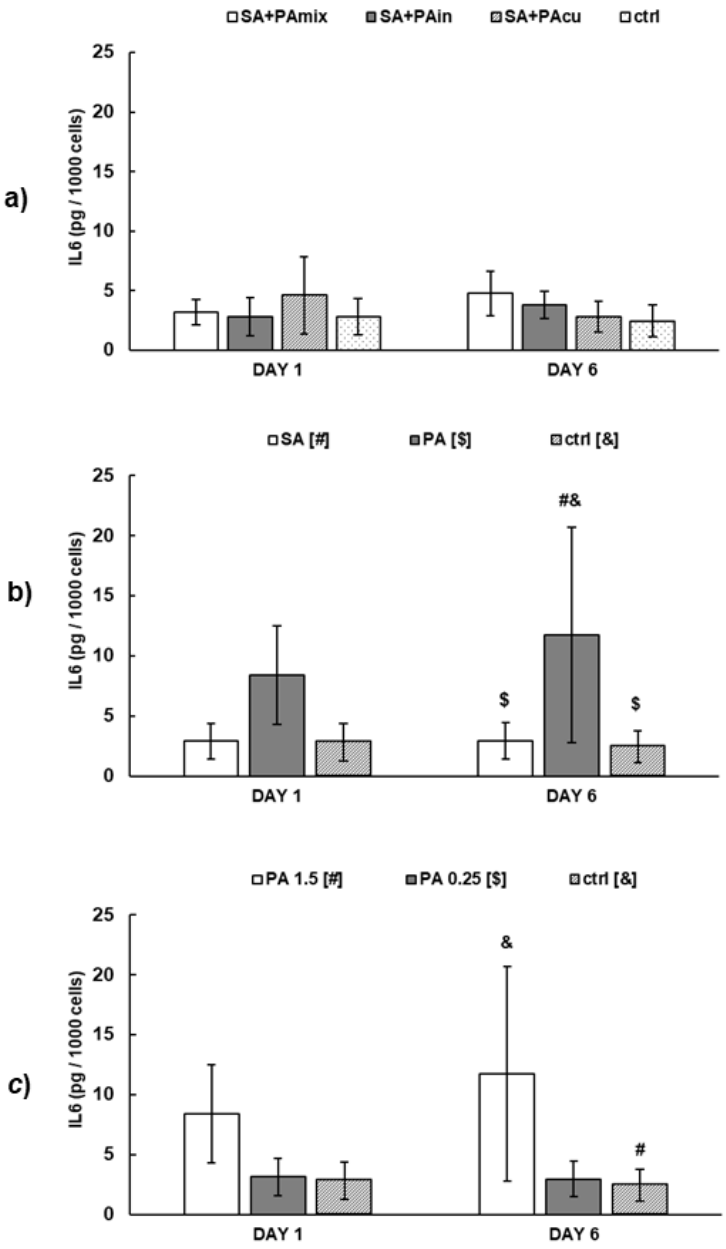

Figure 16 The production of IL6 by dermal fibroblasts is not affected by polybacterial conditions at day 1 and 6 (a). The production of IL6 is potentiated by *PA* conditions compared with *SA* and *ctrl* conditions at day 6 (b). The increase in IL6 production is dependent on the concentration of bacterial soluble factors in the media (c). The production of IL6 was estimated by ELISA. The change in the production of IL6 is expressed as pg of IL6 produced by 1 000 cells at days 1 and 6. The results are expressed as the mean ± standard deviation (n=4-6) (Kruskal-Wallis test; $p<0.05$). *Ctrl* = normal medium; *SA* = medium with soluble factors from *S. aureus*; PA = medium with soluble factors from *P. aeruginosa*, strain originated in CCM; *SA+PAmix* = medium with soluble factors from *SA* and *PA* cultivated separately, incubated separately, but mixed together just before application on the cells; *SA+PAin* = medium with soluble factors from *SA* and *PA* cultivated separately and incubated together; *SA+PAcu* = medium with soluble factors from *SA* and *PA* cultivated together and incubated together. # = a significant difference from the *PA 1.5* group, $ = a significant difference from the *PA 0.25*, & = a significant difference from the *ctrl* group.

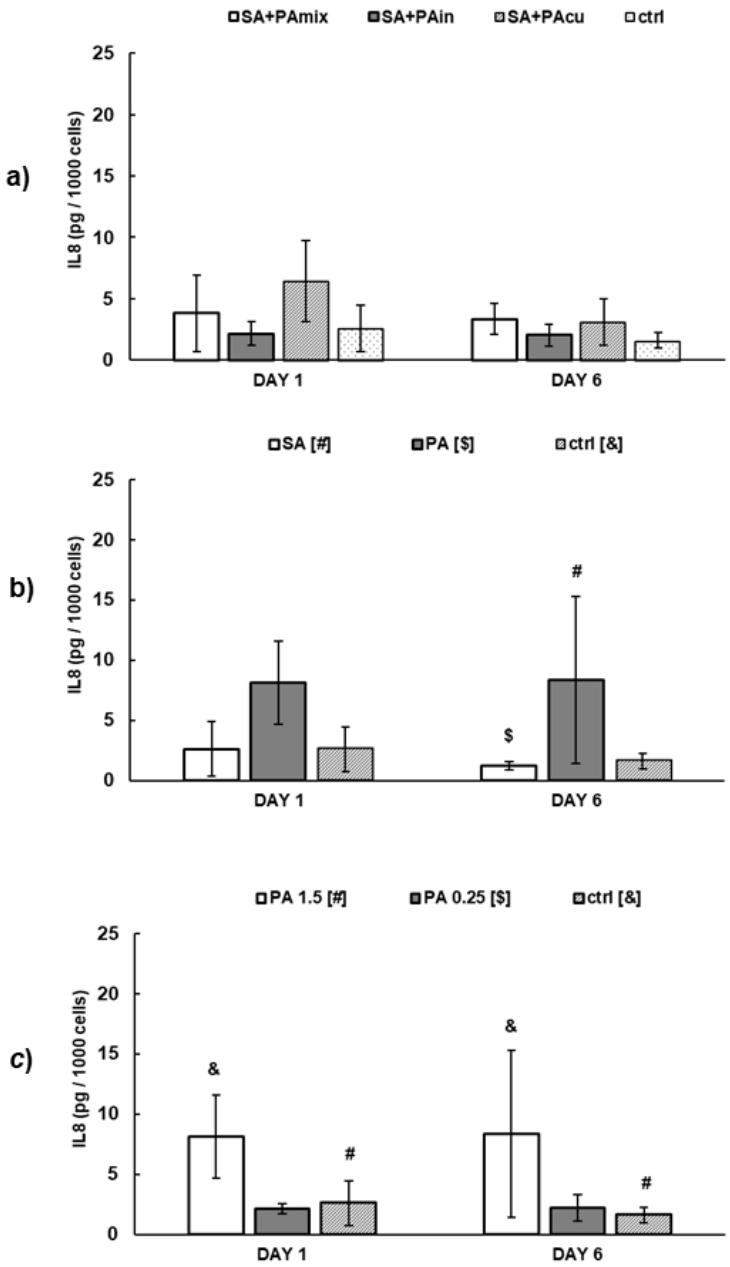

Figure 17 The production of IL8 by dermal fibroblasts is not affected by polybacterial conditions at day 1 and 6 (a). The production of IL8 is potentiated by *PA* conditions compared with *SA* conditions at day 6 (b). The increase in IL8 production is dependent on the concentration of bacterial soluble factors in the media at day 1 and 6 (c). The production of IL8 was estimated by ELISA. The change in the production of IL8 is expressed as pg of IL8 produced by 1 000 cells at days 1 and 6. The results are expressed as the mean ± standard deviation (n=4-6) (Kruskal-Wallis test; $p<0.05$). *Ctrl* = normal medium; *SA* = medium with soluble factors from *S. aureus*; PA = medium with soluble factors from *P. aeruginosa*, strain originated in CCM; *SA+PAmix* = medium with soluble factors from *SA* and *PA* cultivated separately, incubated separately, but mixed together just before application on the cells; *SA+PAin* = medium with soluble factors from *SA* and *PA* cultivated separately and incubated together; *SA+PAcu* = medium with soluble factors from *SA* and *PA* cultivated together and incubated together. # = a significant difference from the *PA 1.5* group, $ = a significant difference from the *PA 0.25*, & = a significant difference from the *ctrl* group.

4.1.2.6 Collagen type I synthesis

The structural function of the NHDF in bacterial conditions was estimated via the quantification of collagen type I and normalized to 1 000 cells at time points of 1 and 6 days. The production of collagen type I by NHDF was compared a) in different types of polybacterial conditions (*SA+PAmix*, *SA+PAin* and *SA+PAcu*), b) in bacterial conditions of the same concentration of soluble factors (1.5×10^7 CFU/ml) from two species (*SA* and *PA*) and c) in *PA* conditions of two concentrations – *PA 1.5* (1.5×10^7 CFU/ml) and *PA 0.25* (0.25×10^7 CFU/ml).

The different types of polybacterial conditions did not affect the production of collagen type I by NHDF neither at day 1, nor at day 6; however, the change in time was significantly higher at day 6 compared to day 1 in all tested conditions (**Figure 18a**). The production of collagen type I by NHDF cultured in *PA* and *SA* conditions for 6 days did not differ, however, the change in time was significantly higher at day 6 compared to day 1 in all tested conditions, (**Figure 18b**). The production of collagen type I by dermal fibroblasts was not dependent on the concentration of bacterial soluble factors in the media at day 1 and 6; however, the change in time was significantly higher at day 6 compared to day 1 in all tested conditions (**Figure 18c**) (Mann-Whitney U test; $p<0.05$ for the same group-between time points testing).

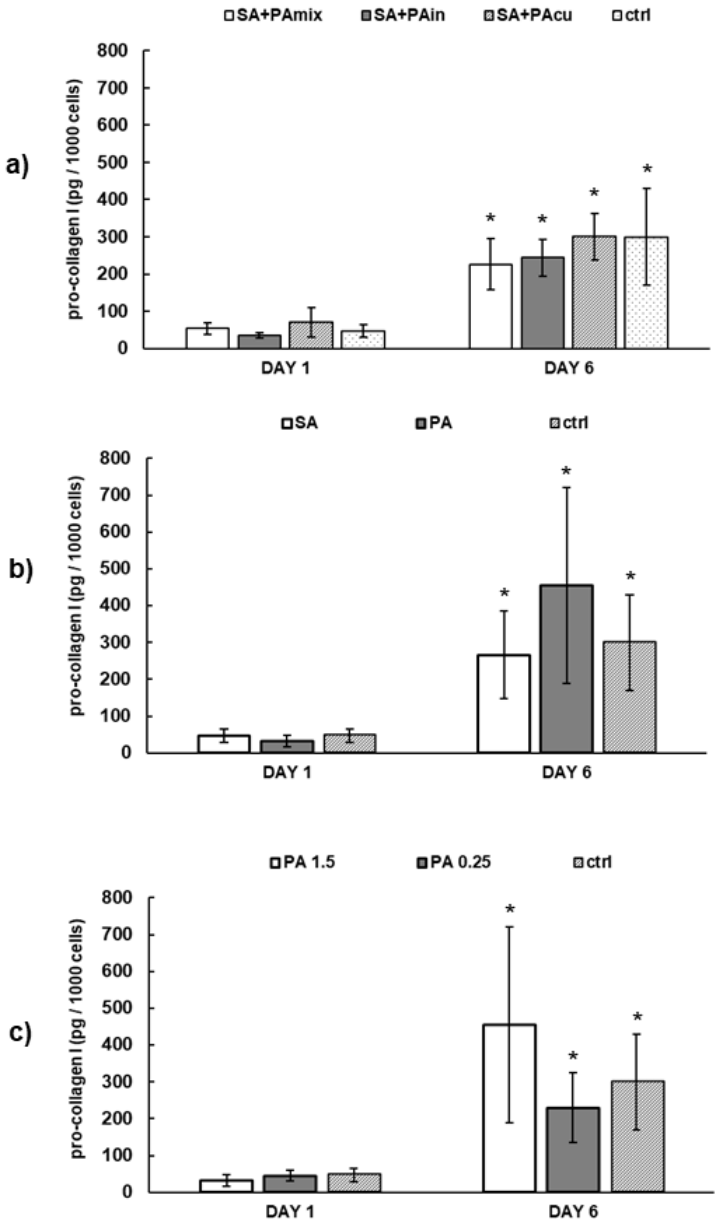

Figure 18 The production of collagen type I by dermal fibroblasts treated by (a) polybacterial conditions or (b) *PA* and *SA* conditions is not affected within each time point 1 and 6 days, but the change in time is significantly higher in all tested conditions. The production of collagen type I by dermal fibroblasts is not dependent on the concentration of bacterial soluble factors in the media at day 1 and 6 (c). The production of collagen type I was estimated by ELISA. The change in the production of collagen type I is expressed as pg of collagen type I produced by 1 000 cells at days 1 and 6. The results are expressed as the mean ± standard deviation (n=4-6) (Mann-Whitney U test; $p<0.05$). * = significant difference of the value at day 6 compared to the value of the same group at day 1. *Ctrl* = normal medium; *SA* = medium with soluble factors from *S. aureus*; PA = medium with soluble factors from *P. aeruginosa*, strain 1; *SA+PAmix* = medium with soluble factors from SA and PA cultivated separately, incubated separately, but mixed together just before application on the cells; *SA+PAin* = medium with soluble factors from SA and PA cultivated separately and incubated together; *SA+PAcu* = medium with soluble factors from SA and PA cultivated together and incubated together.

4.2 Response of fibroblasts to normal and wound conditions in 3D culture

4.2.1 Normal culture conditions

4.2.1.1 Collagen hydrogel contraction by dermal fibroblasts

The contraction ability of the NHDF was evaluated via the diameter measurement of collagen hydrogels seeded with NHDF and compared with collagen hydrogels without NHDF at time points of 7, 14, 21 and 28 days (**Figure 19a**). The contraction of the collagen hydrogels was promoted by NHDF significantly at each time point, when the cell-seeded collagen hydrogel diameter was 9.3 ± 0.6 mm at day 7, 8 ± 0.5 mm at day 14, 6 ± 1.2 mm at day 21 and 5.2 ± 1.0 mm at day 28, while the diameter of collagen hydrogels without cells was 13.2 ± 0.8 mm at day 7, 13.4 ± 0.5 mm at day 14, 12.5 ± 0.7 mm at day 21 and 12.8 ± 1.2 mm at day 28 (Wilcoxon paired test; $p<0.05$). The change in the collagen hydrogel diameter forced by NHDF was visible to the naked eye for each time point (**Figure 19b**).

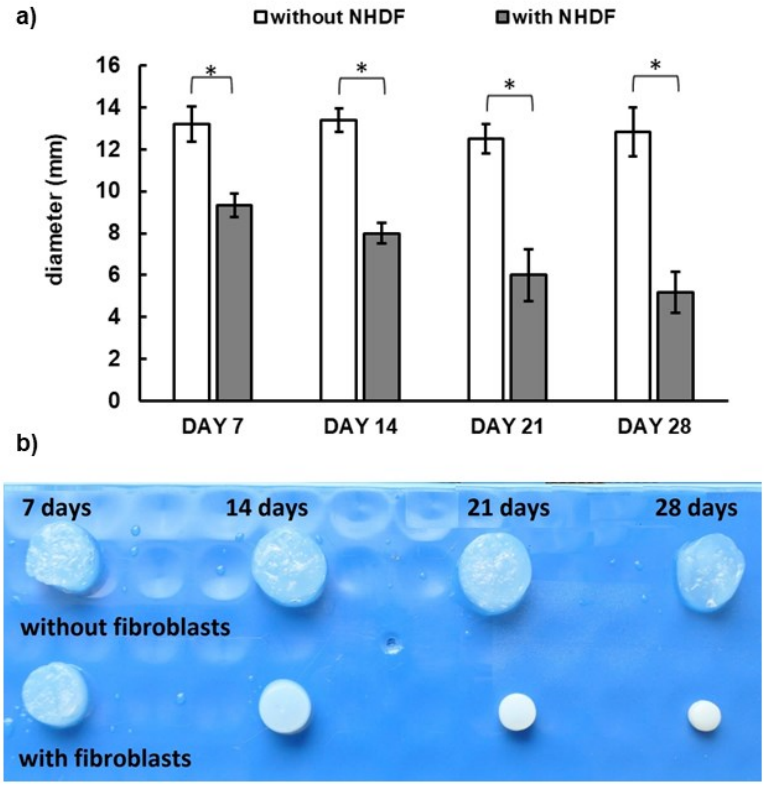

Figure 19 Dermal fibroblasts promote contraction of the collagen hydrogels. The diameter of the collagen hydrogels decreases in time. The contraction ability was measured by diameter measurement of the collagen hydrogels in time points 7, 14, 21 and 28 days. The results are expressed as the mean ± standard deviation (n=4-8). * = a significant difference between particular groups (Wilcoxon paired test; $p<0.05$).

4.2.1.2 Metabolic activity

Metabolic activity of NHDF in 3D culture (collagen hydrogels) was compared with the metabolic activity of NHDF in 2D cell culture (plastic plates) by means of AlamarBlue assay. NHDF were cultured 6 days in both 2D and 3D environment and the metabolic activity was estimated after 0, 1, 2, 3 and 6 days (**Figure 20**). NHDF in 3D culture exhibited no significant difference in metabolic activity compared with NHDF in 2D culture. The metabolic activity of NHDF had an increasing tendency in both types cultures (Mann-Whitney U test; $p<0.05$).

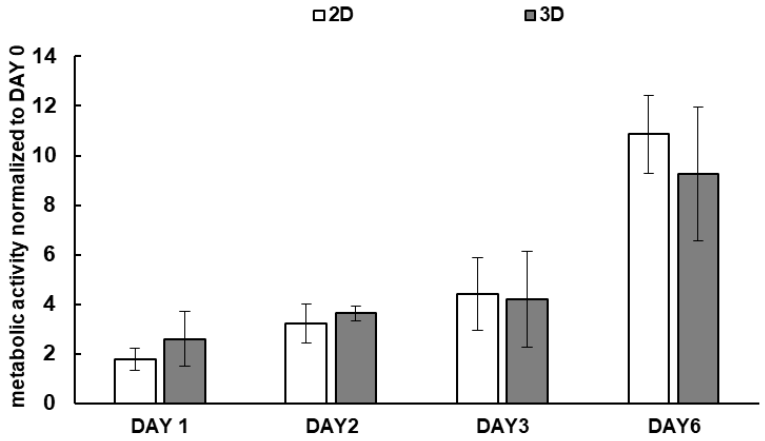

Figure 20 The metabolic activity of dermal fibroblasts cultured in 3D does not differ from metabolic activity of dermal fibroblasts in 2D culture and is increasing in time in both types of culture. Dermal fibroblasts were cultured in 2D and 3D conditions for 6 days. The cell metabolic activity was measured by AlamarBlue assay every 24 hours and the change in the metabolic activity was expressed as a ratio of the signal at days 1-6 to the signal at day 0. The results are expressed as the mean ± standard deviation (n=4-8) (Mann-Whitney U test; $p<0.05$).

4.2.1.3 Cell proliferation

Proliferation of NHDF in 3D culture (collagen hydrogels) was compared with the proliferation of NHDF in 2D cell culture (plastic plates) by means of fluorescent signal measurement of a Calcein-AM stained NHDF after collagen hydrogel digestion (in the case of 3D cultures). NHDF were cultivated 6 days in both 2D and 3D cultures and the proliferation was estimated after 0, 1, 2, 3 and 6 days (**Figure 21**). The proliferation of NHDF in 3D culture did not differ from the proliferation of the cells in 2D culture significantly at each time point (Mann-Whitney U test; $p<0.05$).

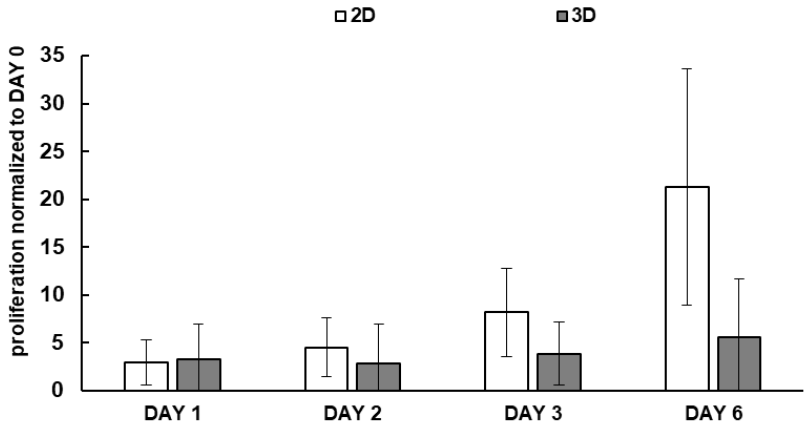

Figure 21 The dermal fibroblasts cultured in 3D does not proliferate in time. The cells were cultured in 2D and 3D environment for 6 days. The cell proliferation was estimated after collagen digestion (in the case of 3D cultures) and dermal fibroblasts´ fluorescence staining (Calcein-AM) and lysis every 24 hours. The change in the proliferation was expressed as a ratio of the signal at days 1-6 to the signal at day 0. The results are expressed as the mean ± standard deviation (n=3) (Mann-Whitney U test; $p<0.05$).

4.2.1.4 Cell morphology

The comparison of NHDF morphology in 2D and 3D culture was observed the day after seeding by phase contrast microscopy (**Figure 22a**) and fluorescence microscopy after Calcein-AM staining (**Figure 22b**). In 2D culture, the NHDF were flattened and spindle-shaped while in 3D culture the NHDF were elongated and stellate.

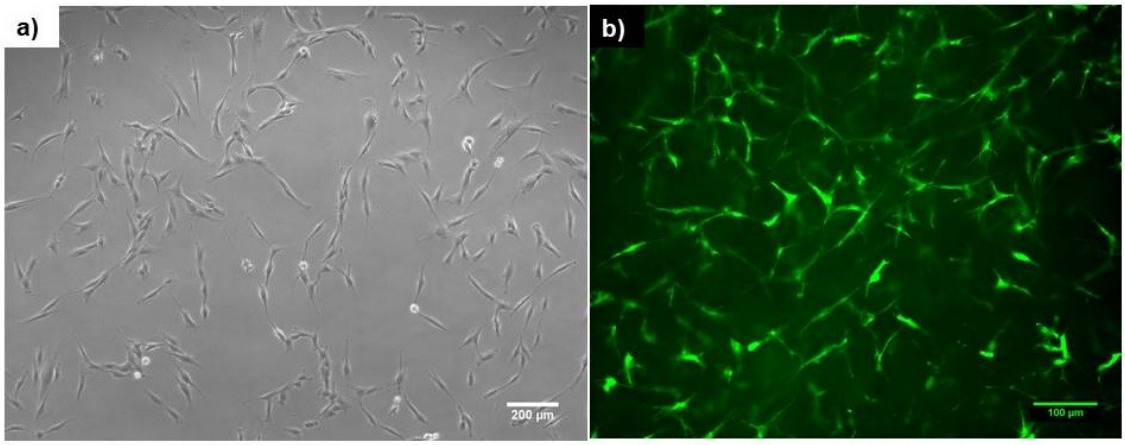

Figure 22 The morphology of dermal fibroblasts in 2D and 3D culture is spindle-shaped. The morphology was observed by phase contrast microscopy (left) and by fluorescence microscopy after Calcein-AM staining of the cells (right) the day after seeding. The spindle-shaped morphology of the cells was more flattened in (a) 2D culture (plastic plate) compared to more elongated and stellate cells in (b) 3D culture (collagen hydrogels). The scale bar represents 200 µm.(left), 100 µm (right).

4.2.2 Low nutrition and inflammation

4.2.2.1 Collagen hydrogel contraction by dermal fibroblasts

The impact of *low nutrition* and *low nutrition+LPS* conditions on the contraction ability of the NHDF was evaluated via the diameter measurement of cell-seeded collagen hydrogels at time points of 3, 6 and 13 days (**Figure 23**). After 1 day and 6 days culturing under the *control*, *low nutrition* and *low nutrition+LPS* conditions, the contraction ability of the NHDF was found not to have changed. After 13 days of culturing, the highest NHDF contraction ability was observed in the *control* medium with a scaffold diameter of 10.27 ± 1.3 mm (*control*) versus 11.60 ± 0.99 mm (*low nutrition*) and 11.89 ± 1.33 mm (*low nutrition+LPS*) (Kruskal-Wallis test; $p<0.05$).

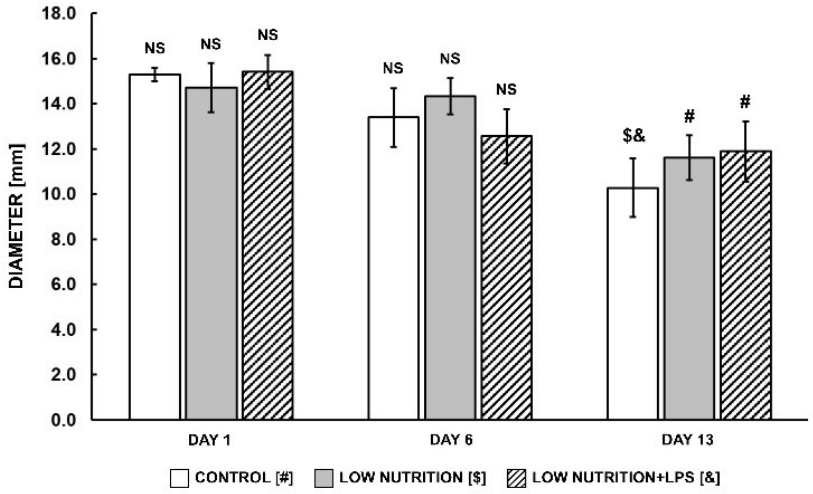

Figure 23 The contraction ability of dermal fibroblasts is affected by both the *low nutrition* and *low nutrition+LPS* wound stress factors. The contraction ability was estimated from changes in the diameter of cell-seeded collagen hydrogels at distinct time points. The diameters of the hydrogels were measured at days 1, 6 and 13. The results are expressed as the mean ± standard deviation (n=6) (Kruskal-Wallis test; $p<0.05$). *Control* = medium with 10% of FBS; *low nutrition* = medium with 2% of FBS; *low nutrition+LPS* = medium with 2% of FBS and 0.1 μg/ml of LPS. # = a significant difference from the *control* group, $ = a significant difference from the *low nutrition* group, & = a significant difference from the *low nutrition+LPS* group, NS = no significant difference between particular groups.

4.2.2.2 Metabolic activity

Metabolic activity of NHDF in 3D culture under *low nutrition+LPS* conditions was compared with the metabolic activity of NHDF in 3D culture in *control* conditions as well as in 2D conditions. NHDF were cultured in the conditions 6 days and the metabolic activity was estimated after 0, 1, 2, 3 and 6 days by AlamarBlue assay (**Figure 24**). NHDF cultured under *low nutrition+LPS* conditions exhibited no significant difference in metabolic activity compared with NHDF cultured in *control* conditions in both 2D and 3D culture (Mann-Whitney U test; $p<0.05$).

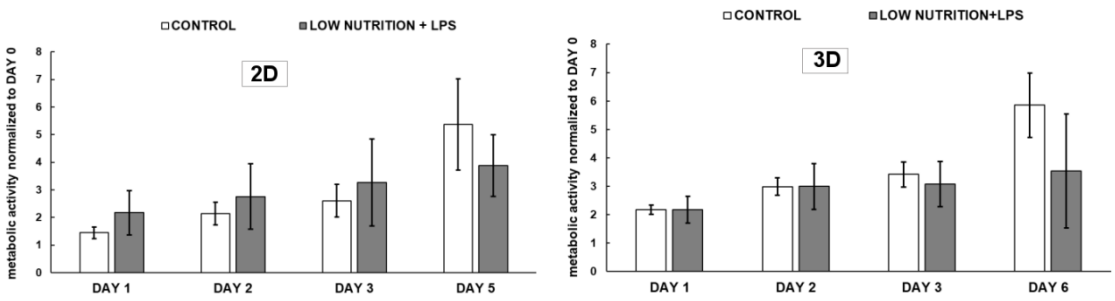

Figure 24 The metabolic activity of NHDF in 2D and 3D culture is not affected by *low nutrition+LPS* conditions. NHDF were cultured in *low nutrition+LPS* and *control* conditions in 3D culture for 6 days. The cell metabolic activity was measured by AlamarBlue assay every 24 hours and the change in the metabolic activity was expressed as a ratio of the signal at days 1-6 to the signal at day 0. The results are expressed as the mean ± standard deviation (n=8 for 2D culture; n=3 for 3D culture) (Mann-Whitney U test; $p<0.05$).

4.2.2.3 Cell proliferation

Proliferation of NHDF under *low nutrition+LPS* and *control* conditions in 2D culture was compared to the 3D culture by means of fluorescent signal measurement of a Calcein-AM stained NHDF after collagen hydrogel digestion (in the case of the 3D culture) (**Figure 25**). NHDF did not proliferate under *low nutrition+LPS* conditions in both 2D and 3D cultures. In *control* conditions the proliferation tended to be increasing in time in 2D culture while the proliferation of NHDF in 3D culture was non-increasing. However, the difference was not significant at any time point (Mann-Whitney U test; $p<0.05$).

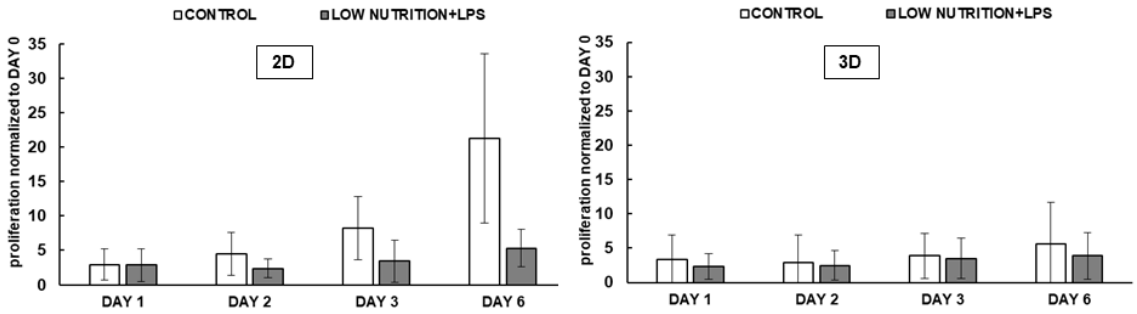

Figure 25 The proliferation of NHDF in 2D and 3D cultures is not affected by *low nutrition+LPS* conditions. NHDF were cultured in *low nutrition+LPS* and *control* conditions in 2D and 3D cultures for 6 days. The cell proliferation was estimated after collagen digestion (in the case of 3D culture) and dermal fibroblasts´ fluorescence staining (Calcein-AM) and lysis every 24 hours. The change in the proliferation was expressed as a ratio of the signal at days 1-6 to the signal at day 0. The results are expressed as the mean ± standard deviation (n=3) (Mann-Whitney U test; $p<0.05$).

4.3 Optimization of selected methods necessary for the following research

4.3.1 Cell number determination in 2D culture

We optimized the image analysis for the cell number determination in Fiji software from the compiled pictures of cell nuclei in the whole well area, since the up to date available methods use only estimation of nuclei count from selected visual fields of the well area. Our method was used for further cell number determination of NHDF and monitoring of the cell proliferation in the experiments. The example of the data processing from four NHDF donors is to be found in **Table 3**.

Table 3 Cell number determined by fluorescence microscopy followed by image analysis in Fiji software from 4 independent donors the day after seeding of 2 000 cells/well (N = number of technical repetitions; SD = standard deviation; CV = coefficient of variation).

	cell number			
N	**donor 1**	**donor 2**	**donor 3**	**donor 4**
1	2129	2339	2279	2501
2	2076	2125	2238	2627
3	2245	2239	2618	2656
4	2009	2365	2526	2632
5	2238	2400	2703	2710
6	2302	2377	2720	2623
7	2463	2314	2825	2647
8	2011	2572	2882	2599
mean	**2184**	**2341**	**2599**	**2624**
SD	**158**	**129**	**238**	**59**
CV [%]	**7.21**	**5.51**	**9.14**	**2.27**

4.3.2 Cell number determination in 3D culture

The cell-seeded collagen hydrogels were stained with DAPI after fixation and the unbiased (accurate) method for cell number determination was developed using stereological principles for cell sampling and freely available Fiji software for image analysis. Determined cell numbers were equal to the seeding densities of 125 000, 250 000 and 375 000 cells in collagen hydrogel, while for 10 000 cells in collagen

hydrogel did not (verified by the One-sample t-test; $p<0.05$) (**Table 4**). The data distribution is visualized (**Figure 26)** for seeding densities a) 10 000 cells, b) 125 000 cells, c) 250 000 cells and d) 375 000 cells.

Table 4 Comparison of cell seeding densities and corresponding cell numbers determined with the use of Fiji software (N = number of technical repetitions; SD = standard deviation). The mean of the determined cell count is equal to the seeding densities 125 000, 250 000 and 375 000 cells, while the mean of the determined cell count is not equal to the seeding density of 10 000 cells (One-sample t-test; $p<0.05$).

seeding density (cells in collagen hydrogel)	cell number evaluated by Fiji software		
	mean	SD	N
10 000	13 851	2 505	18
125 000	121 020	11 182	19
250 000	232 027	46 292	17
375 000	455 095	133 195	7

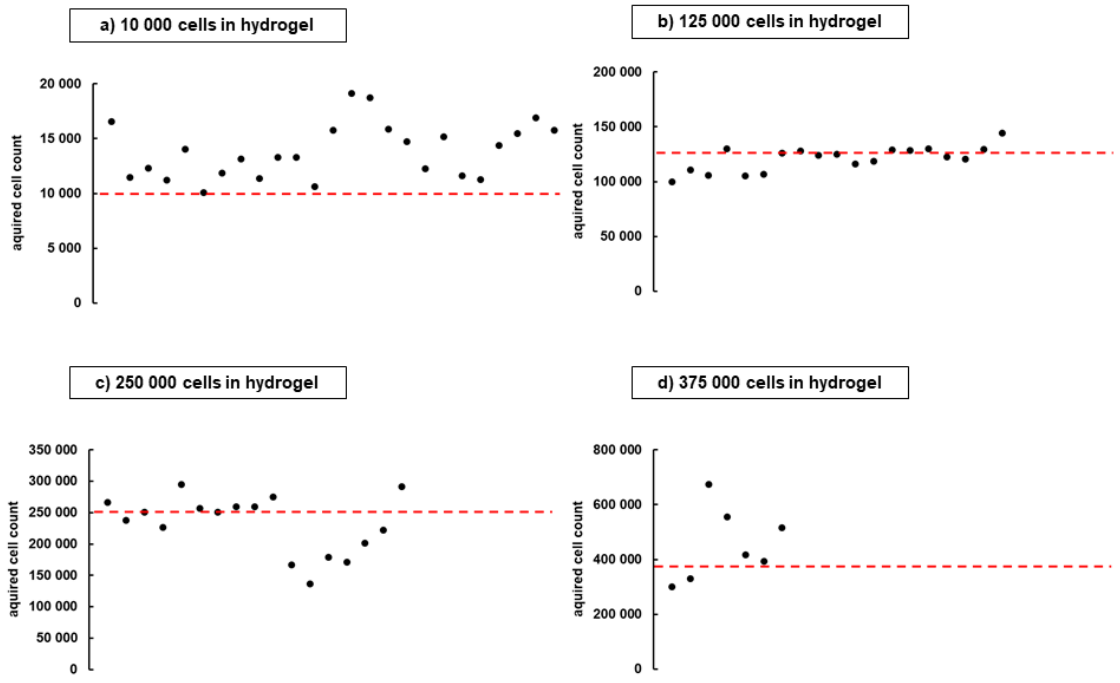

Figure 26 The data distribution of the cell number determined by Fiji software for seeding densities a) 10 000, b) 125 000, c) 250 000 and d) 375 000 cells in collagen hydrogel. Each point represents one collagen hydrogel.

5. DISCUSSION

The response of dermal fibroblasts on the two key stress factor, low nutrition and LPS, was studied. As an extension, two bacterial species were used for simulating of wound contamination since not only G^- bacteria LPS is present in non-healing wounds. G^+ *S. aureus* and G^- *P. aeruginosa* were used separately or in combination as a model of polybacterial conditions. The response of dermal fibroblasts exposed to the bacterial soluble factors was described.

The functions of dermal fibroblasts in 3D culture were compared to those of in 2D culture. Moreover, the impact of the simultaneously acting low nutrition with LPS on dermal fibroblasts in 3D culture was described.

In addition, the two methods for the determination of the cell number in 2D and 3D culture were developed as a tool for cell proliferation examination since we realized that methods for determination of the total cell count in a whole sample is missing.

5.1 Response of fibroblasts to wound conditions in 2D culture

5.1.1 Low nutrition and inflammation

The approach taken herein involved the study of dermal fibroblast responses to low nutrition and inflammation. We studied the impact of the *low nutrition* (medium containing 2% of FBS) and the *low nutrition+LPS* (medium containing 2% of FBS and 0.1 μg/ml of LPS). The parameters used to describe the behavior of the dermal fibroblasts consisted of metabolic activity, proliferation, cell morphology, migration, the production of the IL6 and IL8 pro-inflammatory cytokines, production of MMP2 and MMP9, synthesis of contractile marker α-SMA and the production of collagen type I.

The dermal fibroblasts cultured under *low nutrition* conditions exhibited a slightly higher metabolic activity level than those cultured under the *control* conditions; however, the increase was significant at day 3 only. When dermal fibroblasts were cultured in *low nutrition* conditions (a medium with 0.1% of FBS) a quiescence phenotype in dermal fibroblasts occurred and pathways generating NADPH were induced (Lemons et al., 2010). AlamarBlue, the substrate used in this study for the estimation of metabolic activity, can be reduced by NADPH (Rampersad, 2012). Therefore, we hypothesize that *low nutrition* conditions (a culture medium with 2% of FBS) induce a quiescence phenotype and that the metabolic activity of the dermal fibroblasts under *low nutrition* and *low nutrition+LPS* conditions is paradoxically increased due to the generation of increased levels of NADPH produced by activated metabolic pathways. The available results describing the metabolic activity response of fibroblasts on LPS in the culture media are inconsistent. 0.2 μg/ml of LPS in a serum-free medium that contained another components supporting proliferation and plating efficiency did not affect the metabolic activity of dermal fibroblasts (Eleftheriadis et al., 2011). 10 μg/ml of LPS in a medium with 10% of FBS decreased the metabolic activity of gingival fibroblasts (Basso et al., 2015) or 25 μg/ml of LPS in a medium containing 10% of FBS increased the metabolic activity of gingival fibroblasts (Xi et al., 2016). The inconsistency in available data is probably caused by different source of fibroblasts and by different experimental set up. Therefore we cannot generalize the effect of LPS

on dermal fibroblasts and we have to stay only with the results from our experimental set up and correlate them with our other results.

Our results showed that dermal fibroblasts did not proliferate under *low nutrition* and *low nutrition+LPS* conditions compared to *control* conditions. Similarly, a serum free medium exhibited a sharp decrease in the cell count (Ejiri et al., 2015). Regarding the addition of LPS, 1 μg/ml of LPS in a medium containing 10% of calf serum increased the proliferation of mouse lung fibroblasts (He et al., 2012). On the other hand, 10 μg/ml of LPS in a medium with 10% FBS decreased the proliferation of gingival fibroblasts (Basso et al., 2015). Based on the information provided in the studies mentioned above, we propose that the 0.1 μg/ml of LPS used in this thesis was too low concentration to exert an impact on the proliferation of dermal fibroblasts. Thus, we conclude that the dermal fibroblasts in our study did not proliferate due to the *low nutrition* conditions rather than the presence of LPS, which is supported by the results obtained by Ejiri et al. Importantly, the comparison of the metabolic activity and proliferation presented in our paper provided evidence that while the two methods are sometimes erroneously interchanged (Cai et al., 2010; Zhang et al., 2011; Xi et al., 2016), the metabolic activity is not the same as proliferation. While the dermal fibroblasts under both *low nutrition* and *low nutrition+LPS* conditions exhibited increasing metabolic activity, they did not proliferate, which suggests that the culturing conditions of the experiment have the potential to increase the metabolic activity of the cells as a reflection of cellular activity aimed at overcoming the "uncomfortable" culturing conditions accompanied by the non-proliferative state of the cells.

The dermal fibroblasts (3^{rd} passage) under *low nutrition* and *low nutrition+LPS* conditions retained the normal morphology for 5 days. Yang et al. observed diversified morphological changes in the ultrastructure of fibroblasts after 0.1 μg/ml LPS treatment dependent on the increasing passage (4^{th} – 10^{th}) of the cells. Interestingly, the morphological changes in treated fibroblasts mimicked the morphology of fibroblasts isolated from hypertrophic scars (Yang et al., 2013). Unfortunately, the authors did not state the duration of the LPS treatment. In our study, we did not observe any morphological changes in dermal fibroblasts (4^{th} passage) isolated from a different donor (data not shown).

Scratch wound assay was found to provide an appropriate method for the assessment of cell migration into the wounded area (Liang et al., 2007). We demonstrated that dermal fibroblasts cultured in the presence of LPS migrate to a greater extent than do dermal fibroblasts cultured without LPS. The enhanced migration rate of mouse advential fibroblasts was observed in a culture medium with 10 μg/ml of LPS (Cai et al., 2010). Similarly, treatment with 0.4 μg/ml of LPS increased the migration of mouse embryo cell line fibroblasts through the positive feedback between β-Catenin and cyclooxygenase-2 in concentration and time-dependent manner (Li et al., 2018). The results of both studies are consistent with our results, i.e. that LPS exerts a stimulatory effect on dermal fibroblast migration.

The production of IL6 was seen to be significantly enhanced when dermal fibroblasts were cultured under *low nutrition+LPS* conditions independent of the cell count. Similarly, other researchers showed that the secretion of IL6 increased when gingival fibroblasts were cultivated with 0.1 μg/ml of LPS from *E. coli* in a medium containing 10% of fetal calf serum. The NFκB signaling pathway was found to play an essential role in the regulation of the expression of IL6 by LPS-stimulated fibroblasts (Jin et al., 2012). Similarly, 10 μg/ml of LPS from *P. aeruginosa* significantly enhanced the production of IL6 by nasal polyp-derived fibroblasts (Cho et al., 2014). Therefore, we propose that the presence of LPS has a primary effect on the production of IL6. In addition, a complex of IL6 with the IL6 receptor suppresses IL1β-, TNFα- and PDGF-AA-induced dermal fibroblast proliferation (Mihara et al., 1996). These findings correlate well with not proliferating fibroblasts in our experiment. An increased level of IL6 following LPS treatment was also observed *in vivo*. Research has demonstrated that a gel containing 10 mg/g (g of gel) of LPS from *S. typhi* applied to incision-wounded mice increased the production of IL6 (Kostarnoy et al., 2013). Lung fibroblasts cultured with 1 μg/ml of LPS in a 10% calf serum medium produced increased levels of IL6 and IL8, which resulted in a decrease in the metabolic activity of the fibroblasts in an autocrine manner (Zhang et al., 2011). However, the origin of the fibroblasts and the origin and concentration of the bacterial LPS appear to be of significant importance. For instance, 0.05 and 0.1 μg/ml of LPS from *P. aeruginosa* did not affect the production of IL6 and IL8 by corneal fibroblasts. Moreover, it is necessary to take into account the age of the patients that provided the corneal samples, i.e. the samples were provided by

elderly persons as opposed to the mostly young donors of the dermal fibroblasts used in this thesis. Interestingly, when the same LPS treatment was performed using ulcerated corneal fibroblasts, the production of IL6 and IL8 were enhanced significantly (Wong et al., 2011). Biopsies from burn wounds produced increased levels of IL8 compared with those from healed wounds and intact skin (Iocono et al., 2000). The production of IL8 following treatment with 0.2 µg/ml of LPS in a serum-free medium that contained components supporting proliferation and plating efficiency was significantly increased. It should be noted that the authors did not state the bacterial species origin of the LPS (Eleftheriadis et al., 2011). Similarly, 10 µg/ml of LPS from *P. aeruginosa* significantly increased the production of IL8 by nasal polyp-derived fibroblasts (Cho et al., 2014). Our results suggest that the dermal fibroblasts did not produce higher level of IL8 under *low nutrition+LPS* conditions; however, due to high variability of data set, the increase was not statistically significant. The analysis of IL8 production by dermal fibroblasts under the same conditions as used in this study has not been reported in the literature. Therefore, we can only speculate about the general impact of LPS on IL8 production by dermal fibroblasts.

The presence of MMPs in wounded tissue is essential with respect to cell migration, tissue remodeling and the regulation of the level of cytokines. The *control* conditions applied in this thesis contained more FBS (10%) than did the *low nutrition* and *low nutrition+LPS* conditions (2%). Our results revealed that the FBS contained MMPs regardless of those produced by the cells (**Figure 9a**; culture media without cells). Nevertheless, our results show increased levels of MMP2 under the *low nutrition* and *low nutrition+LPS* conditions compared to that of the *control* conditions over time and independent of the cell count. Since the MMP2 level was enhanced in both of the stress media, we propose that this enhancement was due primarily to *low nutrition* rather than the presence of LPS. The level of MMP9 remained unchanged under both stress conditions. After 48 hours of the exposure of bovine dermal fibroblasts to LPS (5 µg/ml) that originated in *E. coli* the increased levels of MMP2 and MMP9 were observed (Akkoc et al., 2016). In our study, the dermal fibroblasts were cultured in 0.1 µg/ml LPS. Based on our and the previous findings, LPS was capable of increasing the production of MMP2 and MMP9 by dermal fibroblasts in concentrations higher than 0.1 µg/ml. The release of MMPs was dependent not only upon the origin of the LPS but

also that of the fibroblasts (Lindner et al., 2012). An increased level of MMP9 in nasal polyp-derived fibroblasts followed the exposure to 10 μg/ml LPS (*P. aeruginosa*) for 12 hours (Cho et al., 2014). We conclude that with respect to our experimental set up, the dermal fibroblast secretion of MMP2 was induced primarily by *low nutrition* and that LPS concentration of 0.1 μg/ml is too low to enable the release of the active form of MMP9.

α-SMA constitutes one of the typical characteristics of myofibroblasts, a contractile type of fibroblast that appears later in the proliferative phase of the wound healing process (Darby et al., 1990; Tomasek et al., 2002; Hinz et al., 2007). We observed a decrease in the expression of α-SMA under the *low nutrition* conditions and a more pronounced decrease under the *low nutrition+LPS* conditions independent of the cell count which goes hand-in-hand with a decrease in the contraction ability (discussed in chapter 5.2.1). Dermal fibroblasts isolated from chronic wounds expressed increased level of α-SMA compared with fibroblasts isolated from properly healing wounds (Schwarz et al., 2013). Weak migration ability of fibroblasts from venous ulcers was correlated with a high myofibroblast differentiation and increased α-SMA expression (Raffetto et al., 2001). In our study, dermal fibroblasts cultured in *low nutrition+LPS* conditions exhibited higher migration ability and decreased α-SMA expression pointing out the decreased myofibroblast differentiation, which interestingly reflects the opposite correlation between fibroblast migration and contraction (or myofibroblast phenotype) compared to Raffetto's study. Putting together data from α-SMA expression, contraction ability and MMP2 production, dermal fibroblasts cultured under *low nutrition+LPS* conditions exhibited the decreased level of α-SMA-positive cells, decreased contraction ability and increased activity of MMP2 compared to the *control* conditions, which negatively correlates with results of another study observing increasing myofibroblast phenotype and suppressed levels of MMP2 pro-migratory gene (Howard et al., 2012).

We observed that the dermal fibroblasts produced the same amount of collagen type I under all the test conditions. The production of collagen type I by dermal fibroblasts was verified in this thesis via the application of two independent methods – quantification in cell culture media by ELISA and immunocytochemistry staining of intracellular collagen. Another study has shown that the production of collagen type I

and hyaluronan in dermal fibroblasts is dependent on cytokine- and growth factor changes. The researchers determined that neither IL6 nor IL8 exerted a change with concern to the production of either of the molecules compared with the control (Kim et al., 2014). These findings corresponds to our results, i.e. that the production of collagen by dermal fibroblasts is not affected by pro-inflammatory conditions modeled in the form of increased levels of LPS or IL6/IL8 in the medium.

5.1.2 Contamination by bacterial strains

The wounds are not contaminated only by lipopolysaccharide from G^- bacteria but also by other soluble factors produced by both G^+ and G^- bacteria. *S. aureus* and *P.aeruginosa* are the most common bacterial species in wounds (Wong et al., 2015; Wolcott et al., 2016). Therefore, we used conditioned media from *S. aureus* (*SA*) and *P.aeruginosa* (*PA*) (bacterial conditions) and investigated their effect on the dermal fibroblasts.

The first part of the approach taken herein involved the study of dermal fibroblast responses to the single strain bacterial conditions: soluble factors from *S. aureus* (*SA*), soluble factors from *P. aeruginosa*, strain originated from CCM database (*PA*) and soluble factors from *P. aeruginosa*, strain originated in patient wound (*PA2*).

The second part of this study focused on the response of dermal fibroblasts to the three polybacterial conditions differing in preparation steps. The bacterial species were 1) incubated and cultivated together (*SA+PAcu*), 2) cultivated separately but incubated together (*SA+PAin*), or 3) cultivated separately, incubated separately but mixed together just before application on the cells (*SA+PAmix*). The parameters used to describe the behavior of the dermal fibroblasts consisted of proliferation, cell morphology, migration, the production of the IL6 and IL8 pro-inflammatory cytokines, and the production of collagen type I. The gelatinase, hyaluronidase and leukocidal activity of the bacterial strains were characterized.

5.1.2.1 Single strain bacterial contamination

In our study, the dermal fibroblasts did not proliferate in *PA* conditions originated in CCM, while they did proliferate in *PA2* conditions which originated in a patient sample.

This finding goes hand in hand with the cytotoxic effect of the strains on leukocytes. We therefore conclude that *PA* strain originated in CCM have a greater cytostatic effect not only on leukocytes but also on the dermal fibroblasts. Chemically prepared pyocyanin, a virulence factor produced by PA, decreased the proliferation of dermal fibroblasts in a concentration-dependent manner (Muller et al., 2009). Similar results were obtained by other researchers who tested commercial di-rhamnolipid (BAC-3), the heat-stable hemolysin or glycolipid secreted by PA (Stipcevic et al., 2005).

The spindle-shaped morphology of dermal fibroblasts was not affected by single strain bacterial conditions. Since any other similar study was performed we have to stay only with the results from our experimental set up.

In our study, the migration of dermal fibroblasts was not affected by *SA* while it was slightly potentiated by *PA* conditions; however, the effect was not significant. The similar effect of PA was observed on keratinocytes, when the migration was accelerated to over 300% of the control. Unlike our results SA prevented the cell migration (Jeffery Marano et al., 2015). The impact of PA expressing or not expressing quorum sensing-regulated virulence genes on dermal fibroblasts was studied. While secreted quorum sensing-regulated virulence factors from the wild-type PA suppressed the cell migration, the isogenic double-knockout mutant did not. The culture medium was supplemented with bacterial supernatants (conc. 1×10^9 CFU/ml). The authors provide that bacterial supernatants at concentration of 5% of the total media volume (i.e. final conc. 5×10^7 CFU/ml) did not have an impact on the cell migration. The *PA* conditions used in our study contained only 1.5×10^7 CFU/ml. Therefore we hypothesize that the lower concentration of soluble factors promoted the dermal fibroblasts´ migration, while the higher concentrations had an adverse effect which was also dependent on the spectrum of quorum sensing molecules produced by the PA strains.

Dermal fibroblasts produced low level of IL6 in *SA* and *PA* conditions like in a *ctrl* conditions at day 1. The production increased and was significantly higher in *PA* conditions compared to *ctrl* and also to *SA* conditions at day 6. The increase was concentration dependent. At day 6, the production of IL8 was increased in *PA* conditions compared to *ctrl*. Interestingly, *SA* conditions did not affect the production of both IL6 and IL8. After the treatment with purified elastase from PA (Elastin Products Company), IL8 production by lung fibroblasts was increased. The increase was

concentration dependent (Azghani et al., 2014). Significantly higher production of IL6 and IL8 by dermal fibroblasts was observed after 4 hours (IL8) and 12 hours (IL6) culture in MRSA conditioned medium (2×10^9 CFU/ml). The authors suppose that the increase in IL6 and IL8 by dermal fibroblasts under the conditions tested was caused by the soluble toxins i.e. protein A, lipoteichoic acid, peptidoglycans and enterotoxin A (Kirker et al., 2012). Increased level of IL6 and IL8 was produced by skin equivalents consisted of normal human keratinocytes and fibroblasts exposed to MRSA suspension (10^6 CFU/ml) (Haisma et al., 2013). Compared to our study, the researchers did not rid of the bacteria before the exposition to the cells. From this reason we can suggest that not only soluble factors but also the presence of the bacteria stimulated the interleukin production by the skin equivalents. Based on our results and previous studies we conclude that the production of IL6 and IL8 by dermal fibroblasts is very dependent on the bacterial strain the cells are exposed to. Moreover, the production of the both cytokines by dermal fibroblasts seems to be dependent on the concentration of the SA and PA soluble factors in the medium.

In our study, we observed low level of collagen I production at day 1, while at day 6 it was significantly higher in all single strain conditions. We conclude that bacterial soluble factors did not affect normal collagen production by dermal fibroblasts.

The dermal fibroblasts were affected the most by *PA* conditions. Interestingly, the cells did not proliferate compared to *ctrl*, while the cell morphology was normal and the migration was slightly potentiated. Moreover, the dermal fibroblasts produced increased level of the both pro-inflammatory cytokines, IL6 and IL8 in the *PA* conditions. Unlike *SA* conditions, which showed no cytotoxic effect on the cells, we suppose that the *PA* conditions are the main source of the soluble factors negatively influencing the behavior of dermal fibroblasts.

5.1.2.2 Polybacterial contamination

In this thesis the dermal fibroblasts did not proliferate under the bacterial conditions containing soluble factors from *PA*, i.e. *SA+PAcu*, *SA+PAin* and *SA+PAmix* conditions, although the proliferation arrest was significant only in the *SA+PAmix* conditions. We presume that the significantly affected proliferation of dermal fibroblasts by the

SA+PAmix conditions was caused by the non-restriction of soluble factors secretion by the both bacterial species during the separated cultivation and incubation.

The morphology of dermal fibroblasts was affected by *SA+PAmix* conditions and *SA+PAcu* conditions while in the rest bacterial conditions the morphology of the cells was normal. While in *SA+PAmix* conditions the cells were a little rounded after 6 days of the treatment, in *SA+PAcu* conditions, shrinkage fibroblasts occurred and the cells were detaching from the bottom of the culture dish. We presume that the fibroblasts underwent cell death; however, this hypothesis would be a subject for future studies. From our microscopic analysis of the cell morphology we presume that the *SA+PAcu* conditions had the most toxic impact on dermal fibroblasts´ morphology due to the longest time of exposure of the bacterial species (and the soluble factors they produced) to each other before the application on the dermal fibroblasts compared to the other polybacterial conditions (*SA+PAin* and *SA+PAmix*).

The migration of dermal fibroblasts was suppressed by *SA+PAmix* conditions compared with *ctrl* while the other polybacterial conditions did not affect the cell migration. Similarly like in the case of the proliferation determination we presume that the significantly affected migration of dermal fibroblasts by the *SA+PAmix* conditions was caused by the non-restriction of soluble factors secretion by the both bacterial species during the separated cultivation and incubation. However, we have to stay only with the results from our experiments while any other study of polybacterial conditions was performed on dermal fibroblasts or other cell type.

The dermal fibroblasts did not produce IL6 or IL8 in polybacterial conditions neither at day 1, nor at day 6. The production of collagen I by the dermal fibroblasts in all polybacterial conditions was low at day 1, while it was significantly higher at day 6. We conclude that soluble factors produced by the bacteria in all polybacterial conditions did not increase the pro-inflammatory molecule secretion and kept normal collagen production by dermal fibroblasts.

Based on the results from the single strain bacterial contamination we presume that the *PA* component in the polybacterial conditions had the major effect as the cells was significantly affected by the single strain *PA* conditions while the *SA* conditions did not, although, interestingly, the major component of the polybacterial conditions was *SA* (10:1). The morphology and the migration of dermal fibroblasts were affected in

polybacterial conditions while the pro-inflammatory phenotype of the cells was affected by single strain *PA* conditions and was not affected by the polybacterial condtions. It has been shown that the virulence of PA was increased by presence of SA. The N-Acetyl glucosamine, cell wall peptidoglycan of SA, induced the virulence of PA by enhancing the quinolone signal in PA which controls the production of extracellular virulence factors (e.g. pyocyanin, elastase and rhamnolipids). On the other hand, PA produced a wide variety of molecules that inhibit SA *in vitro* ((Hotterbeekx et al., 2017). It has been shown that the simultaneously acting SA and PA resulted in delayed wound healing compared to single species infection *in vivo* (Dalton et al., 2011; Seth et al., 2012; Pastar et al., 2014).

We are aware that the observations on dermal fibroblasts under the conditions used in this thesis have not been reported in another study since now. The choice of different bacterial strains (whether from CCM or patient samples) or different concentrations of bacterial soluble factors in media may provide different results.

5.2 Response of fibroblasts to normal and wound conditions in 3D culture

The ECM is an important component establishing the environment providing mechanical support and a scaffold for dermal fibroblasts. Dermal fibroblasts are completely surrounded by ECM. The cell-matrix interactions and molecular composition of ECM are crucial for the organization of skin with specific structural and mechanical properties. The 3D culture system provides a tissue-like environment for study of functional and biomechanical properties of cell-matrix interactions.in normal as well as pathological conditions (Rhee, 2009). The 3D dermal fibroblast culture introduced and characterized in this work serves as an extension of the knowledge about dermal fibroblast´s behavior in 2D culture. We used self-made collagen hydrogels as scaffolds for dermal fibroblasts to study the effect of specific extracellular microenvironments on proliferation, metabolic activity and contraction of dermal fibroblasts in 3D culture.

5.2.1 Normal culture conditions

Remodeling was measured by collagen hydrogel contraction by dermal fibroblasts. The cells promoted the contraction of the collagen hydrogels at each time point. From the other side, stiffness of the collagen hydrogels regulates the contraction and matrix remodeling by dermal fibroblasts (Karamichos et al., 2007). When fibroblasts are placed within 3D culture as collagen, cell locomotion results in translocation of the flexible collagen fibrils of the matrix. Several integrins (i.e. α1β1, α2β1, α11β1 αvβ3) and fibronectin are involved in collagen hydrogel remodeling (Tamariz and Grinnell, 2002).

The metabolic activity of dermal fibroblasts was increasing in time in both 2D and 3D cultures and did not differ between the groups. The increasing metabolic activity of dermal fibroblasts cultured in 3D collagen hydrogel in normal culture conditions for 5 days was observed also by Garcia et al. (Garcia et al., 2007).

The proliferation of dermal fibroblasts cultured in 2D had an increasing tendency compared to the non-increasing proliferation of the cells cultured in 3D. Contrary to our results another studies observed the increasing proliferation of dermal

fibroblasts in 3D cultures (Bott et al., 2010; Helary et al., 2012). Dermal fibroblasts in 3D collagen culture of the same collagen and cell density showed an increasing proliferation in time. The number of dermal fibroblasts increased gradually – ca. 2.3 times the initial fibroblast number after 7 days, while only 1.7 times the initial fibroblast number after 6 days in our study. We assume that the lower proliferation rate was given by the big data dispersion. We attribute the big variations in the data to 1) the fact that in our study the primary cells from various donors were used - however, the significantly different proliferation rates of fibroblasts from different donors cultured in 3D was also observed by Bott et al. (Bott et al., 2010) - and 2) the use of the not fully suitable method for proliferation assay in this study. The proliferation was measured by Calcein-AM staining followed by fluorescence detection. We are fully aware that Calcein-AM dye is primarily used for metabolic activity determination. However, this dye was the only one which did not produce non-specific bindings and worked well in our experiments (in contrast with protocols using DNA fluorescent dyes for proliferation assay). Based on this experience we were developing a new method for cell number determination and the study of cell proliferation in collagen hydrogels discussed in chapter 5.4.

Compared with 2D cultures, much less is known about cell–matrix interactions in 3D cultures. In our study, dermal fibroblasts were spindle-shaped in both 2D and 3D cultures. However, while in 2D cultures the shape of the cells was more flattened in 3D cultures the shape of the cells was stellate. The morphology of the cells is consistent with Grinnel´s finding of dermal fibroblast morphology in restrained (attached to dish) collagen hydrogels (Grinnell, 2003). In a bigger enlargement, the cells cultured in 2D created an artificial cell polarity between upper and lower surfaces of the cell which did not exist in 3D cultured cells (Green and Yamada, 2007). The findings indicate that the effect of 3D conditions on dermal fibroblasts is dependent on the mechanical environment. Fibroblast microtubules and the degree of tension are the essential features in the star-like shape of fibroblasts in 3D collagen hydrogels (Tamariz and Grinnell, 2002; Rhee et al., 2007).

5.2.2 Low nutrition and inflammation

Our study revealed that the contraction ability of dermal fibroblasts decreased under both *low nutrition* and *low nutrition+LPS* conditions, most likely due to the decreased number of cells under the *low nutrition* conditions. These results are consistent with those obtained from an *in vivo* study; 10 μg *K. pneumoniae*-derived LPS subcutaneously injected prior to wounding delayed the wound closure process (Crompton et al., 2016) (in this case the LPS originated from *K. pneumoniae* rather than *E. coli* as used in our study). Other researchers determined similar results using an *in vivo* experimental set up. Gels containing 0.2, 2 and 10 mg/g (g of gel) of LPS from *S. typhi* were applied to the incision-wounded skin of mice. The wound closure process was enhanced in the presence of LPS and was dose-dependent (Kostarnoy et al., 2013). On the other hand, the opposite effect *in vitro* was observed. 2 and 5 μg/ml of LPS in a culture medium (origin not specified) with 1% of FBS enhanced the contraction of intestine fibroblast-mediated collagen in a dose dependent manner (Burke et al., 2010). Whether the differences in the types of fibroblasts and/or concentrations of LPS used in our (0.1μg/ml) and Burke's (2 and 5 μg/ml) study were responsible for the discrepancies in the results remains open to debate.

The metabolic activity of dermal fibroblasts cultured under *low nutrition+LPS* conditions exhibited not a significant difference with *control* conditions in 3D culture. There are not available another data observing metabolic activity of dermal fibroblasts in 3D wound conditions. Therefore we have to stay only with the results from our experimental set up.

It seems that dermal fibroblasts cultured under *low nutrition+LPS* did not proliferate at all while in *control* conditions there is a little hint of increasing tendency of cell proliferation in 2D culture. The slight increase at day 6 in 2D *control* conditions was not significant probably due to the small data set (n=3) and the Calcein-AM-based method which is not fully suitable for a proliferation assay. Our results of non-increasing proliferation of dermal fibroblasts in 3D *control* conditions are not consistent with the other researches. In the studies the dermal fibroblasts proliferate in time (Bott et al., 2010; Helary et al., 2012). Any other work on fibroblasts in 3D collagen hydrogel was not performed.

5.3 Optimization of cell number determination in 2D culture

Presently, several methods for cell number estimation based on different principles and detection systems are usually used (**Table 5**). A very common strategy of cell quantification is based on conversion of various substrates by cellular enzymes to highly fluorescent products e.g. MTT, MTS (Cory et al., 1991), WST-1 (Wang et al., 2015), WST-8 (Xi et al., 2016; Chamchoy et al., 2019; Lee et al., 2019) and AlamarBlue assay (Voytik-Harbin et al., 1998). These methods are however dependent on the metabolic activity of the cells and therefore reflect the metabolic activity of the cells rather than the proliferation.

The methods using labeling of DNA are independent on metabolic activity of the cells. Many of them however determine the relative number of cells. To determine the absolute number of cells, the calibration curves using samples containing a known cell number are necessary. The detection is based on the measurement of the fluorescent signal using the plate reader.

Table 5 Commonly used methods for measuring of the cell proliferation.

Name	Principle	Detection	Reference
Trypan blue	Viable cells do not take up the dye, while the permeable dead cells do	Light microscopy	(Kanafi et al., 2013)
BrdU	BrdU is incorporated into replicating DNA and detected by anti-BrdU antibodies	Fluorescent microscopy, FACS, ELISA	(He et al., 2013; Roberts et al., 2018)
Ki-67 protein	Detection of the nuclear protein by anti-Ki-67 antibodies	Fluorescent microscopy, WB	(Sabetkam et al., 2018)
CyQuant®, SYBR green I, DAPI, Hoechst	Labeling of a cellular DNA content	Microplate reader	(McCaffrey et al., 1988; Myers, 1998; Jones et al., 2001)

In this thesis, we have developed a method for the estimation of the absolute cell number. It enables to observe the cell nuclei distribution with use of fluorescent microscope with picture compilation employing VisiView®, which is a necessary tool of this method. The advantages of the method are low material demand, low detection

limit (single cell detection), it does not require fixation or cell lysis, it does not require calibration curve, it determines the absolute cell numbers, it is independent on metabolic activity, it uses a freeware for data analysis and last but not least it is fast and cheap. The disadvantages of the method are the requirement of VisiView® software for a picture compilation (or any other software with the function of a picture compilation), the upper detection limit which is given by overlapping nuclei and the cell type limitation when the separated (not overlapping) cell nuclei are required (i.e. it does not work for epithelial cells). The method for cell number determination was used in this thesis for the quantitative analysis of cell proliferation in 2D culture and for IL6, IL8, MMPs and collagen type I relation to cell number.

5.4 Optimization of cell number determination in 3D culture

The estimation of cell number in 3D cultures is more complicated compared to 2D cultures, while the usually used methods require collagen hydrogel digestion before labeling of cellular DNA content followed by the detection of a fluorescent signal using plate reader. Collagen hydrogels are usually digested by collagenase. The cells are then stained by Trypan blue and counted from a titer using Coulter counter or after cell lysis the DNA is stained by Hoechst (Mio et al., 1996) or PicoGreen (Ng et al., 2005). The disadvantage of the mentioned methods is a risk of loss of the cells during cell collection by centrifugation, the necessary step of the protocols. Until today, the most promising method for estimation of cell proliferation in 3D cultures is DNA labeling with CyQuant after hydrogel digestion with proteinase K (Wang et al., 2005; Bott et al., 2010). The advantage of this protocol is an avoidance of centrifugation step. However, this method requires calibration curve using DNA standard and thus do not determine the absolute cell number.

As well as in 2D cultures, strategies of cell quantification based on conversion of various substrates by cellular enzymes to highly fluorescent products are very common e.g. MTS (Thevenot et al., 2008; Sirivisoot et al., 2014) and MTT (Lohrasbi et al., 2020) assay. These methods are however equally dependent on the metabolic activity of the cells as in 2D cultures and therefore reflect the metabolic activity of the cells rather than the proliferation.

Rarely, histology methods for cell number estimation in 3D collagen hydrogels are used. The collagen hydrogels were embedded into paraffin, sectioned with a microtome after the routine histology processing (dewaxing and rehydrating) the cells were stained with hemalun and observed with use of light microscopy (Helary et al., 2005). The disadvantage of the method is that it requires complete histology equipment, it is time consuming and the problem of proper sampling strategy occurs.

Although strategies of cell number determination based on conversion of various substrates by cellular enzymes to highly fluorescent products are very common, they provide only information about the amount of DNA and it is not possible to determine the absolute cell number by these methods much less so cell distribution. Therefore we

developed a new method for determination of the absolute cell number in cell-seeded 3D collagen hydrogels based on stereology. It enables to observe the cell nuclei distribution with use of fluorescent microscope. The advantages of the method are low material demand, low detection limit (single cell detection), it does not require calibration curve, it determines the absolute cell numbers, it is independent on metabolic activity, it does not require digestion of the collagen hydrogels and it uses a freeware for data analysis. The disadvantages of the method are the extensiveness of the data analysis, the upper detection limit which is given by overlapping nuclei, the cell type limitation when the separated cell nuclei are required (i.e. it does not work for epithelial cells) and since the absolute cell number is determined from the sample, homogenous cell distribution in the collagen hydrogels is required as the method does not take into account reduction of collagen hydrogel diameter (a result of the cell contraction in time **Figure 27A, B**) and non-homogenous cell density (a result of the cell migration in time **Figure 27C, D**).

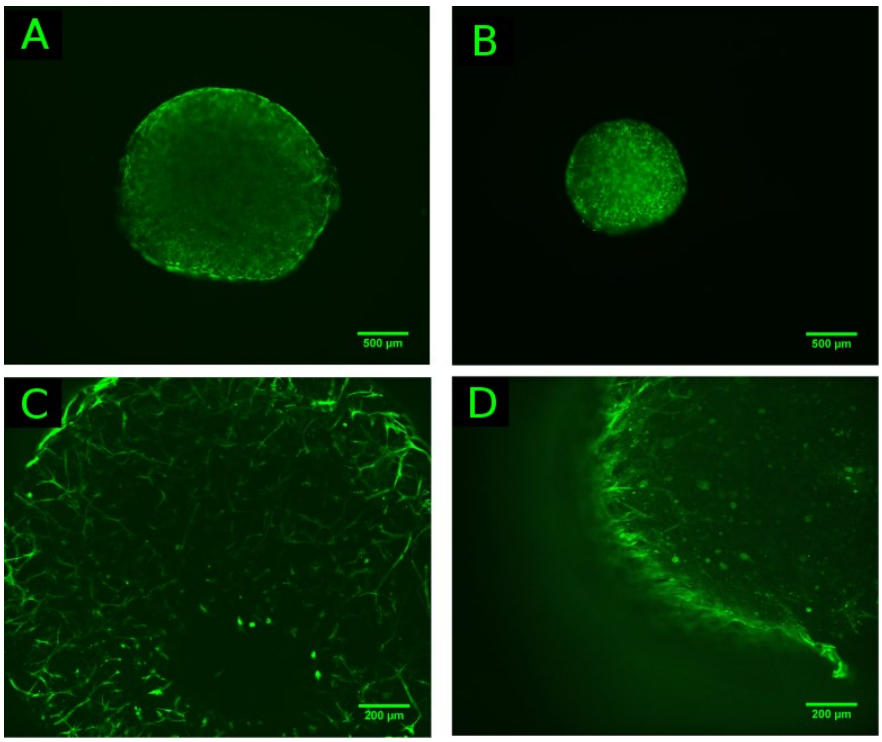

Figure 27 The contraction of collagen hydrogel by dermal fibroblasts after (A) 3 days and (B) 24 days in *control* medium. The distribution of dermal fibroblasts in collagen hydrogel after (C) 3 days and (D) 24 days in *control* medium. The dermal fibroblasts were stained by Phalloidin-Alexa 488, green (A12379, ThermoFisher Scientific, USA). The scale bar represents 500 µm (A, B) 200 µm (C, D).

6. CONCLUSIONS

This thesis provides new observations of the behavior of dermal fibroblasts via the analysis of the typical functions of dermal fibroblasts under wound conditions studied *in vitro* in 2D cultures and self-made 3D collagen hydrogel cultures. Based on our results we can conclude that:

1. Both conditions, the low nutrition and the low nutrition+LPS, promoted metabolic activity of the cells; however, this promotion was not followed by promoted proliferation. Morphology of the cells was not affected by any condition. Further, only the LPS potentiated migration of the cells. The pro-inflammatory phenotype of the cells evidenced by increased production of interleukins IL6 and IL8 was potentiated by only low nutrition+LPS conditions. Moreover, the expression of α-SMA decreased by low nutrition and even more by LPS. The remodeling capability of the cells was influenced only by low nutrition when documented by increased MMP2 and unchanged MMP9 activities. Finally, the production of collagen type I was not affected by any condition.
2. Proliferation of the cells was suppressed by soluble factors from *P. aeruginosa* originated in Czech Collection of Microorganisms (CCM), while it was not affected by soluble factors from *P. aeruginosa* originated in patient wound. Further, morphology and migration of the cells was not affected by any bacterial condition. The pro-inflammatory phenotype of the cells evidenced by increased production of IL6 and IL8 was potentiated by soluble factors from *P. aeruginosa* originated in CCM and was concentration dependent. The production of collagen type I was not affected by any condition. Soluble factors from *S. aureus* did not affect the functions of dermal fibroblasts at all.
3. Metabolic activity of the cells was not affected by any of the three types of polybacterial condition. Further, proliferation of the cells was suppressed by the mixed polybacterial conditions (*P. aeruginosa* and *S. aureus* cultivated separately, incubated separately but mixed together just before application on the cells). Cell morphology was affected by the polybacterial conditions cultivated together, while only the mixed polybacterial conditions suppressed the cell migration. Any of the three types of polybacterial conditions affected

neither the pro-inflammatory response of the cells in the way of IL6 and IL8 production, nor the production of collagen type I.

4. The metabolic activity of the cells was independent on the type of culture and was increasing in time. The proliferation of the cells was increasing in time in 2D culture and constant in 3D culture. The spindle-shaped morphology of the cells was flattened in 2D culture, while in 3D culture the shape was more elongated and stellate utilizing the availability of the third dimension.
5. The contraction ability of the cells in 3D culture was disrupted by both the low nutrition and the low nutrition+LPS conditions. The metabolic activity of the cells as well as the proliferation was not affected by the wound conditions in both types of culture.
6. The unique point of the thesis was the optimization of two methods for monitoring of cell distribution and absolute cell number determination in 1) 2D culture and 2) 3D self-made collagen hydrogel culture. This issue was not a part of the primary research. However the methods were required for the most accurate cell proliferation analysis. Moreover, it was essential for IL6, IL8, MMPs and collagen type I relation to cell number throughout the whole thesis. We faced the challenge whereas such methods have not yet been optimized.

6.1 The path of my PhD

At the beginning of the study I was motivated to create a new model of wound conditions *in vitro* based on more than one stress factor as no such a model was available. I wade into the experiments with diligence and with vision of much more than "only two" stress factors acting together. I must admit I did not ask a question "why such a model is not available" at that time. It seemed so simple to combine one and one to make two stress factors.

However, even when solving every single factor I dealt with many questions: How much low should the low nutrition be? What origin should have the LPS? What concentration should be used in the case of contamination by LPS? What bacterial strains should be used? How many of them? How to prepare the bacterial strains? And so on and so forth. And what if we deal with more than one stress factor?!

But now, after the research and especially the experiences, I realized that it depends on everything! I realized that the choice of a different bacterial may provide different results. I realized that the choice of a different concentration of anything may provide different results of anything. The awareness of all of this was very disturbing.

Another story was the experience with difficult paper submission and related defense and demanding review procedure I had to overcome repeatedly. It was hard not to take such experiences personally. Sometimes I doubt myself.

Although the previous paragraphs may sound pessimistic this experience taught me a lot. The knowledge mentioned above I keep in mind in the future work. I already know that I must ask many and many questions and I must read many and many papers before I reach for the pipette. I know I must want to reach the best possible knowledge and experience to design such complicated experiments which sometimes may not seem complicated at the first sight.

During the years I worked on the thesis I learned how to ask myself questions, what it is like to work with other researchers and how difficult sometimes is to discuss problems with others who look at it from a different point of view and how difficult sometimes is to understand to each other. Last but not least I learned that the diligence is not a guarantee of success. I experienced that all the work I done does not always pay off. All of this taught me that I must not be discouraged by the initial failure but be persistent and tenacious.

7. REFERENCES

Abbott, A. (2003). Biology's new dimension. *Nature*. doi:10.1038/424870a.

Agren, M. S., Steenfos, H. H., Dabelsteen, S., Hansen, J. B., and Dabelsteen, E. (1999). Proliferation and mitogenic response to PDGF-BB of fibroblasts isolated from chronic venous leg ulcers is ulcer-age dependent. *J. Invest. Dermatol.* doi:10.1046/j.1523-1747.1999.00549.x.

Akkoc, A., Kahraman, M. M., Vatansever, A., Gunaydin, E., and Akdesir, E. (2016). Lipopolysaccharide (LPS) induces matrix metalloproteinase-2 and -9 (MMP-2 and MMP-9) in bovine dermal fibroblasts. *Pak. Vet. J.*

Arya, A. K. (2014). Recent advances on the association of apoptosis in chronic non healing diabetic wound. *World J. Diabetes*. doi:10.4239/wjd.v5.i6.756.

Ashcroft, G. S., Mills, S. J., and Ashworth, J. J. (2002). Ageing and wound healing. *Biogerontology*. doi:10.1023/A:1021399228395.

Azghani, A. O., Neal, K., Idell, S., Amaro, R., Baker, J. W., Omri, A., et al. (2014). Mechanism of fibroblast inflammatory responses to Pseudomonas aeruginosa elastase. *Microbiol. (United Kingdom)*. doi:10.1099/mic.0.075325-0.

Babaei, B., Davarian, A., Lee, S. L., Pryse, K. M., McConnaughey, W. B., Elson, E. L., et al. (2016). Remodeling by fibroblasts alters the rate-dependent mechanical properties of collagen. *Acta Biomater.* doi:10.1016/j.actbio.2016.03.034.

Baroni, A., Perfetto, B., Ruocco, E., and Rossano, F. (1998). Lipoteichoic acid and protein-A from Staphylococcus aureus stimulate release of hepatocyte growth factor (HGF) by human dermal fibroblasts. *Arch. Dermatol. Res.* doi:10.1007/s004030050292.

Basso, F. G., Soares, D. G., Pansani, T. N., Turrioni, A. P. S., Scheffel, D. L., De Souza Costa, C. A., et al. (2015). Effect of LPS treatment on the viability and chemokine synthesis by epithelial cells and gingival fibroblasts. *Arch. Oral Biol.* doi:10.1016/j.archoralbio.2015.04.010.

Bedran, T. B. L., Mayer, M. P. A., Spolidorio, D. P., and Grenier, D. (2014). Synergistic anti-inflammatory activity of the antimicrobial peptides human beta-defensin-3 (hBD-3) and cathelicidin (LL-37) in a three-dimensional co-culture model of gingival epithelial cells and fibroblasts. *PLoS One*. doi:10.1371/journal.pone.0106766.

Behm, B., Babilas, P., Landthaler, M., and Schreml, S. (2012). Cytokines, chemokines and growth factors in wound healing. *J. Eur. Acad. Dermatology Venereol.* doi:10.1111/j.1468-3083.2011.04415.x.

Bessa, L. J., Fazii, P., Di Giulio, M., and Cellini, L. (2015). Bacterial isolates from infected wounds and their antibiotic susceptibility pattern: Some remarks about wound infection. *Int. Wound J.* doi:10.1111/iwj.12049.

Bill, T. J., Ratliff, C. R., Donovan, A. M., Knox, L. K., Morgan, R. F., and Rodeheaver, G. T. (2001). Quantitative swab culture versus tissue biopsy: a comparison in chronic wounds. *Ostomy. Wound. Manage.*

Böhm, S., Strauß, C., Stoiber, S., Kasper, C., and Charwat, V. (2017). Impact of source and manufacturing of collagen matrices on fibroblast cell growth and platelet aggregation. *Materials (Basel).* doi:10.3390/ma10091086.

Bott, K., Upton, Z., Schrobback, K., Ehrbar, M., Hubbell, J. A., Lutolf, M. P., et al. (2010). The effect of matrix characteristics on fibroblast proliferation in 3D gels. *Biomaterials*. doi:10.1016/j.biomaterials.2010.07.046.

Breit, S., Bubel, M., Pohlemann, T., and Oberringer, M. (2011). Erythropoietin ameliorates the reduced migration of human fibroblasts during in vitro hypoxia. *J. Physiol. Biochem.* doi:10.1007/s13105-010-0043-5.

Brinkmann, V., Reichard, U., Goosmann, C., Fauler, B., Uhlemann, Y., Weiss, D. S., et al. (2004). Neutrophil Extracellular Traps Kill Bacteria. *Science (80-.).* doi:10.1126/science.1092385.

Bullen, E. C., Longaker, M. T., Updike, D. L., Benton, R., Ladin, D., Hou, Z., et al. (1995). Tissue inhibitor of metalloproteinase-1 is decreased and activated gelatinases are increased in chronic wounds. *J. Invest. Dermatol.* doi:10.1111/1523-1747.ep12612786.

Burke, J. P., Cunningham, M. F., Watson, R. W. G., Docherty, N. G., Coffey, J. C., and O'Connell, P. R. (2010). Bacterial lipopolysaccharide promotes profibrotic activation of intestinal fibroblasts. *Br. J. Surg.* doi:10.1002/bjs.7045.

Cai, X. J., Chen, L., Li, L., Feng, M., Li, X., Zhang, K., et al. (2010). Adiponectin inhibits lipopolysaccharide-induced adventitial fibroblast migration and transition to myofibroblasts via AdipoR1-AMPK-iNOS pathway. *Mol. Endocrinol.* doi:10.1210/me.2009-0128.

Caley, M. P., Martins, V. L. C., and O'Toole, E. A. (2015). Metalloproteinases and Wound Healing. *Adv. Wound Care*. doi:10.1089/wound.2014.0581.

Caliari, S. R., and Burdick, J. A. (2016). A practical guide to hydrogels for cell culture. *Nat. Methods*. doi:10.1038/nmeth.3839.

Carter, M., and Shieh, J. (2015). Chapter 14 - Cell Culture Techniques. *Guid. to Res. Tech. Neurosci.* doi:10.1016/B978-0-12-800511-8.00014-9.

Castilla, D. M., Liu, Z.-J., and Velazquez, O. C. (2012). Oxygen: Implications for Wound Healing. *Adv. Wound Care*. doi:10.1089/wound.2011.0319.

Cha, J., Kwak, T., Butmarc, J., Kim, T. A., Yufit, T., Carson, P., et al. (2008). Fibroblasts from non-healing human chronic wounds show decreased expression of βig-h3, a TGF-β inducible protein. *J. Dermatol. Sci.* doi:10.1016/j.jdermsci.2007.10.010.

Chamchoy, K., Pakotiprapha, D., Pumirat, P., Leartsakulpanich, U., and Boonyuen, U. (2019). Application of WST-8 based colorimetric NAD(P)H detection for quantitative dehydrogenase assays. *BMC Biochem.* doi:10.1186/s12858-019-0108-1.

Cho, J. S., Kang, J. H., Um, J. Y., Han, I. H., Park, I. H., Heung, H., et al. (2014). Lipopolysaccharide induces pro-inflammatory cytokines and mmp production via TLR4 in nasal polyp-derived fibroblast and organ culture. *PLoS One*. doi:10.1371/journal.pone.0090683.

Connelly, L., Palacios-Callender, M., Ameixa, C., Moncada, S., and Hobbs, A. J. (2001). Biphasic Regulation of NF-κB Activity Underlies the Pro- and Anti-Inflammatory Actions of Nitric Oxide. *J. Immunol.* doi:10.4049/jimmunol.166.6.3873.

Cory, A. H., Owen, T. C., Barltrop, J. A., and Cory, J. G. (1991). Use of an aqueous soluble tetrazolium/formazan assay for cell growth assays in culture. *Cancer Commun.* doi:10.3727/095535491820873191.

Crompton, R., Williams, H., Ansell, D., Campbell, L., Holden, K., Cruickshank, S., et al. (2016). Oestrogen promotes healing in a bacterial LPS model of delayed cutaneous wound repair. *Lab. Investig.* doi:10.1038/labinvest.2015.160.

Dalton, T., Dowd, S. E., Wolcott, R. D., Sun, Y., Watters, C., Griswold, J. A., et al.

(2011). An in vivo polymicrobial biofilm wound infection model to study interspecies interactions. *PLoS One*. doi:10.1371/journal.pone.0027317.

Darby, I., Skalli, O., and Gabbiani, G. (1990). α-Smooth muscle actin is transiently expressed by myofibroblasts during experimental wound healing. *Lab. Investig.*

De Mattei, M., Ongaro, A., Magaldi, S., Gemmati, D., Legnaro, A., Palazzo, A., et al. (2008). Time- and dose-dependent effects of chronic wound fluid on human adult dermal fibroblasts. *Dermatologic Surg.* doi:10.1111/j.1524-4725.2007.34068.x.

DeLeon, S., Clinton, A., Fowler, H., Everett, J., Horswill, A. R., and Rumbaugh, K. P. (2014). Synergistic interactions of Pseudomonas aeruginosa and Staphylococcus aureus in an In vitro wound model. *Infect. Immun.* doi:10.1128/IAI.02198-14.

Demaria, M., Ohtani, N., Youssef, S. A., Rodier, F., Toussaint, W., Mitchell, J. R., et al. (2014). An essential role for senescent cells in optimal wound healing through secretion of PDGF-AA. *Dev. Cell*. doi:10.1016/j.devcel.2014.11.012.

Demidova-Rice, T. N., Hamblin, M. R., and Herman, I. M. (2012). Acute and impaired wound healing: Pathophysiology and current methods for drug delivery, part 1: Normal and chronic wounds: Biology, causes, and approaches to care. *Adv. Ski. Wound Care*. doi:10.1097/01.ASW.0000416006.55218.d0.

DiPietro, L. A. (2016). Angiogenesis and wound repair: when enough is enough. *J. Leukoc. Biol.* doi:10.1189/jlb.4mr0316-102r.

Dong, C., and Lv, Y. (2016). Application of collagen scaffold in tissue engineering: Recent advances and new perspectives. *Polymers (Basel).* doi:10.3390/polym8020042.

Donlan, R. M., and Costerton, J. W. (2002). Biofilms: Survival mechanisms of clinically relevant microorganisms. *Clin. Microbiol. Rev.* doi:10.1128/CMR.15.2.167-193.2002.

Dow, G., Browne, A., and Sibbald, R. G. (1999). Infection in chronic wounds: controversies in diagnosis and treatment. *Ostomy. Wound. Manage.*

Driskell, R. R., Lichtenberger, B. M., Hoste, E., Kretzschmar, K., Simons, B. D., Charalambous, M., et al. (2013). Distinct fibroblast lineages determine dermal architecture in skin development and repair. *Nature*. doi:10.1038/nature12783.

Ejiri, H., Nomura, T., Hasegawa, M., Tatsumi, C., Imai, M., Sakakibara, S., et al. (2015). Use of synthetic serum-free medium for culture of human dermal fibroblasts to establish an experimental system similar to living dermis. *Cytotechnology*. doi:10.1007/s10616-014-9709-0.

Eleftheriadis, T., Liakopoulos, V., Lawson, B., Antoniadi, G., Stefanidis, I., and Galaktidou, G. (2011). Lipopolysaccharide and hypoxia significantly alters interleukin-8 and macrophage chemoattractant protein-1 production by human fibroblasts but not fibrosis related factors. *Hippokratia*.

Eming, S. A., Krieg, T., and Davidson, J. M. (2007). Inflammation in wound repair: Molecular and cellular mechanisms. *J. Invest. Dermatol.* doi:10.1038/sj.jid.5700701.

Farel, P. B. (2003). Principles and Practices of Unbiased Stereology: An Introduction for Bioscientists . By Peter R Mouton. Baltimore (Maryland): Johns Hopkins University Press. $34.95 (paper). xi + 214 p; ill.; index. ISBN: 0–8018–6797–5. 2002. . *Q. Rev. Biol.* doi:10.1086/377827.

Formichi, P., Radi, E., Battisti, C., Tarquini, E., Leonini, A., Di Stefano, A., et al. (2006). Human fibroblasts undergo oxidative stress-induced apoptosis without internucleosomal DNA fragmentation. *J. Cell. Physiol.* doi:10.1002/jcp.20662.

Füller, J., and Müller-Goymann, C. C. (2018). Anti-proliferative and anti-migratory effects of hyperforin in 2D and 3D artificial constructs of human dermal fibroblasts – A new option for hypertrophic scar treatment? *Eur. J. Pharm. Biopharm.* doi:10.1016/j.ejpb.2017.03.003.

Gabbiani, G. (2003). The myofibroblast in wound healing and fibrocontractive diseases. *J. Pathol.* doi:10.1002/path.1427.

Garcia, Y., Collighan, R., Griffin, M., and Pandit, A. (2007). Assessment of cell viability in a three-dimensional enzymatically cross-linked collagen scaffold. *J. Mater. Sci. Mater. Med.* doi:10.1007/s10856-007-3091-9.

Germain, L., Jean, A., Auger, F. A., and Garrel, D. R. (1994). Human Wound Healing Fibroblasts Have Greater Contractile Properties Than Dermal Fibroblasts. *J. Surg. Res.* doi:10.1006/jsre.1994.1143.

Giampieri, F., Alvarez-Suarez, J. M., Mazzoni, L., Forbes-Hernandez, T. Y., Gasparrini, M., Gonzàlez-Paramàs, A. M., et al. (2014). An anthocyanin-rich strawberry extract protects against oxidative stress damage and improves mitochondrial functionality in human dermal fibroblasts exposed to an oxidizing agent. *Food Funct.* doi:10.1039/c4fo00048j.

Glass, D., Viñuela, A., Davies, M. N., Ramasamy, A., Parts, L., Knowles, D., et al. (2013). Gene expression changes with age in skin, adipose tissue, blood and brain. *Genome Biol.* doi:10.1186/gb-2013-14-7-r75.

Greaves, N. S., Ashcroft, K. J., Baguneid, M., and Bayat, A. (2013). Current understanding of molecular and cellular mechanisms in fibroplasia and angiogenesis during acute wound healing. *J. Dermatol. Sci.* doi:10.1016/j.jdermsci.2013.07.008.

Green, J. A., and Yamada, K. M. (2007). Three-dimensional microenvironments modulate fibroblast signaling responses. *Adv. Drug Deliv. Rev.* doi:10.1016/j.addr.2007.08.005.

Grinnell, F. (2003). Fibroblast biology in three-dimensional collagen matrices. *Trends Cell Biol.* doi:10.1016/S0962-8924(03)00057-6.

Grinnell, F., B. Rocha, L., Iucu, C., Rhee, S., and Jiang, H. (2006). Nested collagen matrices: A new model to study migration of human fibroblast populations in three dimensions. *Exp. Cell Res.* doi:10.1016/j.yexcr.2005.10.001.

Haisma, E. M., Rietveld, M. H., Breij, A., Van Dissel, J. T., El Ghalbzouri, A., and Nibbering, P. H. (2013). Inflammatory and antimicrobial responses to methicillin-resistant Staphylococcus aureus in an in vitro wound infection model. *PLoS One*. doi:10.1371/journal.pone.0082800.

He, Z., Gao, Y., Deng, Y., Li, W., Chen, Y., Xing, S., et al. (2012). Lipopolysaccharide induces lung fibroblast proliferation through toll-like receptor 4 signaling and the phosphoinositide3-kinase-Akt pathway. *PLoS One*. doi:10.1371/journal.pone.0035926.

He, Z., Wang, X., Deng, Y., Li, W., Chen, Y., Xing, S., et al. (2013). Epigenetic regulation of Thy-1 gene expression by histone modification is involved in lipopolysaccharide-induced lung fibroblast proliferation. *J. Cell. Mol. Med.* doi:10.1111/j.1582-4934.2012.01659.x.

Hehenberger, K., Kratz, G., Hansson, A., and Brismar, K. (1998). Fibroblasts derived from human chronic diabetic wounds have a decreased proliferation rate, which is recovered by the addition of heparin. *J. Dermatol. Sci.* doi:10.1016/S0923-1811(97)00042-X.

Helary, C., Foucault-Bertaud, A., Godeau, G., Coulomb, B., and Giraud Guille, M. M. (2005). Fibroblast populated dense collagen matrices: Cell migration, cell density and metalloproteinases expression. *Biomaterials*. doi:10.1016/j.biomaterials.2004.05.016.

Helary, C., Zarka, M., and Giraud-Guille, M. M. (2012). Fibroblasts within concentrated collagen hydrogels favour chronic skin wound healing. *J. Tissue Eng. Regen. Med.* doi:10.1002/term.420.

Hinz, B., Phan, S. H., Thannickal, V. J., Galli, A., Bochaton-Piallat, M. L., and Gabbiani, G. (2007). The myofibroblast: One function, multiple origins. *Am. J. Pathol.* doi:10.2353/ajpath.2007.070112.

Honardoust, D., Varkey, M., Marcoux, Y., Shankowsky, H. A., and Tredget, E. E. (2012). Reduced decorin, fibromodulin, and transforming growth factor-β3 in deep dermis leads to hypertrophic scarring. *J. Burn Care Res.* doi:10.1097/BCR.0b013e3182335980.

Hopf, H. W., Hunt, T. K., West, J. M., Blomquist, P., Goodson, W. H., Jensen, J. A., et al. (1997). Wound tissue oxygen tension predicts the risk of wound infection in surgical patients. *Arch. Surg.* doi:10.1001/archsurg.1997.01430330063010.

Hopf, H. W., and Rollins, M. D. (2007). Wounds: An overview of the role of oxygen. *Antioxidants Redox Signal.* doi:10.1089/ars.2007.1641.

Hotterbeekx, A., Kumar-Singh, S., Goossens, H., and Malhotra-Kumar, S. (2017). In vivo and In vitro interactions between Pseudomonas aeruginosa and Staphylococcus spp. *Front. Cell. Infect. Microbiol.* doi:10.3389/fcimb.2017.00106.

Howard, E. W., Crider, B. J., Updike, D. L., Bullen, E. C., Parks, E. E., Haaksma, C. J., et al. (2012). MMP-2 expression by fibroblasts is suppressed by the myofibroblast phenotype. *Exp. Cell Res.* doi:10.1016/j.yexcr.2012.03.007.

Hynes, R. O. (2009). The extracellular matrix: Not just pretty fibrils. *Science (80-.).* doi:10.1126/science.1176009.

Iocono, J. A., Colleran, K. R., Remick, D. G., Gillespie, B. W., Ehrlich, H. P., and Garner, W. L. (2000). Interleukin-8 levels and activity in delayed-healing human thermal wounds. *Wound Repair Regen.* doi:10.1046/j.1524-475X.2000.00216.x.

Janson, D. G., Saintigny, G., Van Adrichem, A., Mahé, C., and El Ghalbzouri, A. (2012). Different gene expression patterns in human papillary and reticular fibroblasts. *J. Invest. Dermatol.* doi:10.1038/jid.2012.192.

Jeffery Marano, R., Jane Wallace, H., Wijeratne, D., William Fear, M., San Wong, H., and O'Handley, R. (2015). Secreted biofilm factors adversely affect cellular wound healing responses in vitro. *Sci. Rep.* doi:10.1038/srep13296.

Jin, H. C., Jin, Y. S., Hai, R. C., Mi, K. L., Choon, S. Y., Rhie, G. E., et al. (2001). Modulation of skin collagen metabolism in aged and photoaged human skin in vivo. *J. Invest. Dermatol.* doi:10.1046/j.0022-202X.2001.01544.x.

Jin, J., Sundararaj, K. P., Samuvel, D. J., Zhang, X., Li, Y., Lu, Z., et al. (2012). Different signaling mechanisms regulating IL-6 expression by LPS between gingival fibroblasts and mononuclear cells: Seeking the common target. *Clin. Immunol.* doi:10.1016/j.clim.2012.01.019.

Jones, L. J., Gray, M., Yue, S. T., Haugland, R. P., and Singer, V. L. (2001). Sensitive determination of cell number using the CyQUANT® cell proliferation assay. *J. Immunol. Methods*. doi:10.1016/S0022-1759(01)00404-5.

Jonsson, K., Jensen, J. A., Goodson, W. H., Scheuenstuhl, H., West, J., Hopf, H. W., et al. (1991). Tissue oxygenation, anemia, and perfusion in relation to wound healing

in surgical patients. *Ann. Surg.* doi:10.1097/00000658-199111000-00011.
Kanafi, M. M., Ramesh, A., Gupta, P. K., and Bhonde, R. R. (2013). Influence of hypoxia, high glucose, and low serum on the growth kinetics of mesenchymal stem cells from deciduous and permanent teeth. *Cells Tissues Organs*. doi:10.1159/000354901.
Kapałczyńska, M., Kolenda, T., Przybyła, W., Zajączkowska, M., Teresiak, A., Filas, V., et al. (2018). 2D and 3D cell cultures – a comparison of different types of cancer cell cultures. *Arch. Med. Sci.* doi:10.5114/aoms.2016.63743.
Karamichos, D., Brown, R. A., and Mudera, V. (2007). Collagen stiffness regulates cellular contraction and matrix remodeling gene expression. *J. Biomed. Mater. Res. - Part A*. doi:10.1002/jbm.a.31423.
Kaur, G., and Dufour, J. M. (2012). Cell lines: Valuable tools or useless artifacts. *Spermatogenesis*. doi:10.4161/spmg.19885.
Kim, D. J., Mustoe, T., and Clark, R. A. (2015). Cutaneous wound healing in aging small mammals: A systematic review. *Wound Repair Regen.* doi:10.1111/wrr.12290.
Kim, M. S., Song, H. J., Lee, S. H., and Lee, C. K. (2014). Comparative study of various growth factors and cytokines on type I collagen and hyaluronan production in human dermal fibroblasts. *J. Cosmet. Dermatol.* doi:10.1111/jocd.12073.
Kirker, K. R., James, G. A., Fleckman, P., Olerud, J. E., and Stewart, P. S. (2012). Differential effects of planktonic and biofilm MRSA on human fibroblasts. *Wound Repair Regen.* doi:10.1111/j.1524-475X.2012.00769.x.
Knighton, D. R., Fiegel, V. D., Halverson, T., Schneider, S., Brown, T., and Wells, C. L. (1990). Oxygen as an Antibiotic: The Effect of Inspired Oxygen on Bacterial Clearance. *Arch. Surg.* doi:10.1001/archsurg.1990.01410130103015.
Kostarnoy, A. V., Gancheva, P. G., Logunov, D. Y., Verkhovskaya, L. V., Bobrov, M. A., Scheblyakov, D. V., et al. (2013). Topical bacterial lipopolysaccharide application affects inflammatory response and promotes wound healing. *J. Interf. Cytokine Res.* doi:10.1089/jir.2012.0108.
Kreimendahl, F., Marquardt, Y., Apel, C., Bartneck, M., Zwadlo-Klarwasser, G., Hepp, J., et al. (2019). Macrophages significantly enhance wound healing in a vascularized skin model. *J. Biomed. Mater. Res. - Part A*. doi:10.1002/jbm.a.36648.
Krishnaswamy, V. R., Mintz, D., and Sagi, I. (2017). Matrix metalloproteinases: The sculptors of chronic cutaneous wounds. *Biochim. Biophys. Acta - Mol. Cell Res.* doi:10.1016/j.bbamcr.2017.08.003.
Kruger, T. E., Miller, A. H., and Wang, J. (2013). Collagen scaffolds in bone sialoprotein-mediated bone regeneration. *Sci. World J.* doi:10.1155/2013/812718.
Kruse, C. R., Singh, M., Sørensen, J. A., Eriksson, E., and Nuutila, K. (2016). The effect of local hyperglycemia on skin cells in vitro and on wound healing in euglycemic rats. *J. Surg. Res.* doi:10.1016/j.jss.2016.08.060.
Krzyszczyk, P., Schloss, R., Palmer, A., and Berthiaume, F. (2018). The role of macrophages in acute and chronic wound healing and interventions to promote pro-wound healing phenotypes. *Front. Physiol.* doi:10.3389/fphys.2018.00419.
Kumar, P., Kumar, S., Udupa, E. P., Kumar, U., Rao, P., and Honnegowda, T. (2015). Role of angiogenesis and angiogenic factors in acute and chronic wound healing. *Plast. Aesthetic Res.* doi:10.4103/2347-9264.165438.
Kumar, S., Vinci, J. M., Millis, A. J., and Baglioni, C. (1993). Expression of

interleukin-1 alpha and beta in early passage fibroblasts from aging individuals. *Exp Gerontol*.

Kunkemoeller, B., and Kyriakides, T. R. (2017). Redox Signaling in Diabetic Wound Healing Regulates Extracellular Matrix Deposition. *Antioxidants Redox Signal.* doi:10.1089/ars.2017.7263.

Kurahashi, T., and Fujii, J. (2015). Roles of antioxidative enzymes in wound healing. *J. Dev. Biol.* doi:10.3390/jdb3020057.

Landén, N. X., Li, D., and Ståhle, M. (2016). Transition from inflammation to proliferation: a critical step during wound healing. *Cell. Mol. Life Sci.* doi:10.1007/s00018-016-2268-0.

Lee, S. E., Kwon, T. R., Kim, J. H., Lee, B. C., Oh, C. T., Im, M., et al. (2019). Anti‐photoaging and anti‐oxidative activities of natural killer cell conditioned medium following UV‐B irradiation of human dermal fibroblasts and a reconstructed skin model. *Int. J. Mol. Med.* doi:10.3892/ijmm.2019.4320.

Lemons, J. M. S., Coller, H. A., Feng, X. J., Bennett, B. D., Legesse-Miller, A., Johnson, E. L., et al. (2010). Quiescent fibroblasts exhibit high metabolic activity. *PLoS Biol.* doi:10.1371/journal.pbio.1000514.

Li, W., Fan, J., Chen, M., Guan, S., Sawcer, D., Bokoch, G. M., et al. (2004). Mechanism of Human Dermal Fibroblast Migration Driven by Type I Collagen and Platelet-derived Growth Factor-BB. *Mol. Biol. Cell*. doi:10.1091/mbc.E03-05-0352.

Li, W. W., Carter, M. J., Mashiach, E., and Guthrie, S. D. (2017). Vascular assessment of wound healing: a clinical review. *Int. Wound J.* doi:10.1111/iwj.12622.

Li, X.-J., Huang, F.-Z., Wan, Y., Li, Y.-S., Zhang, W. K., Xi, Y., et al. (2018). Lipopolysaccharide Stimulated the Migration of NIH3T3 Cells Through a Positive Feedback Between β-Catenin and COX-2. *Front. Pharmacol.* doi:10.3389/fphar.2018.01487.

Liang, C. C., Park, A. Y., and Guan, J. L. (2007). In vitro scratch assay: A convenient and inexpensive method for analysis of cell migration in vitro. *Nat. Protoc.* doi:10.1038/nprot.2007.30.

Lindner, D., Zietsch, C., Becher, P. M., Schulze, K., Schultheiss, H. P., Tschöpe, C., et al. (2012). Differential expression of matrix metalloproteases in human fibroblasts with different origins. *Biochem. Res. Int.* doi:10.1155/2012/875742.

Lohrasbi, S., Mirzaei, E., Karimizade, A., Takallu, S., and Rezaei, A. (2020). Collagen/cellulose nanofiber hydrogel scaffold: physical, mechanical and cell biocompatibility properties. *Cellulose*. doi:10.1007/s10570-019-02841-y.

Lokmic, Z., Musyoka, J., Hewitson, T. D., and Darby, I. A. (2012). "Hypoxia and Hypoxia Signaling in Tissue Repair and Fibrosis," in *International Review of Cell and Molecular Biology* doi:10.1016/B978-0-12-394307-1.00003-5.

Loots, M. A. M., Lamme, E. N., Mekkes, J. R., Bos, J. D., and Middelkoop, E. (1999). Cultured fibroblasts from chronic diabetic wounds on the lower extremity (non-insulin-dependent diabetes mellitus) show disturbed proliferation. *Arch. Dermatol. Res.* doi:10.1007/s004030050389.

Maione, A. G., Brudno, Y., Stojadinovic, O., Park, L. K., Smith, A., Tellechea, A., et al. (2015). Three-dimensional human tissue models that incorporate diabetic foot ulcer-derived fibroblasts mimic in vivo features of chronic wounds. *Tissue Eng. - Part C Methods*. doi:10.1089/ten.tec.2014.0414.

Makrantonaki, E., Wlaschek, M., and Scharffetter-Kochanek, K. (2017). Pathogenesis

of wound healing disorders in the elderly. *JDDG J. der Dtsch. Dermatologischen Gesellschaft*. doi:10.1111/ddg.13199.

Malic, S., Hill, K. E., Playle, R., Thomas, D. W., and Williams, D. W. (2011). In vitro interaction of chronic wound bacteria in biofilms. *J. Wound Care*. doi:10.12968/jowc.2011.20.12.569.

Manuela, B., Milad, K., Anna-Lena, S., Julian-Dario, R., and Ewa Klara, S. (2017). Acute and Chronic Wound Fluid Inversely Influence Wound Healing in an in-Vitro 3D Wound Model. *J. Tissue Repair Regen.* doi:10.14302/issn.2640-6403.jtrr-17-1818.

Martin, P., and Nunan, R. (2015). Cellular and molecular mechanisms of repair in acute and chronic wound healing. *Br. J. Dermatol.* doi:10.1111/bjd.13954.

McCaffrey, T. A., Agarwal, L. A., and Weksler, B. B. (1988). A rapid fluorometric DNA assay for the measurement of cell density and proliferation in vitro. *Vitr. Cell. Dev. Biol. - Anim.* doi:10.1007/bf02623555.

Mendez, M. V., Stanley, A., Park, H. Y., Shon, K., Phillips, T., and Menzoian, J. O. (1998). Fibroblasts cultured from venous ulcers display cellular characteristics of senescence. *J. Vasc. Surg.* doi:10.1016/S0741-5214(98)70064-3.

Mihara, M., Moriya, Y., and Ohsugi, Y. (1996). IL-6-soluble IL-6 receptor complex inhibits the proliferation of dermal fibroblasts. *Int. J. Immunopharmacol.* doi:10.1016/0192-0561(95)00106-9.

Mine, S., Fortunel, N. O., Pageon, H., and Asselineau, D. (2008). Aging alters functionally human dermal papillary fibroblasts but not reticular fibroblasts: A new view of skin morphogenesis and aging. *PLoS One*. doi:10.1371/journal.pone.0004066.

Mio, T., Adachi, Y., Romberger, D. J., Ertl, R. F., and Rennard, S. I. (1996). Regulation of fibroblast proliferation in three-dimensional collagen gel matrix. *Vitr. Cell. Dev. Biol. - Anim.* doi:10.1007/BF02723005.

Muller, M., Li, Z., and Maitz, P. K. M. (2009). Pseudomonas pyocyanin inhibits wound repair by inducing premature cellular senescence: Role for p38 mitogen-activated protein kinase. *Burns*. doi:10.1016/j.burns.2008.11.010.

Myers, M. A. (1998). Direct measurement of cell numbers in microtitre plate cultures using the fluorescent dye SYBR green I. *J. Immunol. Methods*. doi:10.1016/S0022-1759(98)00011-8.

Ng, K. W., Leong, D. T. W., and Hutmacher, D. W. (2005). The challenge to measure cell proliferation in two and three dimensions. *Tissue Eng.* doi:10.1089/ten.2005.11.182.

Nolte, S. V., Xu, W., Rennekampff, H. O., and Rodemann, H. P. (2008). Diversity of fibroblasts - A review on implications for skin tissue engineering. *Cells Tissues Organs*. doi:10.1159/000111805.

O'Leary, L. E. R., Fallas, J. A., Bakota, E. L., Kang, M. K., and Hartgerink, J. D. (2011). Multi-hierarchical self-assembly of a collagen mimetic peptide from triple helix to nanofibre and hydrogel. *Nat. Chem.* doi:10.1038/nchem.1123.

Oberringer, M., Meins, C., Bubel, M., and Pohlemann, T. (2007). A new in vitro wound model based on the co-culture of human dermal microvascular endothelial cells and human dermal fibroblasts. *Biol. Cell*. doi:10.1042/bc20060116.

Omar, A., Wright, J., Schultz, G., Burrell, R., and Nadworny, P. (2017). Microbial Biofilms and Chronic Wounds. *Microorganisms*. doi:10.3390/microorganisms5010009.

Pastar, I., Stojadinovic, O., Yin, N. C., Ramirez, H., Nusbaum, A. G., Sawaya, A., et al. (2014). Epithelialization in Wound Healing: A Comprehensive Review. *Adv. Wound Care*. doi:10.1089/wound.2013.0473.

Peschen, M., Lahaye, T., Hennig, B., Weyl, A., Simon, J. C., and Vanscheidt, W. (1999). Expression of the adhesion molecules ICAM-1, VCAM-1, LFA-1 and VLA-4 in the skin is modulated in progressing stages of chronic venous insufficiency. *Acta Derm. Venereol.* doi:10.1080/000155599750011651.

Raffetto, J. D., Mendez, M. V., Marien, B. J., Byers, H. R., Philips, T. J., Park, H. Y., et al. (2001). Changes in cellular motility and cytoskeletal actin in fibroblasts from patients with chronic venous insufficiency and in neonatal fibroblasts in the presence of chronic wound fluid. *J. Vasc. Surg.* doi:10.1067/mva.2001.113297.

Rahim, K., Saleha, S., Zhu, X., Huo, L., Basit, A., and Franco, O. L. (2017). Bacterial Contribution in Chronicity of Wounds. *Microb. Ecol.* doi:10.1007/s00248-016-0867-9.

Rampersad, S. N. (2012). Multiple applications of alamar blue as an indicator of metabolic function and cellular health in cell viability bioassays. *Sensors (Switzerland)*. doi:10.3390/s120912347.

Reijnders, C. M. A., Van Lier, A., Roffel, S., Kramer, D., Scheper, R. J., and Gibbs, S. (2015). Development of a Full-Thickness Human Skin Equivalent in Vitro Model Derived from TERT-Immortalized Keratinocytes and Fibroblasts. *Tissue Eng. - Part A*. doi:10.1089/ten.tea.2015.0139.

Rhee, S. (2009). Fibroblasts in three dimensional matrices: Cell migration and matrix remodeling. *Exp. Mol. Med.* doi:10.3858/emm.2009.41.12.096.

Rhee, S., Jiang, H., Ho, C. H., and Grinnell, F. (2007). Microtubule function in fibroblast spreading is modulated according to the tension state of cell-matrix interactions. *Proc. Natl. Acad. Sci. U. S. A.* doi:10.1073/pnas.0608030104.

Richards, S. A., Muter, J., Ritchie, P., Lattanzi, G., and Hutchison, C. J. (2011). The accumulation of un-repairable DNA damage in laminopathy progeria fibroblasts is caused by ROS generation and is prevented by treatment with N-acetyl cysteine. *Hum. Mol. Genet.* doi:10.1093/hmg/ddr327.

Roberts, M. J., Broome, R. E., Kent, T. C., Charlton, S. J., and Rosethorne, E. M. (2018). The inhibition of human lung fibroblast proliferation and differentiation by Gs-coupled receptors is not predicted by the magnitude of cAMP response. *Respir. Res.* doi:10.1186/s12931-018-0759-2.

Rolin, G., Binda, D., Tissot, M., Viennet, C., Saas, P., Muret, P., et al. (2014). In vitro study of the impact of mechanical tension on the dermal fibroblast phenotype in the context of skin wound healing. *J. Biomech.* doi:10.1016/j.jbiomech.2014.07.015.

Rossi, A., Appelt-Menzel, A., Kurdyn, S., Walles, H., and Groeber, F. (2015). Generation of a three-dimensional full thickness skin equivalent and automated wounding. *J. Vis. Exp.* doi:10.3791/52576.

Sabetkam, S., Rad, J. S., Khodaie, S. H. P., Maleki, M., and Roshangar, L. (2018). Impact of Mummy Substance on Proliferation and Migration of Human Wharton's Jelly-Derived Stem Cells and Fibroblasts in an In Vitro Culture System. *CRESCENT J. Med. Biol. Sci.*

Schreml, S., Szeimies, R. M., Prantl, L., Karrer, S., Landthaler, M., and Babilas, P. (2010). Oxygen in acute and chronic wound healing. *Br. J. Dermatol.* doi:10.1111/j.1365-2133.2010.09804.x.

Schwarz, F., Jennewein, M., Bubel, M., Holstein, J. H., Pohlemann, T., and Oberringer, M. (2013). Soft tissue fibroblasts from well healing and chronic human wounds show different rates of myofibroblasts in vitro. *Mol. Biol. Rep.* doi:10.1007/s11033-012-2223-6.

Sen, C. K. (2009). Wound healing essentials: Let there be oxygen. *Wound Repair Regen.* doi:10.1111/j.1524-475X.2008.00436.x.

Senthil, K. K. J., Gokila, V. M., Mau, J. L., Lin, C. C., Chu, F. H., Wei, C. C., et al. (2016). A steroid like phytochemical Antcin M is an anti-aging reagent that eliminates hyperglycemia-accelerated premature senescence in dermal fibroblasts by direct activation of Nrf2 and SIRT-1. *Oncotarget*. doi:10.18632/oncotarget.11229.

Serra, R., Grande, R., Butrico, L., Rossi, A., Settimio, U. F., Caroleo, B., et al. (2015). Chronic wound infections: The role of Pseudomonas aeruginosa and Staphylococcus aureus. *Expert Rev. Anti. Infect. Ther.* doi:10.1586/14787210.2015.1023291.

Seth, A. K., Geringer, M. R., Galiano, R. D., Leung, K. P., Mustoe, T. A., and Hong, S. J. (2012). Quantitative comparison and analysis of species-specific wound biofilm virulence using an in vivo, rabbit-ear model. *J. Am. Coll. Surg.* doi:10.1016/j.jamcollsurg.2012.05.028.

Shamis, Y., Hewitt, K. J., Carlson, M. W., Margvelashvilli, M., Dong, S., Kuo, C. K., et al. (2011). Fibroblasts derived from human embryonic stem cells direct development and repair of 3D human skin equivalents. *Stem Cell Res. Ther.* doi:10.1186/scrt51.

Siddiqui, A., Galiano, R. D., Connors, D., Gruskin, E., Wu, L., and Mustoe, T. A. (1996). Differential effects of oxygen on human dermal fibroblasts: Acute versus chronic hypoxia. *Wound Repair Regen.* doi:10.1046/j.1524-475X.1996.40207.x.

Singer, A. J., and Clark, R. (1999). Mechanisms of Disease - Cutaneous Wound Healing. *N. Engl. J. Med.*

Singh, V. P., Bali, A., Singh, N., and Jaggi, A. S. (2014). Advanced glycation end products and diabetic complications. *Korean J. Physiol. Pharmacol.* doi:10.4196/kjpp.2014.18.1.1.

Sirivisoot, S., Pareta, R., and Harrison, B. S. (2014). Protocol and cell responses in threedimensional conductive collagen gel scaffolds with conductive polymer nanofibres for tissue regeneration. *Interface Focus*. doi:10.1098/rsfs.2013.0050.

Smith, R. S., Smith, T. J., Blieden, T. M., and Phipps, R. P. (1997). Fibroblasts as sentinel cells. Synthesis of chemokines and regulation of inflammation. *Am. J. Pathol.*

Smithmyer, M. E., Sawicki, L. A., and Kloxin, A. M. (2014). Hydrogel scaffolds as in vitro models to study fibroblast activation in wound healing and disease. *Biomater. Sci.* doi:10.1039/c3bm60319a.

Soneja, A., Drews, M., and Malinski, T. (2005). Role of nitric oxide, nitroxidative and oxidative stress in wound healing. *Pharmacol. Reports*.

Sorg, H., Tilkorn, D. J., Hager, S., Hauser, J., and Mirastschijski, U. (2017). Skin Wound Healing: An Update on the Current Knowledge and Concepts. *Eur. Surg. Res.* doi:10.1159/000454919.

Sorrell, J. M., and Caplan, A. I. (2004). Fibroblast heterogeneity: More than skin deep. *J. Cell Sci.* doi:10.1242/jcs.01005.

Stadelmann, W. K., Digenis, A. G., and Tobin, G. R. (1998). Physiology and healing

dynamics of chronic cutaneous wounds. *Am. J. Surg.* doi:10.1016/S0002-9610(98)00183-4.
Stipcevic, T., Piljac, T., and Isseroff, R. R. (2005). Di-rhamnolipid from Pseudomonas aeruginosa displays differential effects on human keratinocyte and fibroblast cultures [3]. *J. Dermatol. Sci.* doi:10.1016/j.jdermsci.2005.08.005.
Swift, M. E., Kleinman, H. K., and DiPietro, L. A. (1999). Impaired wound repair and delayed angiogenesis in aged mice. *Lab. Investig.*
Takabe, W. (2001). Oxidative stress promotes the development of transformation: involvement of a potent mutagenic lipid peroxidation product, acrolein. *Carcinogenesis*. doi:10.1093/carcin/22.6.935.
Takahashi, A., Aoshiba, K., and Nagai, A. (2002). Apoptosis of wound fibroblasts induced by oxidative stress. *Exp. Lung Res.* doi:10.1080/01902140252964366.
Tamariz, E., and Grinnell, F. (2002). Modulation of fibroblast morphology and adhesion during collagen matrix remodeling. *Mol. Biol. Cell*. doi:10.1091/mbc.E02-05-0291.
Tandara, A. A., and Mustoe, T. A. (2004). Oxygen in Wound Healing - More than a Nutrient. *World J. Surg.* doi:10.1007/s00268-003-7400-2.
Tanigawa, T., Kanazawa, S., Ichibori, R., Fujiwara, T., Magome, T., Shingaki, K., et al. (2014). (+)-Catechin protects dermal fibroblasts against oxidative stress-induced apoptosis. *BMC Complement. Altern. Med.* doi:10.1186/1472-6882-14-133.
Telgenhoff, D., and Shroot, B. (2005). Cellular senescence mechanisms in chronic wound healing. *Cell Death Differ.* doi:10.1038/sj.cdd.4401632.
Thevenot, P., Nair, A., Dey, J., Yang, J., and Tang, L. (2008). Method to analyze three-dimensional cell distribution and infiltration in degradable scaffolds. *Tissue Eng. - Part C Methods*. doi:10.1089/ten.tec.2008.0221.
Thievessen, I., Fakhri, N., Steinwachs, J., Kraus, V., McIsaac, R. S., Gao, L., et al. (2015). Vinculin is required for cell polarization, migration, and extracellular matrix remodeling in 3D collagen. *FASEB J.* doi:10.1096/fj.14-268235.
Thomson, P. D. (2000). Immunology, microbiology, and the recalcitrant wound. *Ostomy. Wound. Manage.*
Tomasek, J. J., Gabbiani, G., Hinz, B., Chaponnier, C., and Brown, R. A. (2002). Myofibroblasts and mechano: Regulation of connective tissue remodelling. *Nat. Rev. Mol. Cell Biol.* doi:10.1038/nrm809.
Vande Berg, J. S., Rudolph, R., Hollan, C., and Haywood-Reid, P. L. (1998). Fibroblast senescence in pressure ulcers. *Wound Repair Regen.* doi:10.1046/j.1524-475X.1998.60107.x.
Vistejnova, L., Safrankova, B., Nesporova, K., Slavkovsky, R., Hermannova, M., Hosek, P., et al. (2014). Low molecular weight hyaluronan mediated CD44 dependent induction of IL-6 and chemokines in human dermal fibroblasts potentiates innate immune response. *Cytokine*. doi:10.1016/j.cyto.2014.07.006.
Vitellaro-Zuccarello, L., Garbelli, R., and Rossi, V. D. P. (1992). Immunocytochemical localization of collagen types I, III, IV, and fibronectin in the human dermis - Modifications with ageing. *Cell Tissue Res.* doi:10.1007/BF00319157.
Voytik-Harbin, S. L., Brightman, A. O., Waisner, B., Lamar, C. H., and Badylak, S. F. (1998). Application and evaluation of the alamarblue assay for cell growth and survival of fibroblasts. *Vitr. Cell. Dev. Biol. - Anim.* doi:10.1007/s11626-998-0130-x.
Wall, I. B., Moseley, R., Baird, D. M., Kipling, D., Giles, P., Laffafian, I., et al. (2008).

Fibroblast dysfunction is a key factor in the non-healing of chronic venous leg ulcers. *J. Invest. Dermatol.* doi:10.1038/jid.2008.114.

Wang, A. S., and Dreesen, O. (2018). Biomarkers of cellular senescence and skin aging. *Front. Genet.* doi:10.3389/fgene.2018.00247.

Wang, H. J., Pieper, J., Schotel, R., Van Blitterswijk, C. A., and Lamme, E. N. (2004). Stimulation of skin repair is dependent on fibroblast source and presence of extracellular matrix. *Tissue Eng.* doi:10.1089/ten.2004.10.1054.

Wang, H., Pieper, J., Péters, F., Van Blitterswijk, C. A., and Lamme, E. N. (2005). Synthetic scaffold morphology controls human dermal connective tissue formation. *J. Biomed. Mater. Res. - Part A*. doi:10.1002/jbm.a.30232.

Wang, J. (2018). Neutrophils in tissue injury and repair. *Cell Tissue Res.* doi:10.1007/s00441-017-2785-7.

Wang, Z., Liu, X., Zhang, D., Wang, X., Zhao, F., Shi, P., et al. (2015). Coculture with human fetal epidermal keratinocytes promotes proliferation and migration of human fetal and adult dermal fibroblasts. *Mol. Med. Rep.* doi:10.3892/mmr.2014.2798.

Wilson, M. (2001). Bacterial biofilms and human disease. *Sci. Prog.* doi:10.3184/003685001783238998.

Wolcott, R. D., Hanson, J. D., Rees, E. J., Koenig, L. D., Phillips, C. D., Wolcott, R. A., et al. (2016). Analysis of the chronic wound microbiota of 2,963 patients by 16S rDNA pyrosequencing. *Wound Repair Regen.* doi:10.1111/wrr.12370.

Wong, S. Y., Manikam, R., and Muniandy, S. (2015). Prevalence and antibiotic susceptibility of bacteria from acute and chronic wounds in Malaysian subjects. *J. Infect. Dev. Ctries.* doi:10.3855/jidc.5882.

Wong, Y., Sethu, C., Louafi, F., and Hossain, P. (2011). Lipopolysaccharide regulation of toll-like receptor-4 and matrix metalloprotease-9 in human primary corneal fibroblasts. *Investig. Ophthalmol. Vis. Sci.* doi:10.1167/iovs.10-5459.

Woodley, D. T. (2017). Distinct Fibroblasts in the Papillary and Reticular Dermis: Implications for Wound Healing. *Dermatol. Clin.* doi:10.1016/j.det.2016.07.004.

Wulff, B. C., and Wilgus, T. A. (2013). Mast cell activity in the healing wound: More than meets the eye? *Exp. Dermatol.* doi:10.1111/exd.12169.

Xi, Z. De, Xie, C. Y., and Xi, Y. Bin (2016). Macrophage migration inhibitory factor enhances lipopolysaccharide-induced fibroblast proliferation by inducing toll-like receptor 4. *BMC Musculoskelet. Disord.* doi:10.1186/s12891-016-0895-0.

Xia, Y. P., Zhao, Y., Tyrone, J. W., Chen, A., and Mustoe, T. A. (2001). Differential activation of migration by hypoxia in keratinocytes isolated from donors of increasing age: Implication for chronic wounds in the elderly. *J. Invest. Dermatol.* doi:10.1046/j.1523-1747.2001.00209.x.

Xia, Y., Pauza, M. E., Feng, L., and Lo, D. (1997). RelB regulation of chemokine expression modulates local inflammation. *Am. J. Pathol.*

Yang, H., Hu, C., Li, F., Liang, L., and Liu, L. (2013). Effect of lipopolysaccharide on the biological characteristics of human skin fibroblasts and hypertrophic scar tissue formation. *IUBMB Life*. doi:10.1002/iub.1159.

Zhang, J., Wu, L., and Qu, J. M. (2011). Inhibited proliferation of human lung fibroblasts by LPS is through IL-6 and IL-8 release. *Cytokine*. doi:10.1016/j.cyto.2011.02.018.

Zhao, R., Liang, H., Clarke, E., Jackson, C., and Xue, M. (2016). Inflammation in chronic wounds. *Int. J. Mol. Sci.* doi:10.3390/ijms17122085.

8. ABBREVIATIONS

DMEM	Dulbcco´s Modified Eagle Medium
FBS	fetal bovine serum
PDGF	platelet-derived growth factor
TGFβ	transforming growth factor β
FGF	fibroblast growth factor
ROS	reactive oxygen species
VEGF	vascular endothelial growth factor
MMPs	matrix metalloproteinases
IL	interleukin
ECM	extracellular matrix
EGF	epidermal growth factor
HB-EGF	heparin-binding EGF-like growth factor
TNFα	tumor necrosis factor α
KGF	keratinocyte growth factor
α-SMA	α smooth muscle actin
TIMPs	tissue inhibitors of MMPs
ICAM1	intracellular adhesive molecule 1
VCAM1	vascular cell adhesion molecule 1
MRSA	methicillin resistant *Staphylococcus aureus*
HGF	hepatocyte growth factor
AGEs	advanced glycation end products
2D	2 dimensional
LPS	lipopolysaccharide
MCP1	monocyte chemoattractant protein 1
MIP2	macrophage inflammatory protein 2
CINC	cytokine-induced neutrophil chemoattractant
CCL5, RANTES	chemokine (C-C motif) ligand 5
MSCs	mesenchymal stem cells
AAPH	2,2-azobis(2-amidinopropane)dihydrochloride
SIN-1	3-morholinosydnonimine hydrochloride

3D	3 dimensional
HSE	human skin equivalents
NHDF	normal human dermal fibroblast
HBSS	Hank's balanced salt solution
PA (PA 1.5)	*Pseudomonas aeruginosa* used in this study; chosen from a database, 1.5×10^7 CFU/ml
PA (PA 0.25)	*Pseudomonas aeruginosa* used in this study; chosen from a database, 0.25×10^7 CFU/ml
PA2	*Pseudomonas aeruginosa* used in this study; isolated from a patient, 1.5×10^7 CFU/ml
SA	*Staphylococcus aureus* used in this study, 1.5×10^7 CFU/ml
PA	*Pseudomonas aeruginosa*
SA	*Staphylococcus aureus*
CCM	Czech Collection of Microorganisms
TSA	Tryptone Soy Agar
LB	Luria Bertani agar
CFU/ml	colony forming units per ml
SA+PAcu	*SA* (2.7×10^7 CFU/ml) and *PA* (2.7×10^6 CFU/ml) cultivated and incubated together
SA+PAin	*SA* (2.7×10^7 CFU/ml) and *PA* (2.7×10^6 CFU/ml) cultivated separately but incubated together
SA+PAmix	*SA* (2.7×10^7 CFU/ml) and *PA* (2.7×10^6 CFU/ml) cultivated separately, incubated separately, but mixed together just before application on the cells
PBS	phosphate buffer saline
SDS-PAGE	SDS polyacrylamide gel electrophoresis
EDTA	ethylenediaminetetraacetic acid

9. APPENDIX

9.1 Appendix 1 - Cell (nuclei) number determination in 2D culture (Fiji)

1. For series of images open the Image sequence *File* →*Import* → *Image Sequence*

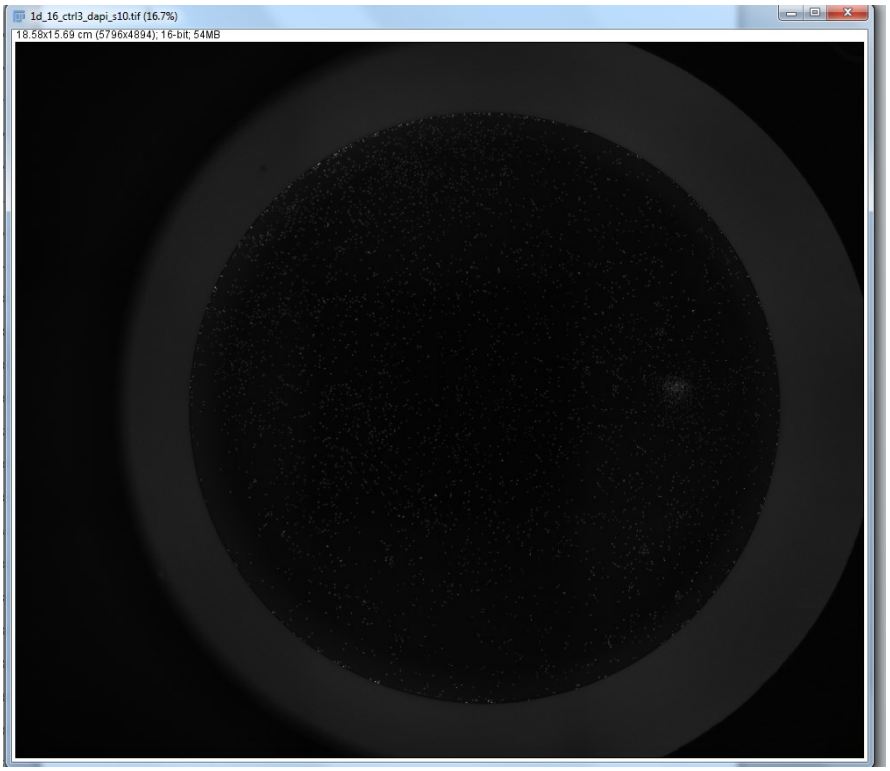

2. *Image* → *Adjust* → *Brightness/Contrast*

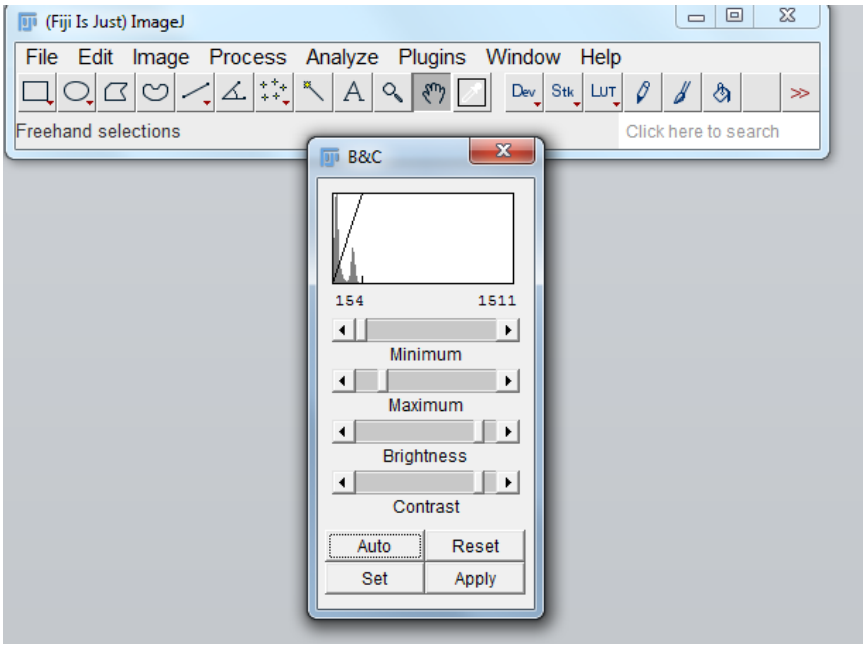

3. Click on **Auto** and **Apply**

4. *Process* → *Subtract Background* – Adjust rolling ball radius to 12 → **Ok**

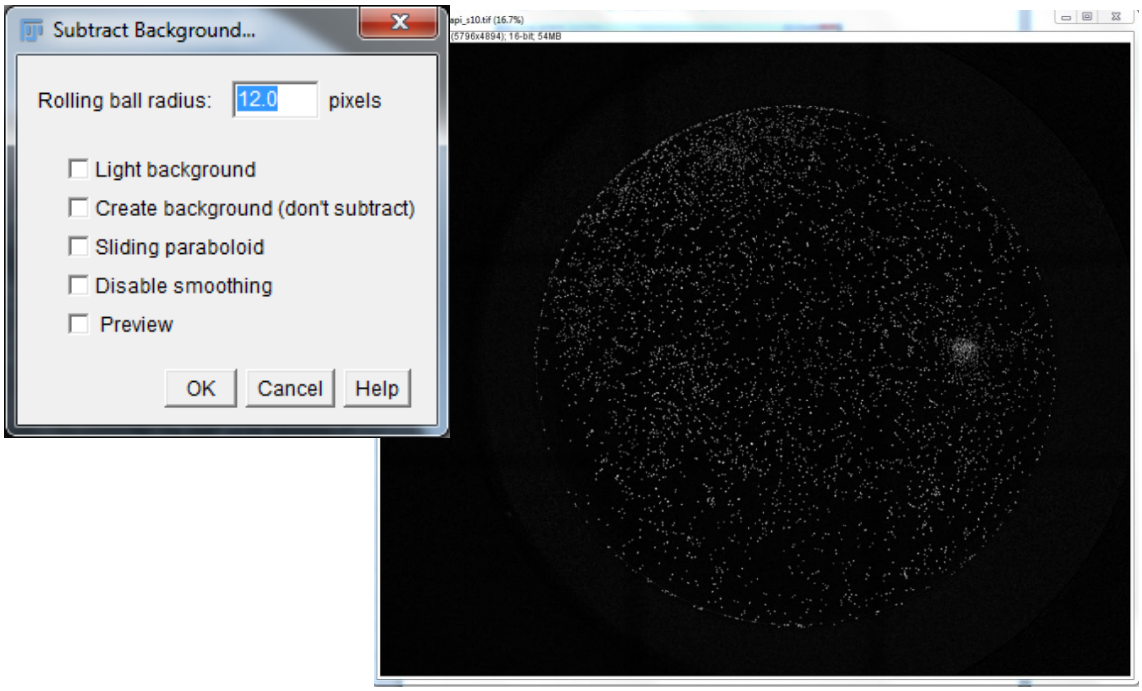

5. *Image* → *Adjust* → *Threshold* - Click **Auto** and **Apply**

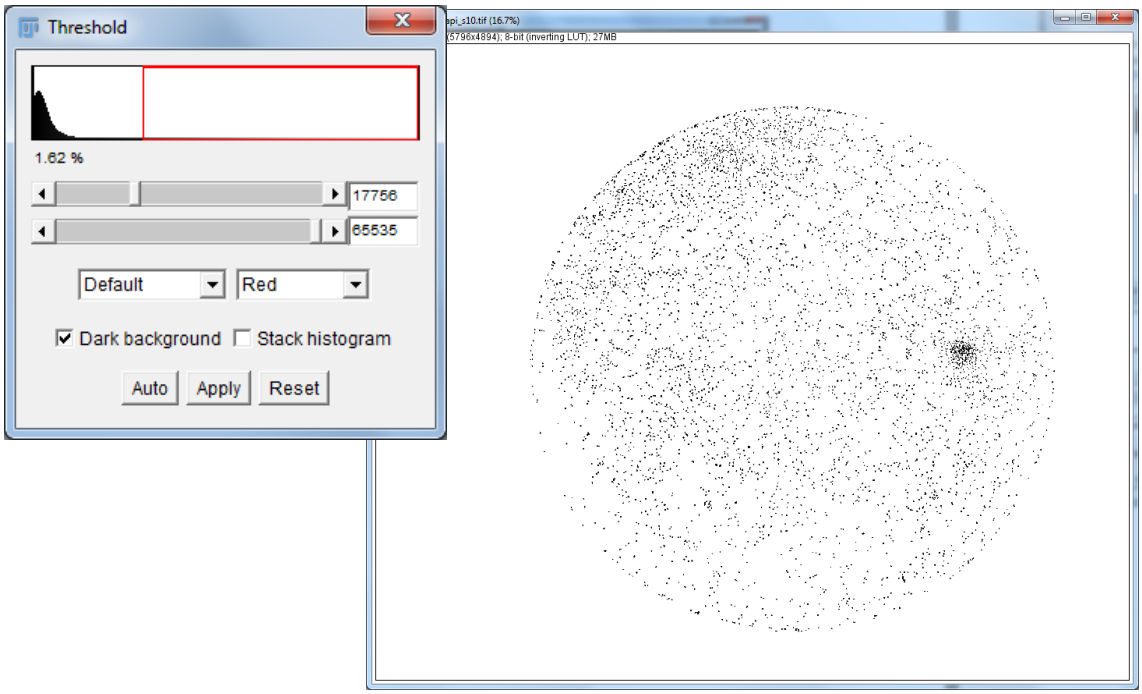

6. *Process* → *Binary* → *Watershed*

7. *Analyze* → *Analyze particles* – Adjust size (cm^2) to 0.00005-10

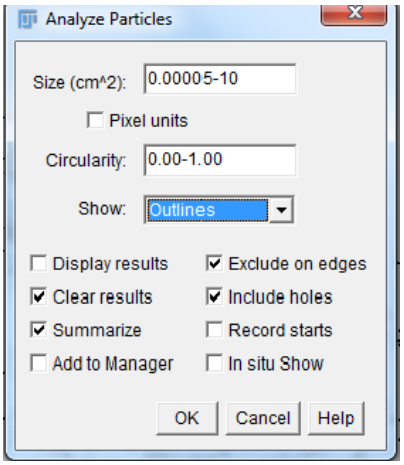

8. Table with results of counted objects + visualization of each object counted

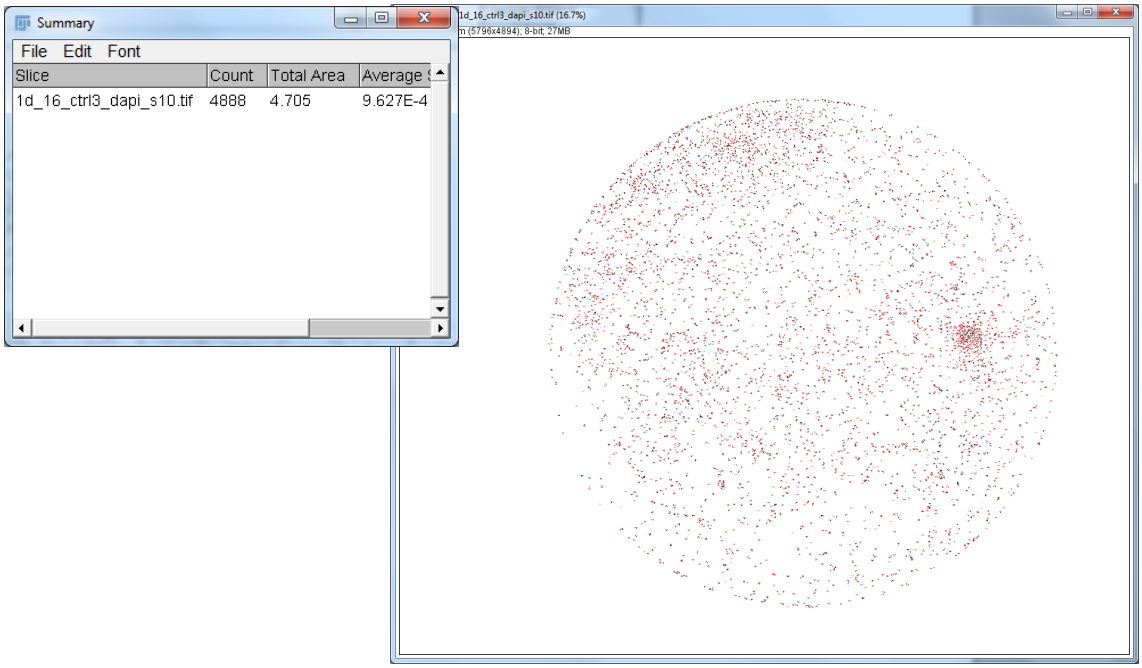

9.2 Appendix 2

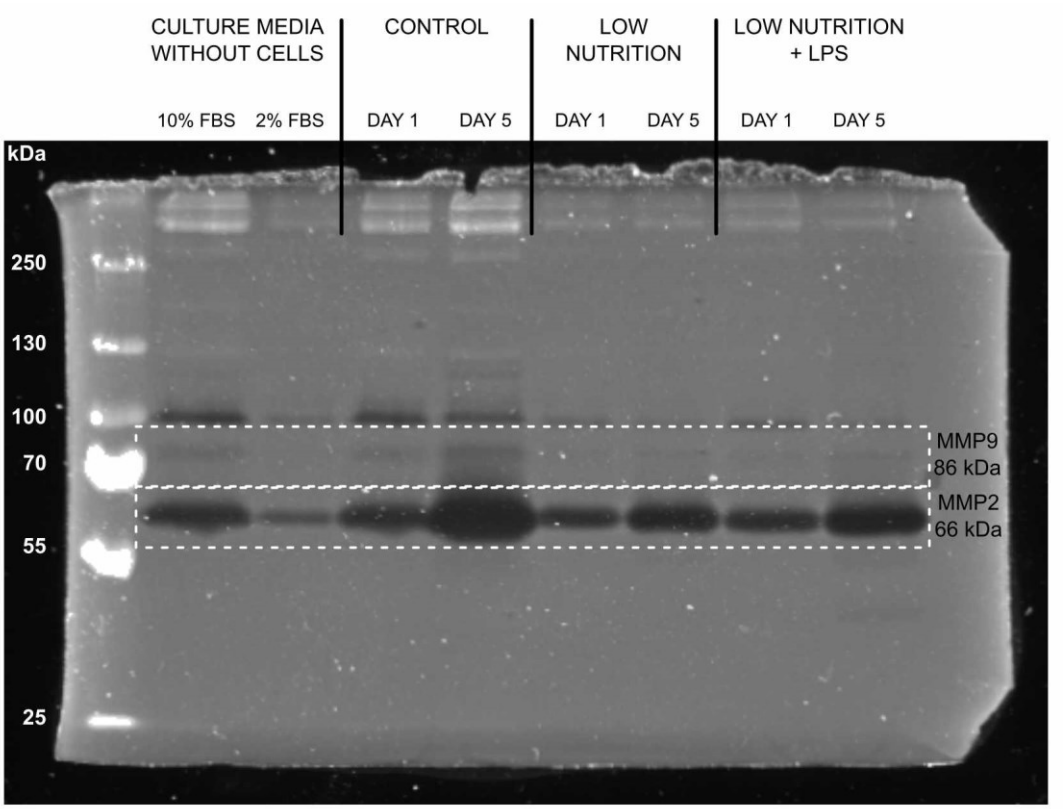

Original scan of the cropped gel in **Figure 9A**. Gels were cropped from one gel as shown by white dashed lines using free Inkscape software (https://inkscape.org/).

9.3 Appendix 3 - Cell (nuclei) number determination in 3D culture (Fiji)

1. Open the FIJI software.

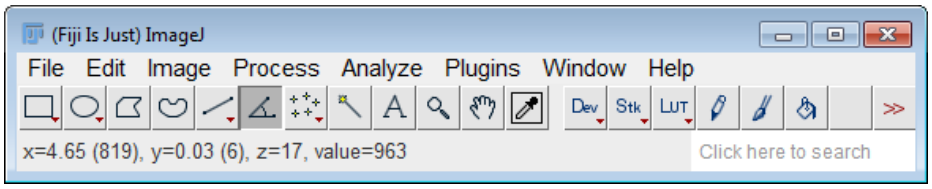

2. Open the .stk file
3. *Image* → *Adjust* → *Size* → Reduce the image file in half
   (The size of .stk files are often very big and the counting by software is slow. The reduced file size does not affect the analysis).

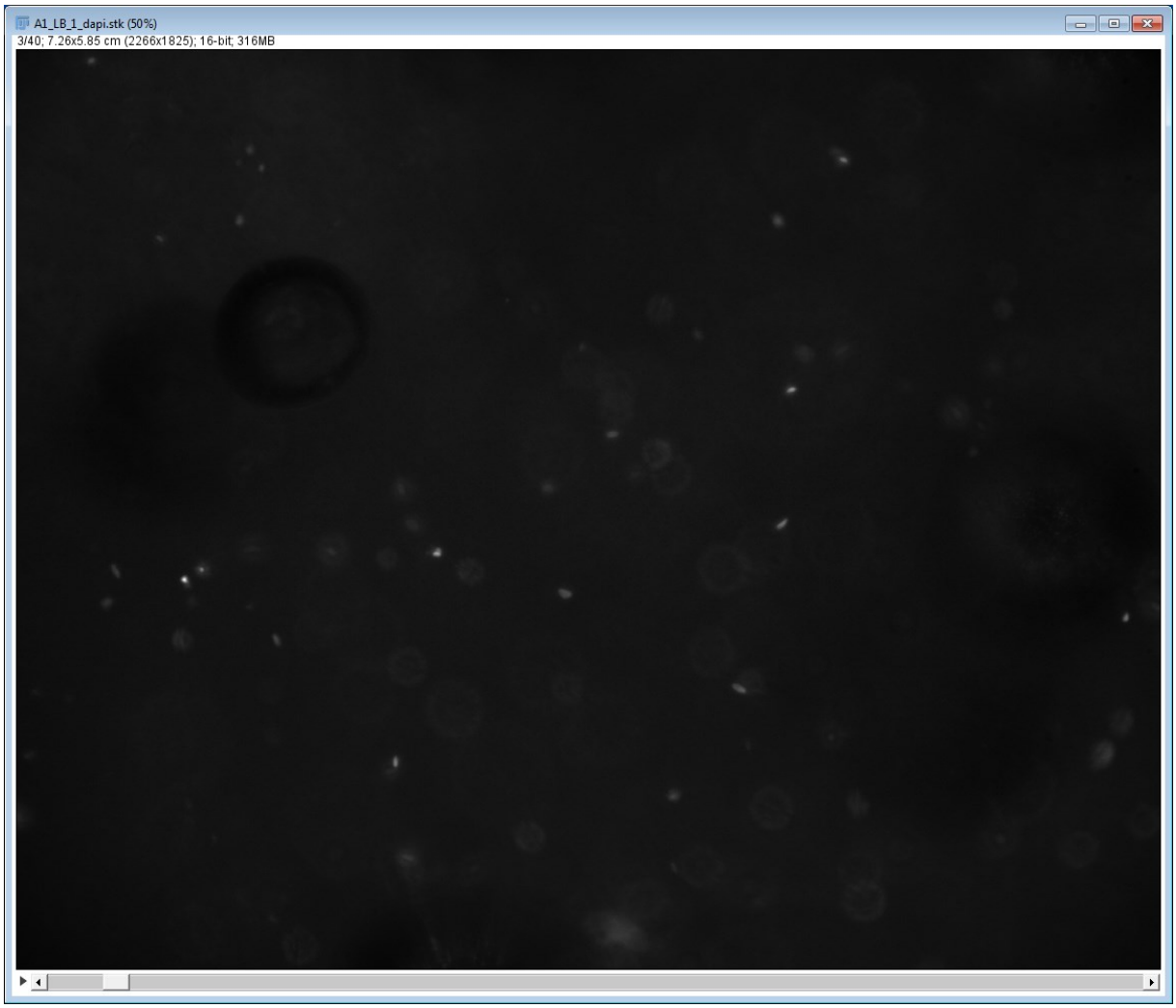

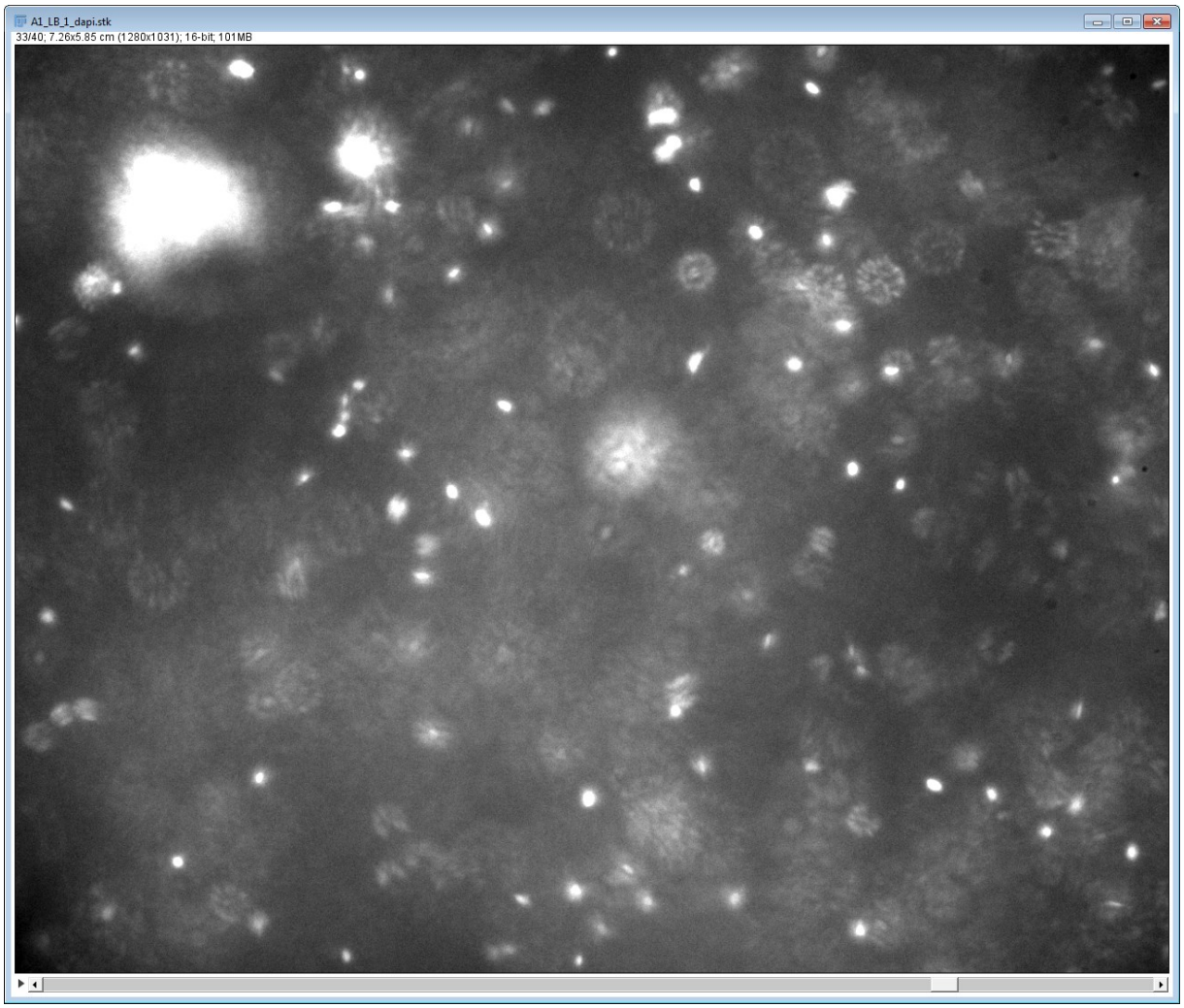

4. *Image* → *Adjust* → *Brightness/Contrast* → Auto → Apply

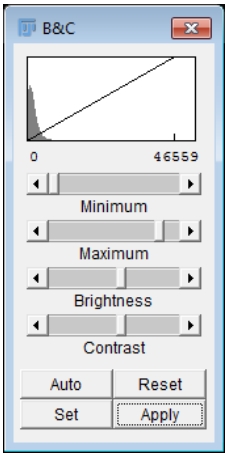

5. *Process* → *Subtract background* →Rolling ball radius: 12 → OK

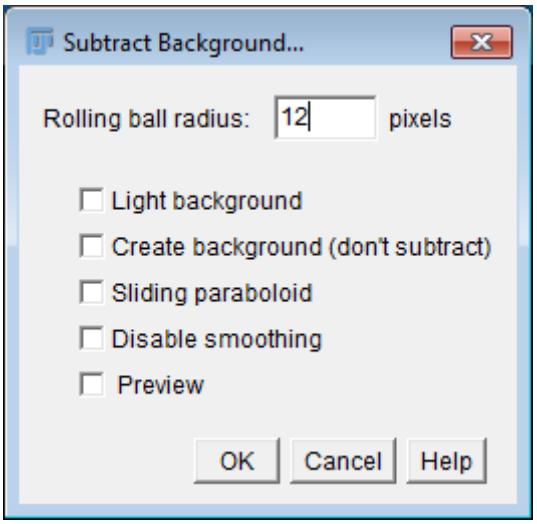

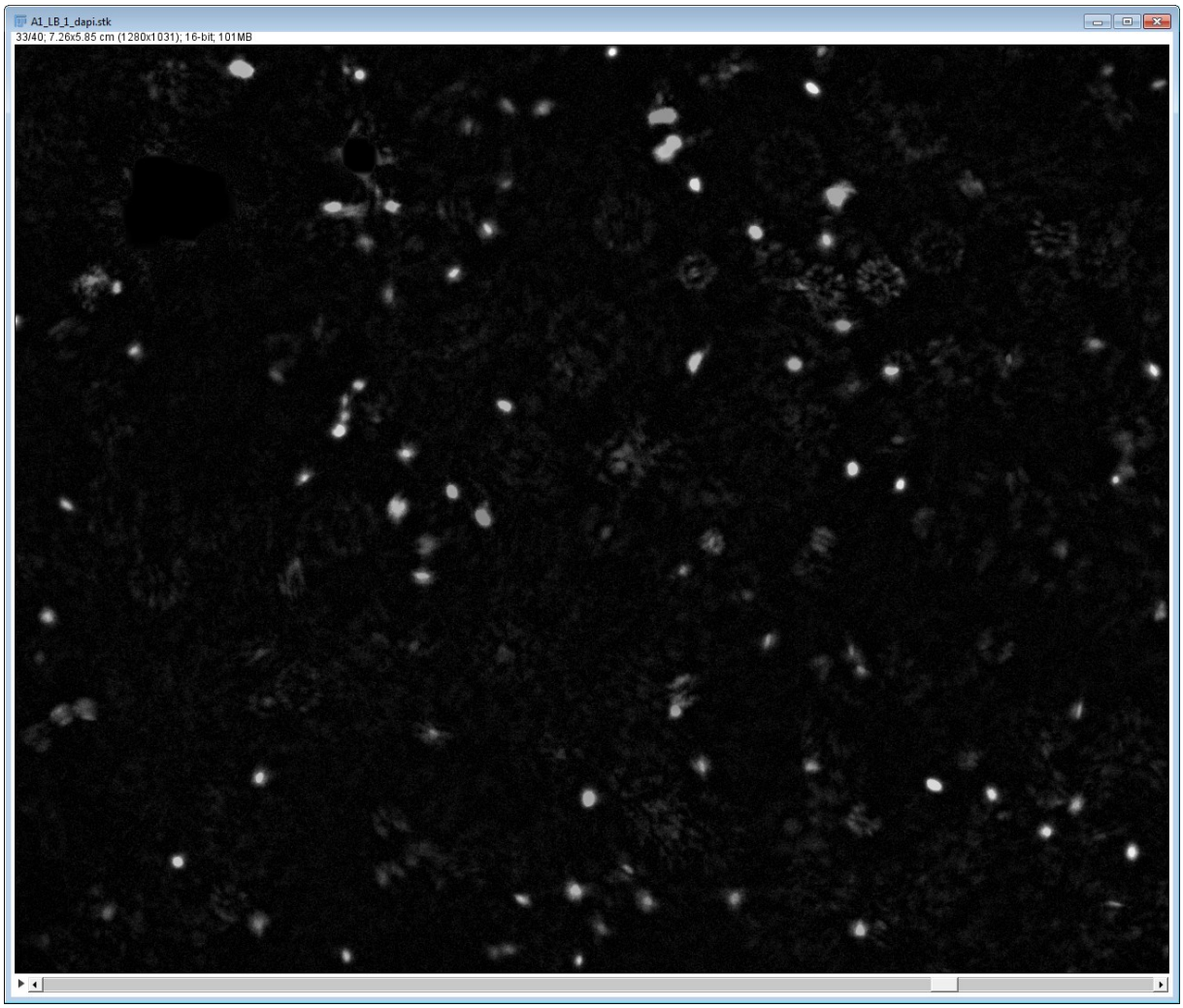

6. *Analyze* → *3D Object Counter* (check or uncheck "Exclude objects on edges"). Shift the Threshold for counting the cell nuclei. Browse the slices with the Slice shift.

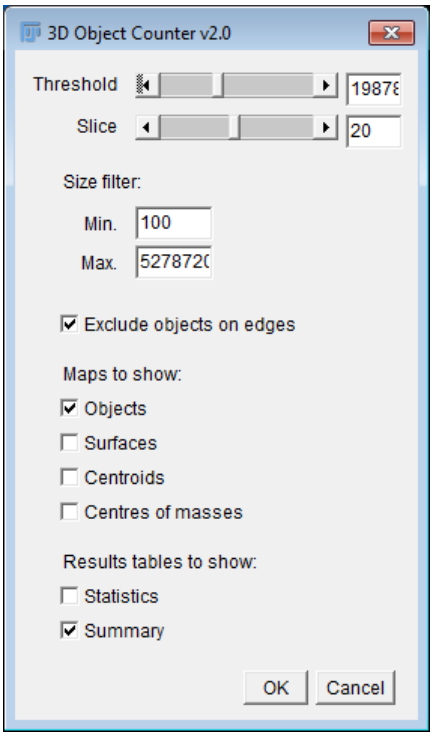

7. The Object map and number of detected objects display. (The lower slices have darker color than the objects above. The digit of counted object displays in the moment of counting by the software).

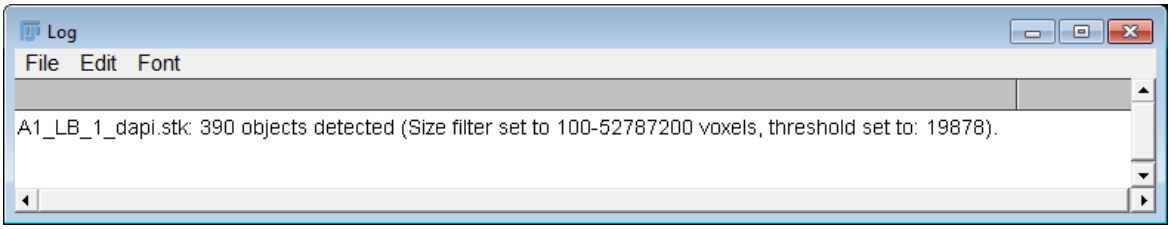

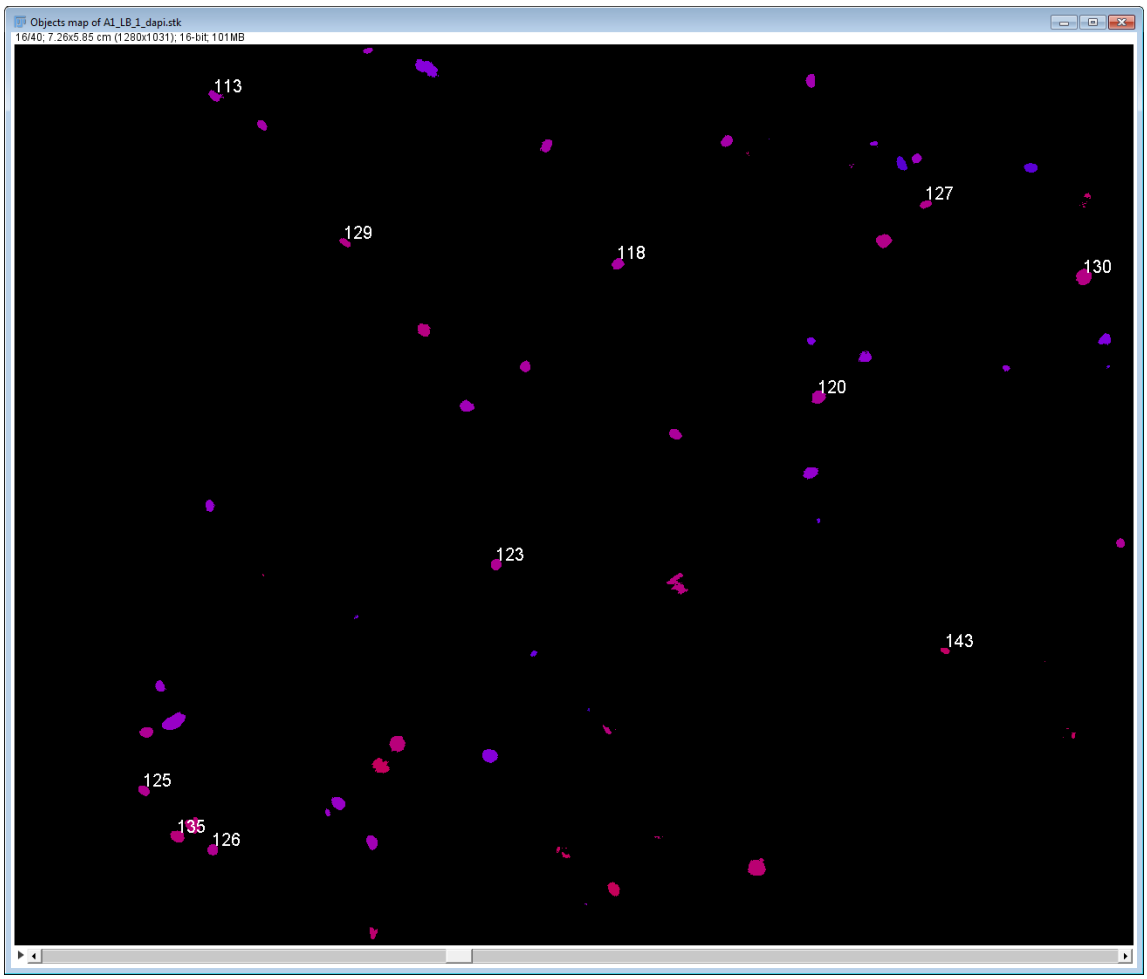
Objects map of A1_LB_1_dapi.stk
16/40; 7.26x5.85 cm (1280x1031); 16-bit; 101MB
113
127
129
118
130
120
123
143
125
135
126

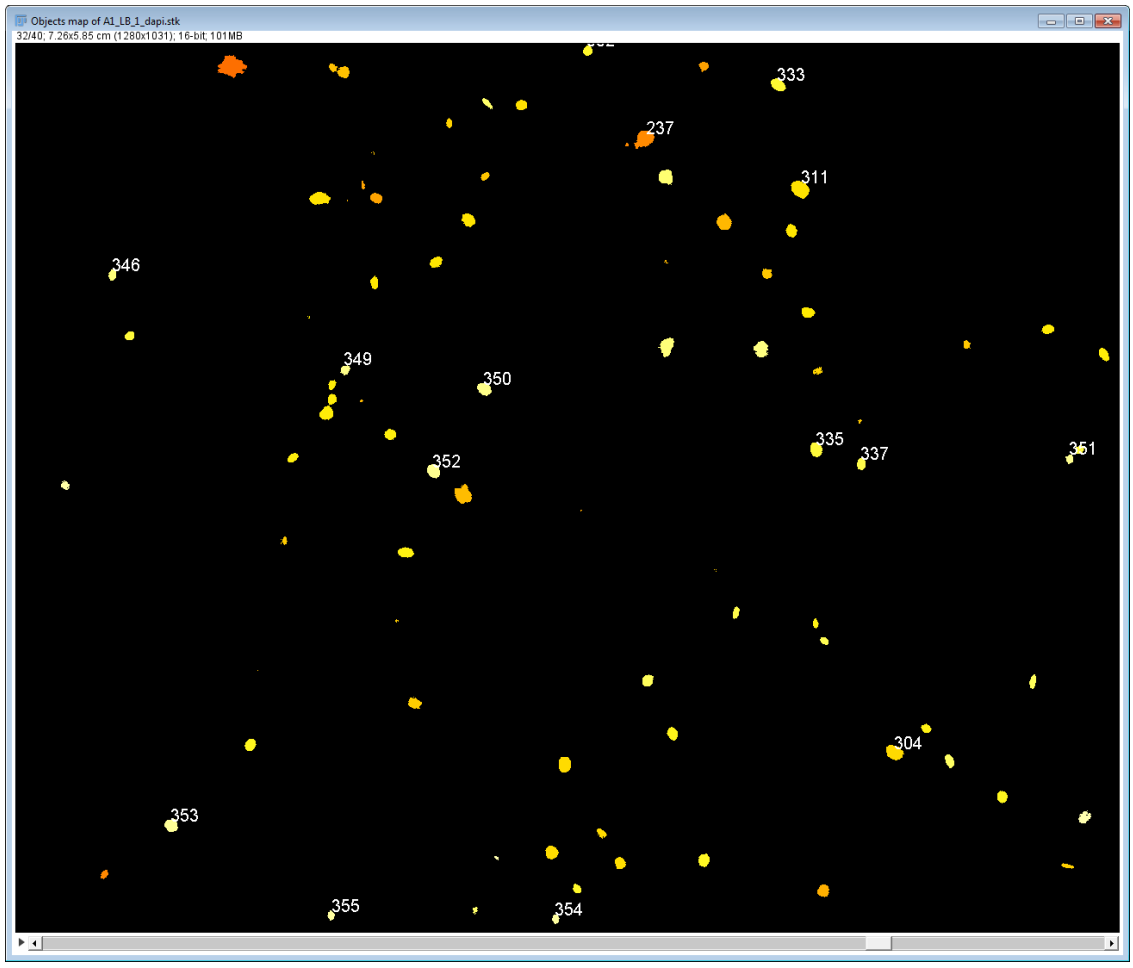
Objects map of A1_LB_1_dapi.stk
32/40; 7.26x5.85 cm (1280x1031); 16-bit; 101MB
333
237
311
346
349
350
335
337
351
352
304
353
355
354

8. It is possible to synchronize the original file with Object Map to verify the correctness of the analysis.

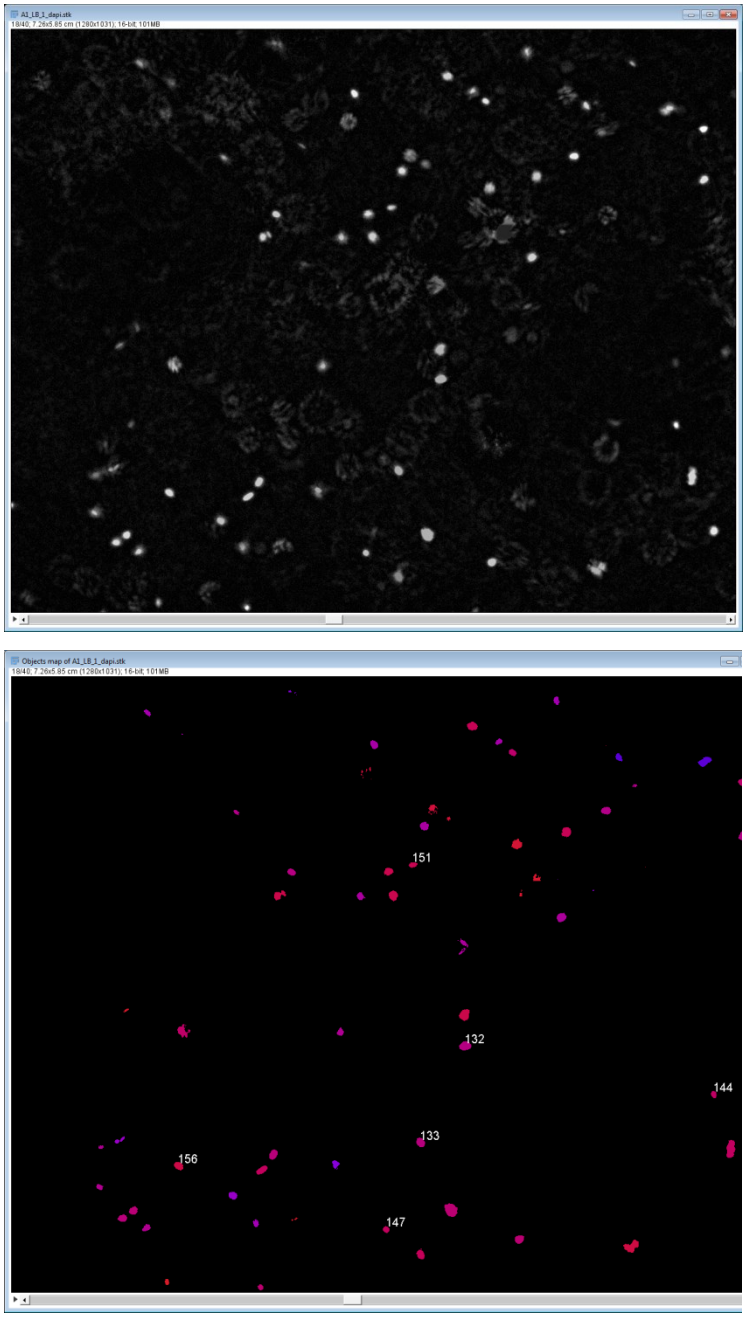

9. *Analyze* → *Tools* → *Synchronize Windows*

Browse the slices with the shift below.

10. AUTHOR´S PUBLICATIONS

Zavadakova, A., Vistejnova, L., and Sauerova, P. (2020). Functional responses of dermal fibroblasts to low nutrition and pro-inflammatory stimuli mimicking wound environment *in vitro*. *Sci. Rep.* Submitted. **IF_{2018}=4.011**

Kanta, J., **Zavadakova, A.** (2020). Role of fibronectin in chronic venous diseases. *Vasc. Med.* Submitted. **IF_{2018}=2.786**

Bacakova, M., Pajorova, J., Broz, A., Hadraba, D., Lopot, F., **Zavadakova, A.**, Vistejnova, L., Beno, M., Kostic, I., Jencova, V., and Bacakova, L. (2019). A two-layer skin construct consisting of a collagen hydrogel reinforced by a fibrin-coated polylactide nanofibrous membrane. *Int. J. Nanomed* 14: 5033-5050. doi: 10.2147/IJN.S200782. **IF_{2018}=4.471**

***Stunova, A**., and Vistejnova, L. (2018). Dermal fibroblasts-A heterogeneous population with regulatory function in wound healing. *Cytokine Growth Factor Rev* 39**,** 137-150. doi:10.1016/j.cytogfr.2018.01.003. **IF_{2018}=6.794 Awarded by Purkyně Endowment Fund 2017**

Leheckova, Z., ***Stunova, A**., and Vistejnova, L. (2018). An overview of wound healing with a brief summary of biomaterials applied in chronic wound healing. *Plzen. Lek. Sborn.* 84: 9-15.

***Stunova = Zavadakova**

11. UPCOMING PUBLICATIONS

The data from this thesis will be processed into three publications:

1. The study of the impact of the contamination by bacterial strains on dermal fibroblasts,
2. the absolute cell number determination in 2D culture,
3. the absolute cell number determination in 3D culture.

12. CONFERENCES

Posters

16th Biomaterials and Surfaces 2018, Horní Mlýn, Czech Republic
Characterization of porcine and rat collagen for 3D cell culture in collagen hydrogels
Biliková D., ***Stunová A.**, Suchý T., Vištejnová L.

4th Future Investigators in Regenerative Medicine, Girona, Spain
Mixture of chronic wound bacteria strains affects dermal fibroblasts in different mode than the individual strains do
***Stunova A.,** Hosek P., Hrabak J., Vistejnova L.

8th Bioimplantology 2016, Brno, Czech Republic
2D and 3D in vitro models of dermal fibroblasts for subsequent chronic wound studies
Zavaďáková A., Vištejnová L., Moravec J., Klein P.

12th International Congress of Cell Biology 2016, Prague, Czech Republic Characterization of Dermal Fibroblasts in New *in vitro* 3D Chronic Wound Model
Zavaďáková A., Moravec J., Klein P. Vištejnová L.

Lectures

27th European Wound Management Association Conference 2017, Amsterdam, Netherlands
Characterization of dermal fibroblasts in novel multifactorial chronic wound 2D and 3D *in vitro* models
The lecture was awarded by the **EWMA First Time International Presenter Award 2017**

16th Biomaterials and Surfaces 2018, Horní Mlýn, Czech Republic
Accurate quantification and spatial distribution of fibroblasts in 3D scaffolds

10th Bioimplantology 2018, Brno, Czech Republic
Simulation of chronic wound bacterial contamination *in vitro*

15th Biomaterials and Surfaces 2017, Horní Mlýn, Czech Republic
Quantification of cell nuclei in 3D culture for determination of cell proliferation

9th Bioimplantology 2017, Brno, Czech Republic
Characterization of dermal fibroblasts in 3D *in vitro* model of chronic wound

14th Biomaterials and Surfaces 2016, Horní Mlýn, Czech Republic
Successes and failures in creating a scaffold for 3D cultivation of skin fibroblasts

***Stunova = Zavadakova**